

SEGMENTED APPROXIMATION
AND
ANALYSIS OF STOCHASTIC PROCESSES

by

ADNAN AKANT

S.B., S.M., Massachusetts Institute of Technology, 1974
E.E., Massachusetts Institute of Technology, 1975

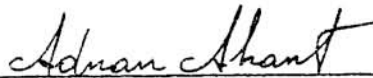
SUBMITTED IN PARTIAL FULFILLMENT
OF THE REQUIREMENTS FOR THE DEGREE OF
DOCTOR OF PHILOSOPHY

at the

MASSACHUSETTS INSTITUTE OF TECHNOLOGY

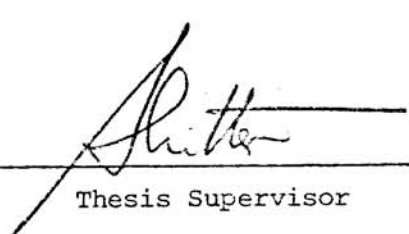
June, 1977

Signature of Author



Department of Electrical Engineering and
Computer Science, June 2, 1977

Certified by:


Thesis Supervisor

Accepted by:

Chairman, Departmental Graduate Committee

SEGMENTED APPROXIMATION AND ANALYSIS OF STOCHASTIC PROCESSES

by

ADNAN AKANT

Submitted to the Department of Electrical Engineering and Computer Science on June 2, 1977 in partial fulfillment of the requirements for the Degree of Doctor of Philosophy.

ABSTRACT

In this thesis a new approach to the approximation and analysis of stochastic processes is developed. A novel formulation of the mathematical approximation problem is introduced for the approximation of sample-functions from a stochastic process defined over a finite (time) interval for which a large but finite set of realizations is available. In this formulation, ensemble, as well as sample-function cost functionals, are considered in order to exploit the statistical nature of the underlying process and to allow approximations to adapt optimally to the particular sample-function being represented. Global measures of the approximation error as well as local constraints on that error over an arbitrary prescribed subset of the global interval are considered. The number of parameters needed to characterize each sample-function of the process via the approximation is obtained by minimizing a cost of feature extraction.

The novel approach is a generalization of the Karhunen-Loève expansion and also incorporates desirable aspects of deterministic piecewise polynomial approximation with free knots. An optimally segmented local Karhunen-Loève expansion is obtained as a result of the novel formulation of the approximation problem in which coefficients, expansion functions, knot locations, local expansion orders, and the total number of segments are determined in an optimal sense. In the new technique, both linear coefficients and highly nonlinear (knot locations, local expansion orders and number of segments) approximation parameters result. Also, arbitrary norms of the error, and in particular the Chebyshev norm, can be used.

Some qualitative and asymptotic results amenable to numerical techniques are derived for the behavior of the estimated expected error of a truncated K-L expansion obtained from a finite data-base.

The techniques developed here are applied to the approximation and analysis of vectorcardiograms. A comparison of the new method with the Karhunen-Loève and piecewise polynomial methods indicates that the new method is generally superior from the point of view of data compression for vectorcardiograms. Furthermore, the nonlinear features that result may carry important diagnostic information not obtainable using linear feature extraction schemes. The off-line and on-line computational time and memory requirements for the new approach are comparable to the requirements for the Karhunen-Loève and piecewise polynomial techniques and indicate that the new approach leads to a viable practical feature extractor for vectorcardiograms. The general approach and techniques developed in this thesis should also be applicable to the analysis of time series and other signals arising from physical processes.

Sanjoy Kumar Mitter, Ph.D.
Professor of Electrical Engineering

ACKNOWLEDGMENTS

I wish to express my deepest appreciation to Professor Sanjoy K. Mitter for supervision, guidance, and support throughout the progress of this thesis and the course of my graduate studies. I would also like to thank Professors T.L. Johnson and A.S. Willsky for acting as readers on my doctoral committee and providing constructive advice.

I have greatly benefited from association with Dr. D.E. Gustafson of Scientific Systems, Inc., during the course of this investigation. His incisive insight and generous efforts are highly appreciated. Our numerous stimulating discussions have contributed in a major way to this thesis and my graduate education.

I would like to thank the M.I.T. Department of Electrical Engineering and Computer Science for a teaching assistantship in my first graduate year. The Charles Stark Draper Laboratory provided me with the opportunity to participate for three years as a Research Assistant and a Draper Fellow in the project that led to this thesis. A Research Assistantship at the M.I.T. Electronic Systems Laboratory through an Air Force grant, and fellowship support from the Vinton-Hayes foundation are also gratefully acknowledged.

I am indebted to the U.S. Air Force School of Aerospace Medicine, and Colonel M. Lancaster in particular, for giving advice on medical matters, providing the cardiograms used in this study, and generally supporting the project that led to this thesis.

I wish to thank Scientific Systems, Inc. for providing me with the possibility to apply the techniques developed in this thesis to the cardiogram approximation problem, and for the final preparation of this report. In particular, I would like to thank William C. Kessel for expert and tireless assistance in computer programming. I also wish to thank Ann C. Mulholland for her skill in typing the text of this manuscript.

To My Parents

TABLE OF CONTENTS

<u>Chapter</u>	<u>Page</u>
1 INTRODUCTION	
1.1 The General Approximation Problem	8
1.2 The Feature Extraction Problem	11
1.3 Overview of Thesis	14
2 THE KARHUNEN LOEVE EXPANSION	
2.1 Introduction	17
2.2 Ensemble Global Cost Function	20
2.3 Determination of Coefficients	21
2.4 Optimization for the Basis Functions	25
2.5 Asymptotic Statistical Analysis for Large Data-Bases	31
2.5.1 Introduction	31
2.5.2 Estimated Eigenvalue Behavior	33
2.5.3 Estimated Expected Error Behavior	36
3 PIECEWISE POLYNOMIAL APPROXIMATION WITH OPTIMAL KNOTS	
3.1 Introduction	43
3.2 Formulation of Approximation Problem	46
3.2.1 Introduction	46
3.2.2 The L_p -Case	49
3.2.3 The Chebyshev Case	51
3.2.4 Constrained Approximations	52
3.3 Determination of Optimal Knots	56
3.3.1 Introduction	56
3.3.2 The L_p -Case	57
3.3.3 The Chebyshev Case	61
3.4 Error Analysis	68
3.4.1 Introduction	68
3.4.2 The Ensemble-Based Problems	69
3.4.3 The Sample-Based Problems	72

4	OPTIMAL SEGMENTED FEATURE EXTRACTION	
4.1	Introduction	77
4.2	Structure of Representations	80
4.3	The L_2 -Case	84
4.3.1	Global-Cost Function	84
4.3.2	Optimal Coefficients	85
4.3.3	Optimal Basis Functions	89
4.3.4	Optimal Knots	95
4.3.5	Local Error Constraints and Optimal Local Expansion Orders	98
4.4	The Chebyshev Case	101
4.4.1	Global-Cost Function	101
4.4.2	Optimal Knots	102
4.4.3	Local Error Constraints and Optimal Local Expansion Orders	103
4.5	Optimal Number of Segments for Feature Extraction	104
4.5.1	Introduction	104
4.5.2	Linear Feature Extraction	105
4.5.3	Nonlinear Feature Extraction	109
4.6	Error Weighting for Improving Smoothness	112
4.7	Comparisons to Global K-L and Piecewise Polynomial Approximations	114
5	APPLICATION TO APPROXIMATION OF CARDIOGRAMS	
5.1	Introduction	118
5.2	Karhunen-Loève Techniques	121
5.3	Piecewise-Polynomial Techniques	126
5.4	Optimally Segmented Karhunen-Loève Techniques	130
5.5	Comparison of Approximation Techniques	141
6	CONCLUSION AND SUGGESTIONS FOR FURTHER RESEARCH	149
	REFERENCES	152
	BIOGRAPHY	157

CHAPTER 1

INTRODUCTION

1.1 The General Approximation Problem

The approximation and analysis of mathematically defined deterministic functions is a highly developed and extensively studied branch of modern mathematics. The linear theory for the approximation of such functions has become fairly well understood [1,2]. On the other hand, a general nonlinear theory of approximation for deterministic functions is yet to be developed, although certain specialized techniques and approaches have been studied for specific problems [3,4].

The approximation and analysis of stochastic processes, however, is an open field with little previous work. The major approximation technique, to date, for second-order stochastic processes, is the truncated (finite-order) Karhunen-Loève (K-L) representation which enjoys certain optimality properties among linear, unconstrained, global techniques. Developing a nonlinear approach for the approximation of stochastic processes has not been previously studied to any extent in the literature.

The problem of approximating curves that arise from the physical world takes on a radically different character than the problem of approximating deterministic mathematical functions. Curves that arise from physical data (i.e., cardiograms, brain waves, seismic waves, economic time series, load-demand data for electric power, etc.) possess certain attributes which distinguish them from mathematical functions (see Rice [5]):

- 1) There usually exists noise in the measurements.
- 2) The underlying physical process is usually stochastic in nature and the measurements are sample-functions of a process. Therefore the uncertainty for a particular realization must be considered, and statistical regularities over the ensemble should be exploited in the approximations.
- 3) The frequent occurrence of "disjointed" behavior is observed. The properties of a curve in one specific region are often independent and little related to its properties in another. In contrast mathematical functions (which are analytic) are determined exactly everywhere by their behavior in any infinitesimal region.

The objectives in approximating data from the physical world also differ from the objectives in the approximation of mathematical functions. Some of these objectives for physical data approximation, discussed by Rice [5] are:

- 1) Representation of certain inherent properties of the process.
- 2) Extraction of information and characterizing features for each sample-function.
- 3) Data compression and compactification by elimination of redundancy.
- 4) Smoothing and noise rejection.
- 5) Computational tractability for obtaining and evaluating approximations.

Of the above objectives, only the last is relevant to the approximation of mathematical functions. The remaining objectives are difficult to translate into quantifiable requirements on the nature of the approximations to be used. Therefore the problem for stochastic processes arising

from the real world must be tackled with a general approach flexible enough to achieve one or more of these desired objectives.

The assumption of disjointed behavior, and the need to extract compact salient characteristics for each sample-function, motivated the formulation of an approach to the approximation of stochastic processes that addresses itself to the following central issues:

- 1) Approximations must minimize well-defined ensemble cost functionals -- they should therefore exploit the statistical regularities and modes of the underlying process.
- 2) The approximation of each sample-function of the process must be accurate enough to capture the particular characteristics of the sample being approximated -- the approximation should therefore be capable to adapt to the sample-function in consideration and not merely reflect how well that sample-function reproduces the statistical regularities of the process in general.
- 3) A global measure of the approximation error in the entire region over which the process is defined must be minimized.
- 4) Imposition of local constraints on approximation error in given specific regions of the global interval should be allowed so that independent control of representation accuracy can be achieved to suit the particular needs of the approximation problem at hand.
- 5) The number of parameters needed to characterize each sample function of the process via the approximations should be minimal.
- 6) Since in practice a full characterization of the stochastic process will not be available, the approximation method must be derived from the statistics of a large but finite data-base of realizations of the process.

The general approach to the classical problem of approximation involves a rather fixed sequence of steps. One first chooses, based on physical intuition or other considerations, the approximating functions and the form of the performance measure to be used (various norms or "distance" functions of the error). Once these choices are made, the existence, uniqueness, and other characterizing properties of the solution are investigated. Then, if possible, a computational scheme for obtaining an optimal solution is developed. The ultimate objective is, of course, to construct an algorithm for obtaining the approximation.

In the present investigations for approximating stochastic processes, the classical approach valid for deterministic functions is considerably generalized to allow the algorithms to deal with the six central issues formulated above. The optimal approximations are explicitly exhibited and algorithms to compute them are provided, which, from the practical point of view, are efficient, reliable, and flexible for constraint imposition. Both the L_p and Chebyshev (L_∞) norms of the error are considered in formulating approximation problems. The use of the L_2 -norm leads to certain elegant optimality properties, whereas the Chebyshev norm is a very valuable norm in practical applications since it imposes absolute bounds on errors.

1.2 The Feature Extraction Problem

The approximation of sample functions from stochastic processes subject to the considerations discussed finds application in the field of feature extraction for pattern recognition and classification studies of line patterns in general, and cardiograms in particular. This study has been initiated and motivated by efforts to develop signal analysis techniques to automatically classify vectorcardiograms into various disease classes [6,7,8].

The feature extraction problem in pattern recognition is concerned with the assignment of analytically and computationally tractable, compact representations to patterns with minimal loss of information for a given number of allowed features. The feature extraction problem arises naturally in the problem of pattern recognition, although its applicability and significance extends to a much wider context [9]. The problem of pattern recognition is generally divided into two stages: feature extraction and classification as depicted in Figure 1.1.

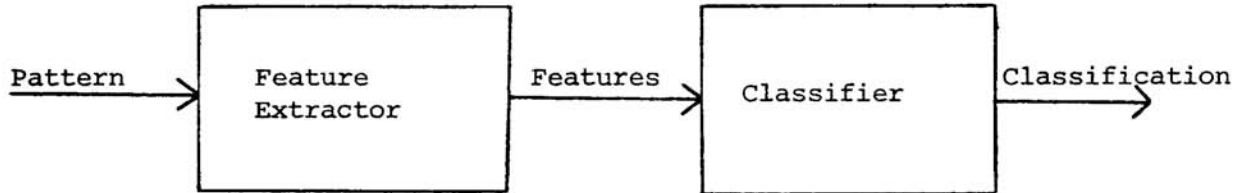


Figure 1.1: The Pattern Recognition Problem

Ideally, the feature extractor preserves only information relevant for classification and neglects all other information. Hence the ideal criterion by which the design of the feature extractor should be carried out is classification error. However, such an overall integrated approach to pattern recognition is in general not feasible. A sub-optimal and widely used approach is the independent design of the feature extractor and the classifier operating on the features.

In such an approach the design of the feature extractor must essentially be guided by the accuracy with which the original data can be reconstructed from the features. Decoupling of the classification and feature

extraction stages therefore makes the feature extraction problem into an approximation problem subject to the considerations discussed in section 1.1.

Feature extraction has received considerable attention in the recent literature [10,11]. Nonlinear feature extraction has been considered by Sebestyen [12], Calvert and Young [9], and others, but to date there is no general approach independent of the geometry of the underlying patterns. In particular, nonlinear feature extraction for highly non-stationary vector stochastic processes, such as cardiograms, has not been considered.

The class of problems to which this study is directed involves non-stationary second-order vector stochastic processes defined over a finite interval of the real line. The averaged, "typical", heartbeat waveform (see [13]) is modeled as such a process. Although the cardiac process is highly non-stationary in time and over the ensemble of possible heart conditions, cardiographers have found it useful to segment the heartbeat cycle into distinct intervals (P,Q,R,S,T waves) each related to a certain phase of the underlying physical process (see e.g. [14]). The appropriate segmentation for each sample waveform is highly variable over the ensemble. However, statistical (ensemble) regularities are observed over these sample-dependent (variable) segments, enabling cardiographers to distinctly identify the various phases.

The Karhunen-Loève expansion has enjoyed a great popularity among theoreticians [15]. Although the K-L expansion is an optimal linear representation, it is based solely on ensemble information (the process covariance function), and takes into account only expected global errors with an L_2 -norm. In the cardiogram approximation problem, the P-wave region, although possessing small signal energy, contains important diagnostic

information and is therefore a local region that needs to be well approximated. The L_2 error criterion, in contrast, will largely ignore the P-wave region due to that region's small contribution to the total signal energy. Similarly, due to the large variance of cardiograms about the ensemble mean a particular sample-function (patient's record) may be poorly approximated although the expected (ensemble) error is made to be very small. The risk associated with misclassifying any single patient makes it mandatory that each sample-function be approximated well, regardless of its being a very rare case in the ensemble. An important feature of the class of problems considered in this study, therefore, is that the actual approximation accuracy for each sample-function must be controlled on a local basis in time.

An approach that allows localization of accuracy, and is compatible with the notion of segmentation of the process, is the generalized variable-knot spline method. This method, however, ignores the statistical nature of the problem and no use is made of ensemble information in representing individual sample waveforms.

It is the above considerations, originally motivated by the feature extraction problem for cardiograms that led to the formulations and general methods developed in this study for the approximation of stochastic processes subject to the central issues discussed earlier.

1.3 Overview of Thesis

In Chapter 2 the K-L expansion for second-order stochastic processes is considered. This expansion is derived from its global L_2 -error minimizing property. Then the effect of the finiteness of the data base used for

estimating the K-L basis functions in practice is analyzed. It is shown how an elegant result of Dyson [16] may be applied to this problem to obtain practical error bounds for the expected error rate of using truncated expansions.

In Chapter 3 piecewise polynomial approximation is considered and a dynamic programming solution for obtaining optimal segmentation is developed for both the L_2 and Chebyshev norm cases. The fixed-knot ensemble and the variable-knot sample-function problems are treated. Error analyses from spline-theory are adapted to obtain performance bounds.

In Chapter 4 a novel representation is developed that combines aspects of the K-L and variable-knot spline techniques. Ensemble and sample-function based, minimal-order representations, allowing for local error constraints, together with global-error optimization, are obtained for both the L_2 and Chebyshev norm cases. Some theoretical comparisons of this novel representation to the K-L and piecewise polynomial methods are discussed.

In Chapter 5 the approximation techniques developed in this thesis are applied to the problem of cardiogram representation and analysis. Evaluation of methods and extensive experimental results are provided for this problem.

In Chapter 6, recommendations for further study in this field are suggested.

The specific contributions of this thesis can be summarized as follows:

- 1) The asymptotic analysis of the K-L eigenvalues and estimation of the expected error rate using Dyson's result.
- 2) The generalization of Bellman's dynamic programming solution for the linear approximation of curves to
 - i) the general piecewise polynomial case.
 - ii) the case for the Chebyshev norm (L_∞).
 - iii) the ensemble case for stochastic problems.
- 3) A novel global-local, ensemble-sample-function formulation of the approximation problem for stochastic processes.
- 4) The derivation of a unified segmented-KL representation with optimal fixed or variable knots and local constraints.
- 5) The application of the techniques developed to feature extraction for cardiograms.

CHAPTER 2

THE KARHUNEN-LOEVE EXPANSION

2.1 Introduction

The Karhunen-Loève expansion is a representation for second-order stochastic processes which is well documented in the theoretical literature [10,15] and which is being used as a practical technique for data reduction [6,15]. The expansion is in terms of orthonormal basis functions and the coefficients of the representation are linear in the data. The basis functions for the expansion are derived from the second order statistics of the process. For a discrete sampled process, the basis functions are the eigenvectors of the covariance matrix. For a continuous waveform they are eigenfunctions of a Fredholm type integral equation [17], and may in general be difficult to obtain. The corresponding eigenvalues measure the expected energy along each eigenvector component. If the terms of the expansion are ordered so that the associated eigenvalues decrease in magnitude, the expansion can be truncated after m -terms. The first m -eigenvectors span the subspace of R^N (in the vector case) which contains on average the greatest proportion of the energy in the process. Some optimality properties of the expansion are:

1) Over the set of all orthonormal functions, for a given number of terms in the expansion, the K-L minimizes the mean-square error [15]; minimizes the coefficient entropy defined by

$$S = - \sum_i \bar{\alpha}_i^2 \log \bar{\alpha}_i^2$$

2.1

here α_i is the coefficient in the representation of the i -th basis function and $\overline{\alpha_i^2}$ denotes the expected value of α_i^2 [15]. The K-L also maximizes the population entropy defined by

$$h = -\mathcal{E} \{ \ln p(\underline{\alpha}) \} \quad 2.2$$

where $\underline{\alpha}$ is the vector of m -coefficients [9]; maximizes the distance between independent samples from a single distribution [10] as defined by the scatter measure:

$$\mathcal{E} \{ d_{\underline{\alpha}}^2 \} = \mathcal{E} \{ |\underline{\alpha}_1 - \underline{\alpha}_2|^2 \} \quad 2.3$$

- 2) The coefficients α_i are uncorrelated and are linear in the data.
- 3) For a wide-sense stationary periodic process the K-L expansion reduces to a Fourier series.
- 4) Young has defined a concept of reliability from an information-theoretic view and proved that K-L is the most "reliable" linear feature extractor [18].

The K-L expansion has also been extended to the case of multiple processes by Chien and Fu [11]. In this section a generalization of the basic K-L method to treat the case when errors over various regions of waveforms are weighted differently is considered. This essentially amounts to redefining the norm of the error using a weighting function. Analogous results follow directly for the weighted K-L expansion [7]. The effect of using a time-weighting in the performance index has been considered in the work reported in [7]. This extension of the K-L expansion is an

interesting modification and has been tried on the cardiographic problem, as discussed in Chapter 5.

In this Chapter the Karhunen-Loève expansion is derived from its error minimizing property. The K-L expansion is obtained by seeking a linear, m-term representation with orthonormal functions, that minimizes the global expected (ensemble) squared error. The original and standard derivation of the K-L is not based on the optimality properties mentioned but rather follows from a Hilbert space approach to random processes [19]. Below is stated the main Karhunen-Loève expansion theorem for reference [20].

Karhunen-Loève Expansion: Let $x(t, \omega), t \in [0, T]$ and $\omega \in \Omega$ (T finite, Ω a probability sample space) be a continuous-parameter second order random process with zero mean and continuous covariance function $R(t, \tau)$.

Then

$$x(t, \omega) = \sum_{i=1}^{\infty} \alpha_i(\omega) \phi_i(t) \quad t \in [0, T] \quad 2.4$$

where the $\{\phi_i\}$ are eigenfunctions of the integral operator corresponding to R :

$$\int_0^T R(t, \tau) \phi_i(\tau) d\tau = \lambda_i \phi_i(t) \quad 2.5$$

and form an orthonormal basis for the space spanned by the eigenfunctions corresponding to the non-zero eigenvalues. The $\alpha_i(\omega)$ are given by

$\int_0^T x(t, \omega) \phi_i(t) dt$ and are orthogonal random variables ($E\{\alpha_i(\omega) \alpha_j(\omega)\} = 0$ for $i \neq j$) with zero mean and variance λ_i , where λ_i is the eigenvalue corresponding to ϕ_i .

The series $\sum_{i=1}^{\infty} \alpha_i(\omega) \phi_i(t)$ converges in mean square to $x(t, \omega)$

uniformly in t , that is

$$\mathbb{E} \left\{ x(t, \omega) - \sum_{k=1}^m \alpha_k(\omega) \phi_k(t) \right\}^2 \rightarrow 0 \quad m \rightarrow \infty \quad 2.6$$

uniformly for all $t \in [0, T]$.

The problems associated with using truncated Karhunen-Loeve expansions that have been derived from a finite data base are also analyzed in this chapter.

2.2 Ensemble Global Cost Function

Let $\{\phi_i\}$ denote a set of complete orthonormal basis functions with respect to the weighting function $w(t)$ over the interval $[0, T]$.

Then, by definition,

$$\int_0^T \phi_i(t) w(t) \phi_j(t) dt = \delta_{ij} \quad 2.7$$

An m -th order truncated representation of the sample-function $x(t, \omega)$ is defined as:

$$\hat{x}(t, \omega) = \sum_{i=1}^m \alpha_i(\omega) \phi_i(t) \quad 2.8$$

The representation error is simply $(x - \hat{x})$. Consider the following ensemble global L_2 -cost, given m , the number of terms in the expansion:

$$J_{\mathbb{E}}(\{\alpha_i\}, \{\phi_i\} | m) = \mathbb{E} \int_0^T [x(t, \omega) - \hat{x}(t, \omega)]^2 w(t) dt \quad 2.9$$

where $w(t) \geq 0 \forall t \in [0, T]$ is a given time-weighting function for the error. The optimization problem considered is to determine

$$J_{\varepsilon}^* = \text{Min}_{\{\alpha_i\}, \{\phi_i\}} J_{\varepsilon} \quad 2.10$$

2.3 Determination of Coefficients

In view of the orthonormality of the basis functions, as given by equation 2.7 any sample function $x(t, \omega)$ can be expanded over the interval $[0, T]$ using the complete orthonormal set $\{\phi_i\}$. That is:

$$x(t, \omega) = \sum_{i=1}^{\infty} \alpha_i(\omega) \phi_i(t) \quad t \in [0, T] \quad 2.11$$

The coefficients can easily be determined by the orthonormality condition for the $\{\phi_i\}$:

$$\int_0^T x(t, \omega) w(t) \phi_k(t) dt = \sum_{i=1}^{\infty} \alpha_i(\omega) \int_0^T \phi_i(t) w(t) \phi_k(t) dt \quad 2.12$$

$$\int_0^T x(t, \omega) w(t) \phi_k(t) dt = \sum_{i=1}^{\infty} \alpha_i(\omega) \delta_{ik} = \alpha_k(\omega) \quad 2.13$$

One may at first suspect that for an m-term truncated expansion of $x(t, \omega)$ one may better approximate by the finite set $\{\phi_1, \phi_2, \dots, \phi_m\}$ using coefficients $\alpha'_i(\omega)$ which are different from those $\alpha_i(\omega)$ given by equation 2.13. It is now shown that this is not so.

$$\mathcal{E} \int_0^T \left[x(t, \omega) - \sum_{i=1}^m \alpha_i(\omega) \phi_i(t) \right]^2 w(t) dt < \mathcal{E} \int_0^T \left[x(t, \omega) - \sum_{j=1}^m \alpha'_j(\omega) \phi_j(t) \right]^2 w(t) dt$$

whenever $\alpha_i(\omega) \neq \alpha'_i(\omega)$. The left hand side of equation 2.14 is simply

$$\mathcal{E} \int_0^T \left\{ \sum_{i=m+1}^{\infty} \alpha_i(\omega) \phi_i(t) \right\}^2 w(t) dt = \mathcal{E} \int_0^T w(t) \sum_{i=m+1}^{\infty} \sum_{j=m+1}^{\infty} \alpha_i(\omega) \alpha_j(\omega) \phi_i(t) \phi_j(t) dt$$

Interchanging the integration and summations (which is allowed due to the uniform convergence in t of the representation) the following is obtained:

$$\mathcal{E} \left\{ \sum_{i=m+1}^{\infty} \sum_{j=m+1}^{\infty} \alpha_i(\omega) \alpha_j(\omega) \int_0^T \phi_i(t) w(t) \phi_j(t) dt \right\} \quad 2.16$$

which is just

$$\mathcal{E} \left\{ \sum_{i=m+1}^{\infty} \sum_{j=m+1}^{\infty} \alpha_i(\omega) \alpha_j(\omega) \delta_{ij} \right\} = \sum_{i=m+1}^{\infty} \overline{\alpha_i^2(\omega)} \quad 2.17$$

Expanding $x(t, \omega)$ on the right hand side of equation 2.14

$$\begin{aligned} \mathcal{E} \int_0^T \left[\sum_{i=1}^{\infty} \alpha_i(\omega) \phi_i(t) - \sum_{j=1}^m \alpha'_j(\omega) \phi_j(t) \right]^2 w(t) dt = \\ \mathcal{E} \int_0^T \left[\sum_{i=1}^m (\alpha_i(\omega) - \alpha'_i(\omega)) \phi_i(t) + \sum_{j=m+1}^{\infty} \alpha_j(\omega) \phi_j(t) \right]^2 w(t) dt \end{aligned} \quad 2.18$$

Expanding the integrand of the right hand side of equation 2.18

$$\begin{aligned} \mathcal{E} \int_0^T \left\{ \sum_{i=1}^m (\alpha_i(\omega) - \alpha'_i(\omega)) \phi_i(t) \right\}^2 w(t) dt + \mathcal{E} \int_0^T \left\{ \sum_{j=m+1}^{\infty} \alpha_j(\omega) \phi_j(t) \right\}^2 w(t) dt \\ + 2 \mathcal{E} \int_0^T \sum_{i=1}^m (\alpha_i(\omega) - \alpha'_i(\omega)) \phi_i(t) \sum_{j=m+1}^{\infty} \alpha_j(\omega) \phi_j(t) w(t) dt \end{aligned} \quad 2.19$$

The last term of 2.19 vanishes due to the orthonormality of the $\{\phi_i\}$

The first two terms of equation 2.19 become, by analogy to equation 2.15

$$\sum_{i=1}^m \overline{[\alpha_i(\omega) - \alpha'_i(\omega)]^2} + \sum_{j=m+1}^{\infty} \overline{\alpha_j^2(\omega)} \quad 2.20$$

Now, using equations 2.20 and 2.17 to rewrite equation 2.14

$$\sum_{i=m+1}^{\infty} \overline{\alpha_i^2(\omega)} < \sum_{j=m+1}^{\infty} \overline{\alpha_j^2(\omega)} + \sum_{i=1}^m \overline{[\alpha_i(\omega) - \alpha'_i(\omega)]^2} \quad 2.21$$

Equation 2.21 holds true whenever $\alpha'_i(\omega) \neq \alpha_i(\omega)$ and the assertion is proved. Therefore the optimal coefficients for an m-term K-L expansion are the $\{\alpha_i(\omega)\}$ given by equation 2.13.

The integrand of the global cost of equation 2.9 can now be expanded and the orthonormality of the basis functions and equation 2.13 for the $\{\alpha_i^*(\omega)\}$ used to obtain:

$$J_{\epsilon} = \mathcal{E} \left\{ \int_0^T x^2(t, \omega) w(t) dt - \sum_{i=1}^m [\alpha_i^*(\omega)]^2 \right\} \quad 2.22$$

Substitute for $\alpha_i^*(\omega)$ from equation 2.13 to obtain

$$J_{\epsilon} = \int_0^T x^2(t, \omega) w(t) dt - \sum_{i=1}^m \mathcal{E} \left\{ \int_0^T x(t, \omega) w(t) \phi_i(t) dt \right\}^2 \quad 2.23$$

But, by definition, $\mathcal{E}\{x(t, \omega) x(t', \omega)\} = R(t, t')$. Thus

$$J_{\epsilon} = \int_0^T R(t, t) w(t) dt - \sum_{i=1}^m \int_0^T \int_0^T R(t, t') w(t) w(t') \phi_i(t) \phi_i(t') dt dt' \quad 2.24$$

Now it remains to minimize J_{ϵ} over the set of $\{\phi_i\}$ subject to the constraints of equation 2.7.

2.4 Optimization for the Basis-Functions.

The following problem must be solved:

$$J_{\epsilon}^* = \underset{\{\phi_i\}}{\text{Min}} J_{\epsilon}(\{\alpha_i(\omega)\}, \{\phi_i(t)\} | m) \quad 2.25$$

such that

$$\int_0^T \phi_i(t) w(t) \phi_j(t) dt = \delta_{ij} \quad 2.26$$

Dynamic programming [21] is used for this minimization.

Define:

$$J_m(\alpha^*, \phi^*) = \text{Min}_{\phi_1 \dots \phi_m} J_m(\alpha^*, \phi) = \text{Min}_{\phi_m} J_{m-1}(\alpha^*, \phi^*) \quad 2.27$$

Equation 2.27 is a recursion relation for the minimal cost (with appropriately simplified notation) where the recursion is on the index m indicating the number of basis functions used. This minimization must be carried out using the constraints of equation 2.26 which are adjoined to the cost using Lagrange multipliers.

Consider using one basis function. From equation 2.24

$$J_1(\alpha^*, \phi) = \int_0^T R(t,t) w(t) dt - \int_0^T \int_0^T \phi_1(t) w(t) R(t,t') w(t') \phi_1(t') dt dt' + \lambda_1 \left\{ \int_0^T \phi_1(t) w(t) \phi_1(t) dt - 1 \right\} \quad 2.28$$

Then set

$$\frac{\partial J_1(\alpha^*, \phi)}{\partial \phi_1(t)} = 0 \quad 2.29$$

which yields

$$\int_0^T R(t, t') w(t) w(t') \phi_1(t') dt = \lambda_1 w(t) \phi_1(t) \quad t \in [0, T] \quad 2.30$$

Since $w(t) \neq 0$ identically on $[0, T]$, it must be that

$$\int_0^T R(t, t') w(t') \phi_1(t') dt' = \lambda_1 \phi_1(t) \quad t \in [0, T] \quad 2.31$$

Rewriting equation 2.28

$$\begin{aligned} J_1(\alpha^*, \phi) = & \int_0^T R(t, t) w(t) dt - \int_{t=0}^T \phi_1(t) \left\{ \int_{t'=0}^T R(t, t') w(t') \phi_1(t') dt' \right\} w(t) dt \\ & + \lambda_1 \left\{ \int_0^T \phi_1(t) w(t) \phi_1(t) dt - 1 \right\} \end{aligned} \quad 2.32$$

The inner integral in the second term of equation 2.32 becomes, using equation 2.31, simply $\lambda_1 \phi_1(t)$. Then that second term reduces to λ_1 due to the normalization of $\phi_1(t)$. The last term of equation 2.32 is cancelled since $\phi_1(t)$ satisfies the constraint.

Thus

$$J_1(\alpha^*, \phi^*) = \int_0^T R(t, t) w(t) dt - \lambda_1^* \quad 2.33$$

Clearly λ_1^* must be the maximum eigenvalue of the integral equation of 2.31 since this will minimize J_1 .

The next stage is to look for $\phi_2^*(t)$. Clearly:

$$J_2(\alpha^*, \phi) = J_1(\alpha^*, \phi^*) - \int_0^T \int_0^T \phi_2(t) w(t) R(t, t') w(t') \phi_2(t') dt dt' \quad 2.34$$

The following optimization is required:

$$\begin{aligned} J_2(\alpha^*, \phi^*) &= \text{Min}_{\phi_2} J_2(\alpha^*, \phi) \\ &= \text{Min}_{\phi_2} \left[J_1(\alpha^*, \phi^*) - \int_0^T \int_0^T \phi_2(t) w(t) R(t, t') w(t') \phi_2(t') dt dt' \right. \\ &\quad \left. + \lambda_2 \left\{ \int_0^T \phi_2(t) w(t) \phi_2(t) dt - 1 \right\} \right] \end{aligned}$$

2.35

Setting

$$\frac{\partial J_2(\alpha^*, \phi)}{\partial \phi_2(t)} = 0 \quad 2.36$$

the integral equation of 2.31 is again obtained

$$\int_0^T R(t, t') w(t') \phi_2(t') dt' = \lambda_2 \phi_2(t) \quad t \in [0, T] \quad 2.37$$

Note that the constraints of equation 2.29 are satisfied when $\phi_2(t)$ is normalized because ϕ_1 and ϕ_2 are eigenfunctions of a symmetric operator, and are therefore already orthogonal. Substituting from equation 2.37 into equation 2.35,

$$J_2(\alpha^*, \phi^*) = J_1(\alpha^*, \phi^*) - \lambda_2^* \quad 2.38$$

where λ_2^* must be the second largest eigenvalue of equation 2.31 or 2.37 in order to minimize J_2 .

Proceeding in this manner it is concluded that if the eigenvalues of the integral equation of 2.31 are ordered monotonically as

$$\lambda_1^* > \lambda_2^* > \dots > \lambda_m^* \quad 2.39$$

then the optimal basis function $\phi_k^*(t)$ is the eigenfunction corresponding to λ_k^* . Therefore the K-L expansion of equations 2.4 and 2.5 has been derived from L_2 global-error minimization using a linear expansion with m-terms.

Finally, Mercer's theorem [19] can be invoked to rewrite the optimal cost. By this theorem

$$R(t, t') = \sum_{i=1}^{\infty} \lambda_i \phi_i(t) \phi_i(t') \quad t, t' \in [0, T] \quad 2.40$$

Hence

$$R(t, t) = \sum_{i=1}^{\infty} \lambda_i \phi_i^2(t) \quad t \in [0, T] \quad 2.41$$

Therefore

$$\int_0^T R(t, t) w(t) dt = \sum_{i=1}^{\infty} \lambda_i \int_0^T \phi_i(t) w(t) \phi_i(t) dt = \sum_{i=1}^{\infty} \lambda_i \quad 2.42$$

Thus the optimal cost using m features is:

$$J_m(\alpha^*, \phi^*) = \sum_{i=m+1}^{\infty} \lambda_i \quad 2.43$$

or in terms of the expected energy of the process $x(t, \cdot)$ this can be restated as:

$$J_m(\alpha^*, \phi^*) = \int_0^T R(t, t) w(t) dt - \sum_{i=1}^m \lambda_i \quad 2.44$$

2.5 Asymptotic Statistical Analysis for Large Data-Bases

2.5.1 Introduction

In practical applications of K-L methods, the discrete case is usually considered. The process $x(t, \cdot)$ is sampled in time and replaced by an n -dimensional vector random variable \underline{x} . The integral equation with the covariance kernel of equation 2.31 is then replaced by the following matrix equation:

$$R^0 \underline{\phi}_j = \lambda_j \underline{\phi}_j \quad j = 1, 2, \dots, n \quad 2.45$$

where

$$R^0 = \mathcal{E} (\underline{x} - \bar{\underline{x}})(\underline{x} - \bar{\underline{x}})^T \quad 2.46$$

with $\bar{\underline{x}} = E(\underline{x})$. Here λ_j and $\underline{\phi}_j$ are the j -th eigenvalue and eigenvector of the covariance matrix R^0 respectively. The Fredholm integral equation problem for the K-L basis functions is therefore transformed into a matrix eigenvalue-eigenvector problem.

In practice the covariance matrix of the n-dimensional random vector \underline{x} is usually not available. Instead, a data-base of sample vectors \underline{x}^i must be used to derive the required ensemble information. Normally, an estimated covariance matrix \hat{R}_p is obtained using the sample-mean of outer products $\{(\underline{x} - \bar{\underline{x}})(\underline{x} - \bar{\underline{x}})^T\}$, and the eigenvectors of this estimated covariance matrix are used as the (estimated) K-L basis functions.

$$\hat{R}_p = \frac{1}{p-1} \sum_{i=1}^p (\underline{x}^i - \bar{\underline{x}}_p)(\underline{x}^i - \bar{\underline{x}}_p)^T = \frac{1}{p-1} \sum_{i=1}^p R^i \quad 2.47$$

The data-base available is assumed to be the set

$$\{\underline{x}^i \mid i=1, 2, \dots, p\} \quad 2.48$$

with each \underline{x}^i representing a particular sample vector from the n-dimensional distribution for \underline{x} . In equation 2.47, $\bar{\underline{x}}_p$ denotes the sample-mean of \underline{x} , and R^i is as given below

$$\bar{\underline{x}}_p = \frac{1}{p} \sum_{i=1}^p \underline{x}^i ; \quad R_i = (\underline{x}^i - \bar{\underline{x}}_p)(\underline{x}^i - \bar{\underline{x}}_p)^T \quad 2.49$$

Note that \hat{R}_p is therefore an estimate of R^o which is derived solely from the data-base. The reason for using (p-1) as the divisor in equation 2.47 rather than p is to make $E(\hat{R}_p)$ exactly equal to R^o , that is, to make \hat{R}_p an unbiased estimator of R^o [22].].

Assuming that the original process $x(t, \cdot)$ possesses fourth order moments, the $\frac{n(n+1)}{2}$ upper diagonal entries of the symmetric random matrix \hat{R}_p will form a k-dimensional distribution $\left(k = \frac{n(n+1)}{2}\right)$ with finite mean $\underline{\mu}$ and positive definite covariance matrix $\{\sigma_{qt}\}$ $q, t = 1, \dots, k$. That is,

define

$$\mathcal{E}(\hat{R}_p)_{lm} = (R^o)_{lm} = (\mu)_s ; \quad \mathcal{E}(\hat{r}_p - \mu)(\hat{r}_p - \mu)^T = \{\sigma_{qt}\} \quad 2.50$$

Here it is assumed that the matrix \hat{R}_p is expressed as a k-dimensional vector \hat{r}_p . The element l,m of \hat{R}_p corresponds to the component s of r_p . The matrix $\{\sigma_{qt}\}$ involves joint fourth-order moments of the components of the original vector x .

As the data-base size increases, the sample-mean estimators \tilde{x}_p and \hat{R}_p can be updated to include new information on the underlying process $x(t, \cdot)$. Then the estimated K-L basis functions should also be updated; they will be the eigenvectors of the updated covariance estimate \hat{R}_p . Since the optimality properties of the K-L method depend on choosing the optimal basis (which in practice can only be estimated using a finite data-base), it is of interest here to analyze the asymptotic behavior of practical K-L schemes as the data base becomes large.

2.5.2 Estimated Eigenvalue Behavior

The eigenvalues of the random matrix \hat{R}_p themselves are random variables. Define the random variable $\lambda_j(\hat{r}_p)$ as the j-th eigenvalue of \hat{R}_p . λ_j is a function from \mathbb{R}^k into \mathbb{R}^1 , i.e.

$$\lambda_j : \mathbb{R}^k \rightarrow \mathbb{R}^1 \quad 2.51$$

It is now shown that $\lambda_j(r)$ possesses first derivatives, $\frac{\partial \lambda_j(r)}{\partial r_s}$ $s=1, \dots, k$, at all points in some neighborhood of $r = \mu$.

A well-known result [23] relates the differential change in a matrix to the differential change in its eigenvalues. If $d\lambda_j$ denotes the differential change in the j -th eigenvalue of a symmetrical matrix A when the matrix changes by dA , and \underline{v}_j denotes the j -th (right and left) eigenvector of A then the result is:

$$d\lambda_j = \underline{v}_j^T dA \underline{v}_j \quad 2.52$$

If only the entry l,m of A changes by $(dA)_{l,m}$ then the resulting change in λ_j is

$$d\lambda_j = (\underline{v}_j)_l \cdot (\underline{v}_j)_m \cdot (dA)_{lm} \quad 2.53$$

where the scalars $(\underline{v}_j)_l$ and $(\underline{v}_j)_m$ denote respectively the l -th and m -th components of the eigenvector \underline{v}_j . Hence it is concluded that in the problem considered here,

$$\left. \frac{\partial \lambda_j}{\partial (\underline{r})_s} \right|_{\underline{r} = \hat{\underline{r}}_p} = (\underline{\phi}_j)_l \cdot (\underline{\phi}_j)_m \quad 2.54$$

where the scalars $(\underline{\phi}_j)_l$ and $(\underline{\phi}_j)_m$ denote respectively the l -th and m -th components of the j -th eigenvector of the estimated covariance matrix \hat{R}_p . The index s refers to the component of the vector form \underline{r} that corresponds

to the entry ℓ, m of the matrix form R .

It is clear that $\frac{\partial \lambda_j}{\partial (r)_s}$ is well-behaved in some neighborhood of $\underline{r} = \underline{\mu}$. (It has been assumed that $\underline{\mu}$ exists and is finite; therefore the eigenvectors $\{\phi_j\}$ corresponding to $\underline{\mu}$, or R^0 , will be well-behaved). It is also clear that not all of $\frac{\partial \lambda_j(r)}{\partial (r)_s}$ $s = 1, \dots, k$ can vanish so that, for at least some s and some j , $\frac{\partial \lambda_j(r)}{\partial (r)_s} \neq 0$.

This is obvious since changing some element of the true covariance matrix R^0 will definitely change at least one eigenvalue. For example, changing a diagonal element will change the trace which is the sum of eigenvalues. Therefore at least one eigenvalue must change.

At this point a theorem by Wilks [22] can be applied to determine the asymptotic behavior of $\lambda_j(\hat{r}_p)$ as $p \rightarrow \infty$. This theorem is stated below using the notation developed in this section:

Theorem: Suppose $\{r^i \mid i = 1, 2, \dots, p\}$ is a sample from a k -dimensional distribution with finite mean $\underline{\mu}$ and positive definite covariance matrix $\{\sigma_{qt}\}$, $q, t = 1, \dots, k$. Let $\lambda_j(r)$ be a function which possesses first derivatives $\frac{\partial \lambda_j(r)}{\partial (r)_s} = g_s$, say, $s = 1, \dots, k$ at all points in some neighborhood of $\underline{\mu}$, and let $g_s^0 \triangleq g_s(\underline{\mu})$. Then if at least one of the g_s^0 is $\neq 0$, then $\lambda_j(\hat{r}_p)$ has the asymptotic gaussian distribution:

$$\mathcal{N}(\lambda_j(\underline{\mu}), \frac{1}{p} \sum_{q,t=1}^k \sigma_{qt} g_q^0 g_t^0)$$

Therefore the eigenvalues of the K-L methods used in practice are asymptotically gaussian random variables with means which correspond exactly to the eigenvalues of the true covariance matrix R^0 and variances which depend on the joint

fourth-moments of the random vector \underline{x} , but converge to zero at the rate of $\left(\frac{1}{p}\right)$, where p is the size of the data-base.

No special assumptions are imposed on the process $x(\underline{t}, \cdot)$ to which the K-L method is applied except that it should possess fourth-order moments. Fukunaga derives equivalent results in [10] but does not consider the asymptotic normality of the eigenvalue estimates.

2.5.3 Estimated Expected Error Behavior

It is now of interest to observe the expected error for a truncated K-L expansion with m -terms, when the K-L functions are estimated using the sample statistics. The expected error is now a random variable dependent on the size of the data base used to estimate the K-L expansion basis functions. The actual expected error for an m -term discrete expansion is:

$$\epsilon_m = \sum_{j=m+1}^n \lambda_j(\underline{\mu}) \quad 2.55$$

where $\{\lambda_j(\underline{\mu})\}$ are the eigenvalues of the true covariance matrix R° (recall that $\underline{\mu}$ denotes the vector form for R°).

Now let

$$(\hat{\epsilon}_m)_p = \sum_{j=m+1}^n \lambda_j(\hat{\underline{r}}_p) \quad 2.56$$

be the expected error using m terms of a K-L basis estimated from a data-base of size p

$$\lim_{p \rightarrow \infty} (\hat{\epsilon}_m)_p = \epsilon_m \quad 2.57$$

$(\hat{\epsilon}_m)_n$ is a random variable which converges to the expected error for an m-th order true K-L expansion as the size of the data base increases to infinity. The behavior of $(\hat{\epsilon}_m)_\rho$ can be analyzed to determine the sensitivity of the K-L approach to the size of the data base. $(\hat{\epsilon}_m)_\rho$ is a r.v. obtained by summing asymptotically normal r.v.'s, the eigenvalues. Since the eigenvalues are not jointly normal it cannot be concluded that $(\hat{\epsilon}_m)_\rho$ is normal. $(\hat{\epsilon}_m)_\rho$ is, however, unbiased.

$$\mathcal{E} (\hat{\epsilon}_m)_\rho = \mathcal{E} \sum_{j=m+1}^n \lambda_j(\hat{r}_\rho) = \sum_{j=m+1}^n \lambda_j(\underline{\mu}) = \epsilon_m \quad 2.58$$

and

$$\text{var} [(\hat{\epsilon}_m)_\rho] = \mathcal{E} \sum_{j=m+1}^n [\lambda_j(\hat{r}_\rho) - \lambda_j(\underline{\mu})]^2 \quad 2.59$$

The λ_j 's are not uncorrelated and hence the above cannot be easily simplified. To advance further a result on the joint density of $\lambda_1, \lambda_2, \dots, \lambda_m$ is needed.

Dyson [16], [24], and others [24,25] have studied correlations between eigenvalues of a random symmetric matrix in the context of statistical theories of nuclear spectroscopy. Dyson [16] has derived a complete, general result concerning the joint distribution of a finite stretch of eigenvalues. $\lambda_1, \lambda_2, \dots, \lambda_m$ of a random Hermitian matrix of order $n \gg m$, in the limit as the order of the matrix, n , tends to infinity. The results obtained involve only trigonometric functions of eigenvalue differences and

a quantity D , denoting the mean level-spacing of the eigenvalue series. For the real symmetric case, the joint density function of m -eigenvalues, in the limit $n \rightarrow \infty$, is

$$f_m(\lambda_1, \lambda_2, \dots, \lambda_m) = \frac{1}{D^m} Q \text{Det} \left[\sigma \left(\frac{\lambda_i - \lambda_j}{D} \right) \right]_{i,j=1, \dots, m} \quad 2.60$$

where

$$\sigma(x) = \begin{pmatrix} s(x) & s'(x) \\ \int_0^x s(x') dx' - u(x) & s(x) \end{pmatrix} \quad 2.61$$

with

$$s(x) = \frac{\sin \pi x}{\pi x} \quad u(x) = \begin{cases} \frac{1}{2} & x > 0 \\ 0 & x = 0 \\ -\frac{1}{2} & x < 0 \end{cases} \quad 2.62$$

$$s'(x) = \frac{ds(x)}{dx}$$

and $Q \text{Det } M$ is the quaternion-determinant for the matrix M of quaternions.

The elements of the $n \times n$ matrix M are themselves 2×2 matrices called quaternions. Then, by definition,

$$Q \text{Det } M = \sum_P (-1)^{n-l} \prod_1^l \frac{\text{tr}}{2} (M_{ab} M_{bc} \dots M_{sa}) \quad 2.63$$

whenever M is self-dual, that is

$$M_{ji} = M_{ij} \quad 2.64$$

P in equation 2.63 is any permutation of the integers $(1, 2, \dots, n)$ consisting of l cycles of the form

$$(a \rightarrow b \rightarrow c \rightarrow \dots \rightarrow s \rightarrow a) \quad 2.65$$

and $(-1)^{n-l}$ is the parity of P .

As a special case, note that

$$f_2(\lambda_1, \lambda_2) = \frac{1}{D^2} \left\{ 1 - s^2(x) + s'(x) \left(\int_0^x s(x') dx' - u(x) \right) \right\} \quad 2.66$$

where $x = \left(\frac{\lambda_1 - \lambda_2}{D} \right)$

Dyson's results can be applied to the K-L problem if the order of the covariance matrix is taken to be very large; i.e. if a very high time-sampling rate is used. Then the joint distribution of any finite set of m eigenvalues for the random matrix \hat{R}_p becomes available for any p (size of data base).

Rewriting equation 2.56

$$(\hat{E}_m)_p = \text{tr}(\hat{R}_p) - \sum_{j=1}^m \lambda_j(\hat{r}_p) \quad 2.67$$

If it is assumed that the expected energy in the process is known or estimated accurately a priori, then a modified expected error can be defined as

$$(\hat{E}_m)'_p = \bar{E} - \sum_{j=1}^m \lambda_j(\hat{r}_p) \quad 2.68$$

where \bar{E} is a known constant, the expected energy in the process, and does not depend on p , the size of the data-base. Then Dyson's result for the finite stretch of eigenvalues $\lambda_1, \dots, \lambda_m$ of the large random matrix \hat{R}_p can be applied to get the distribution function for $(\hat{E}_m)'_p$

$$\text{Prob.}((\hat{E}_m)'_p < E_m) = \text{Prob.}(\bar{E} - \sum_{j=1}^m \lambda_j < E_m) = \text{Prob.}(\sum_{j=1}^m \lambda_j > \bar{E} - E_m)$$

2.69

$$\text{Prob.}((\hat{\epsilon}_m)'_\rho < E_m) = \int_{\lambda_m = \bar{E} - E_m}^{\infty} \dots \int_{\lambda_2 = \bar{E} - E_m - \lambda_3 - \dots - \lambda_m}^{\infty} \int_{\lambda_1 = \bar{E} - E_m - \lambda_2 - \dots - \lambda_m}^{\infty} (\lambda_1 + \lambda_2 + \dots + \lambda_m) f_{\lambda_1, \dots, \lambda_m} d\lambda_1 \dots d\lambda_m$$

2.70

where $f_{\lambda_1, \dots, \lambda_m}$ is given by equation 2.60.

Dyson's result is well adapted for numerical computations and thus the distribution function for $(\hat{\epsilon}_m)'_\rho$ can be calculated exactly using numerical techniques.

It is, in general, difficult to discuss the behavior of the probability of the density function of $(\hat{\epsilon}_m)_\rho$ for arbitrary processes and data bases. However, it is expected that for data bases with randomly selected data, the density function for the expected error will behave as shown in Fig. 2.1. Note that $f((\hat{\epsilon}_m)_\rho)$ is skewed since the probability that $(\hat{\epsilon}_m)_\rho$ is less than zero is identically zero for any ρ ; i.e. the error can never be negative. If the density function is unimodal and otherwise well behaved, the likelihood of the expected error $(\hat{\epsilon}_m)_\rho$ being less than the true rate is higher than the likelihood of its being greater than the true expected error. This implies that the expected error is more likely to be underestimated for any fixed m and finite data base.

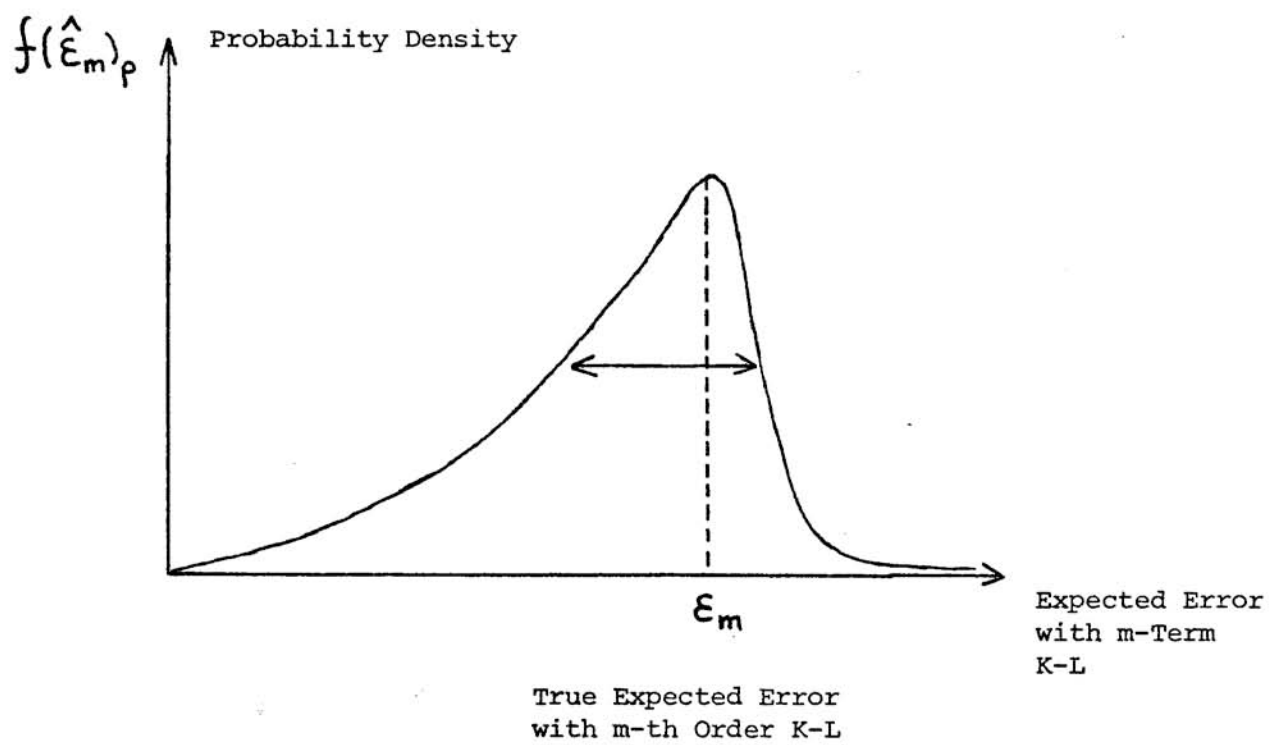


Figure 2.1: Probability Density Function for Finite Data-Base Expected Error of m-Term K-L Expansion.

CHAPTER 3

PIECEWISE POLYNOMIAL APPROXIMATION WITH OPTIMAL KNOTS

3.1 Introduction.

Piecewise polynomial approximation is a subject that has received considerable attention from the mathematical viewpoint only recently. Schoenberg [26] first studied an important subclass of piecewise polynomials, the spline functions, in 1946, and these became the object of intensive research ever since [27,28]. Spline functions are piecewise polynomial functions of m -th degree joined smoothly (at points called knots) so as to have $(m-1)$ continuous derivatives; i.e. the only discontinuity allowed is for the n -th derivative at the knots. Piecewise polynomials are polynomials of m -th degree which are not necessarily smooth across knots (so called deficient splines where knots are allowed a multiplicity $k \leq m$ encompass piecewise polynomials).

When the knots are given, piecewise polynomial and spline approximations are linear in the parameters and approximations are relatively easy to compute. Fixed knot splines and piecewise polynomials have been extensively studied and the theory is well developed and documented for this class of approximation functions (see [29,30]).

It has more recently become clear, however, that the real advantages to splines lie in the possibility to have the knots as variables. This makes them nonlinear approximating functions with a nonlinearity not encountered previously in approximation theory.

Piecewise approximation, as with spline functions, is an approach ideally suited for practical applications. Ordinary polynomials or other (global) functions are inadequate in many situations that arise from the physical rather than the mathematical world. Functions (or data) which express physical relationships are often of a disjointed or disassociated nature and their behavior in one region may be unrelated to their behavior in another region. Global polynomials along with most other smooth global functions have just the opposite property: namely, their behavior in any infinitesimal region determines their behavior everywhere. For example, analytic functions are determined everywhere via Taylor's expansion by the value of the function and all its derivatives at one point. Piecewise polynomials and therefore splines do not suffer this drawback and can be adapted to the functions represented on a local basis. The approximation power of spline functions and, more generally, piecewise polynomial functions, therefore, seems to lie precisely in the possibility of placing the knots in a usually quite non-uniform way to suit the peculiarities of the given function. It being a somewhat nasty nonlinear minimization problem, no satisfactory characterization of a best approximation has been found in general, see e.g. Braess [31] for the case of Chebyshev approximation.

De Boor and Rice [32], De Boor [33], Burchard [34], Schumaker [35], and McClure [36] have worked on the problem of variable-knot splines and their results indicate that approximation with optimal knots is much superior to fixed knot splines. The computational algorithms developed by researchers in the field of variable-knot splines are all based on some descent method (Esch, Eastman [4], De Boor and Rice [32], Dodson [37]) and therefore suffer from the following serious shortcomings.

- (i) Only locally best approximations can be obtained.
- (ii) Initial conditions on knot locations are important for convergence of algorithms.
- (iii) Computational time is quite high.
- (iv) Conjectures and ad hoc schemes are used for optimization (see Rice [3] and Schumaker [28]).

In this chapter piecewise polynomial approximation is considered from the perspective of representing individual sample-functions from a second order vector random process over a finite interval $[0,T]$ of the real line. The starting point for the results of this chapter is Bellman's paper [38] on the approximation of curves by line segments. Bellman's formulation is extended in the following ways:

- (i) The general case of piecewise polynomials with various continuity constraints at the variable knots is considered.
- (ii) The problem for the Chebyshev norm is formulated and considered.
- (iii) An ensemble cost functional is considered for the case of ensemble-optimal knot locations.

The methods developed in this chapter produce globally optimal best knots with computational times comparable to those required by the local descent algorithms mentioned. The development in this chapter forms a basis for the extensions and results of the next chapter where the approximating functions in each interval as well as the knots are selected in an ensemble sense. Moreover the dynamic programming approach to variable-knot splines is also novel.

Obtaining error bounds for the representations formulated here is a difficult problem. Some of the bounds developed in the field of fixed-knot and variable-knot spline theory are adapted to the present formulations, and the limitations of these bounds are discussed.

3.2 Formulation of Approximation Problem.

3.2.1 Introduction

The problem considered is that of polynomial approximation over variable segments of the waveforms. The problem can be visualized as in Figure 3.1. Consider for simplicity the problem of approximating a scalar process; the generalization to the vector case is straightforward. Let $x(t, \omega)$ denote the ω -th sample function over the fixed time interval $0 \leq t \leq T$ and consider segmenting this interval into N regions delimited by the set of knots Π

$$\Pi = \{0, T_1, T_2, \dots, T_{N-1}, T\} \quad 3.1$$

Let $\hat{x}_j(t, \omega)$ denote the approximation to $x(t, \omega)$ over the segment $[T_{j-1}, T_j]$, $j = 1, \dots, N$ (Define $T_0 = 0$ and $T_N = T$). Within each interval between knots the data $x(t, \omega)$ is approximated by a finite order polynomial the coefficients of which must be determined. The $N-1$ interior knots themselves are free, and optimal locations for them must be determined. Various constraints can be imposed on the estimate at the knots (exact fit of function and up to $(m-1)$ st derivatives if m -th order polynomials are used). The parameters of the estimate will therefore be the locations of the optimal knots and the coefficients of the polynomials used for approximation between knots.

There are two possibilities with respect to the knots, which are to determine

- (i) A set of optimal knot locations over the ensemble of waveforms: the ensemble-based problem.
- (ii) Optimal knot locations for each sample waveform: the sample-based problem.

In the first alternative the knot locations are determined once for the entire population and therefore do not form part of the set of features needed to characterize any single sample waveform. The optimal ensemble knots are then analogous to KL basis functions in this sense. They form a canonical basis for segmenting and representing the process. The second alternative, in the case of feature extraction, is computationally much more demanding since this operation has to be performed on-line. In the next chapter it will be shown how the approach taken here for the knots can be extended to the more general case of knots and approximating functions.

The approximation (or representation) problem is considered for the L_p , $1 \leq p < \infty$, and the Chebyshev, $p = \infty$, norms separately. In practice the L_2 and the Chebyshev norms are the most useful ones and therefore examples will be worked out for these cases. The case of the Chebyshev norm is not simply the extension of the L_p norm case and therefore requires independent consideration.

Various variants of the basic formulation can be considered depending on the desired behavior at the knots. In the simplest case no constraints on the representation at the knots are imposed. Another

possibility is to require an exact fit at the knots thereby assuring continuity of the representation. In this case the approximation becomes an interpolation with free knots. Assuming that derivatives of the data are available, yet another variant is to require the representation to fit the data and its derivatives, up to the $(k-1)$ st, at the knots (for k -th order piecewise polynomials).

For the problem to be soluble with the methods of this chapter, the essential requisite is that the estimate $\hat{x}_j(t, \omega)$ in the region $[T_{j-1}, T_j]$ be computable (expressible) solely based on the data (and possibly its derivatives in the region $[T_{j-1}, T_j]$). For the problem to separate recursively the estimate $\hat{x}_j(t, \omega)$ should not depend on parameters or data outside segment j . Hence it cannot be required, for example, that $\hat{x}_j^{(n)}(T_j, \omega) = \hat{x}_{j+1}^{(n)}(T_j, \omega)$, $n=0, 1, \dots$, without specifying further that $\hat{x}_j^{(n)}(T_j, \omega) = x^{(n)}(T_j, \omega)$. The estimates in each segment must be decoupled and independent. This requirement is in line with the philosophy and need for local approximation discussed earlier.

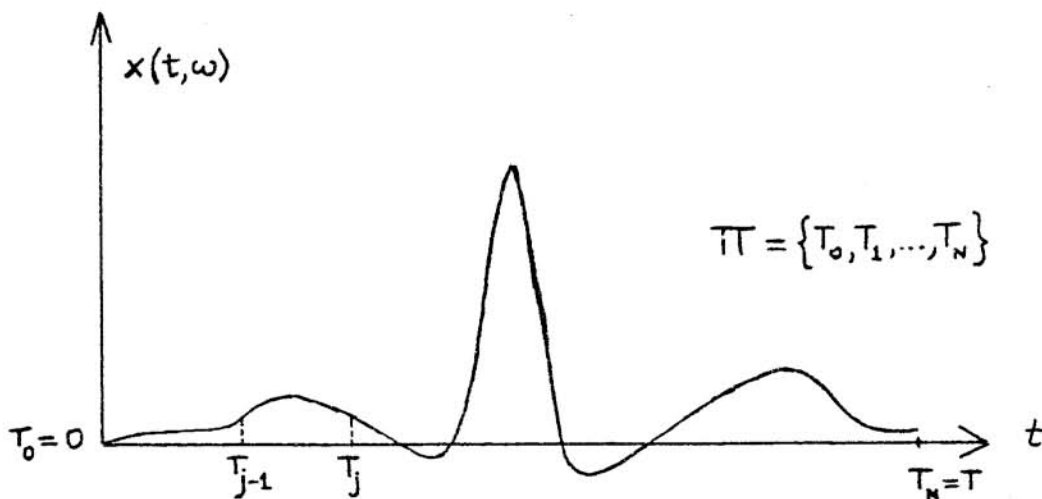


Figure 3.1: Segmentation of Waveform via Knots

3.2.2 The L_p -Case.

The general L_p ($1 \leq p < \infty$) global cost functional appropriate for this class of problems is

$$J_{p,N}(\Pi) = \mathcal{E} \sum_{j=1}^N \mathcal{J}_p^*(T_{j-1}, T_j, \omega) \quad 3.2$$

where the optimal L_p segment cost for sample-function ω is

$$\mathcal{J}_p^*(T_{j-1}, T_j, \omega) = \text{Min}_{\underline{\alpha}_j(\omega) \in A_j(\omega)} \left\{ \int_{T_{j-1}}^{T_j} |e(\underline{\alpha}_j, t, \omega)|^p dt \right\}^{1/p} \quad 3.3$$

and the pointwise approximation error is

$$e(\underline{\alpha}_j, t, \omega) = x(t, \omega) - \hat{x}_j(t, \omega) \quad \begin{matrix} T_{j-1} \leq t \leq T_j \\ j = 1, 2, \dots, N \end{matrix} \quad 3.4$$

with the estimate in segment j given by

$$\hat{x}_j(t, \omega) = \sum_{i=0}^m \alpha_{ij}(\omega) t^i \quad \begin{matrix} T_{j-1} \leq t \leq T_j \\ j = 1, 2, \dots, N \end{matrix} \quad 3.5$$

The coefficient vector $\underline{\alpha}_j(\omega)$ is formed of the set $\{\alpha_{ij}(\omega) \mid i=1, \dots, m\}$

where $m \geq 1$ is the order of polynomials used in each segment. The constraint set $A_j(\omega)$ to which $\underline{\alpha}_j(\omega)$ is restricted accounts for any special conditions that may be imposed on the approximation of sample-function ω over segment j (e.g. exact fit at knots, exact fit of derivatives at knots, exact fit at midpoint of segment j , etc.).

The expectation operation in equation 3.2 is defined by

$$\mathbb{E} f(x(t,\omega)) = \int_{\Gamma} f(x(t,\omega)) dP(x(t,\omega)) \quad 3.6$$

where $dP(x)$ denotes the Lebesgue probability measure for the process $x(t,\cdot)$

The expectation of equation 3.2 can be taken over the complete sample-space. In that case $\Gamma = \Omega$, the underlying sample-space for the stochastic process, and the approximation problem becomes an ensemble-based one.

The second alternative of interest is when $\Gamma = \omega_p$, where ω_p refers to one particular sample-function. In that case the expectation operation is trivial and the approximation problem becomes a sample-based deterministic one.

The partition Π consists of N segments and is defined by equation 3.1. The problem is to minimize $J_{p,N}(\Pi)$ over the set of all possible partitions of the interval

In practice the computation of the expected value of equation 3.2 over the sample space Ω is not possible since the probability density function of $x(t,\cdot)$ is usually not available. However in most statistical problems of interest a large data base of sample-functions will be available; i.e. a set $\{x(t,\omega) \mid \omega = 1, 2, \dots, P\}$ where P , the total number of samples in the population, is large. In such a problem, when $\Gamma = \Omega$ $\mathbb{E} J_p^*(T_{j-1}, T_j, \omega)$ can be replaced by the sample mean $\frac{1}{P} \sum_{\omega=1}^P J_p^*(T_{j-1}, T_j, \omega)$ in computations. In any case the summands of equation 3.2 must be evaluated, or approximated, numerically in any real application. The application of this approach to the cardiographic problem, discussed in

Chapter 5, has shown its use and practical feasibility.

3.2.3 The Chebyshev Case.

The Chebyshev (L_∞) global cost functional appropriate for this class of problems is

$$J_{\infty, N}(\Pi) = \text{Max}_{\omega \in \Gamma} \text{Max}_{1 \leq j \leq N} J_{\infty}^*(T_{j-1}, T_j, \omega) \quad 3.7$$

where the optimal L_∞ segment cost is

$$J_{\infty}^*(T_{j-1}, T_j, \omega) = \text{Min}_{\alpha_j(\omega) \in A_j(\omega)} \text{Max}_{T_{j-1} \leq t \leq T_j} |e(\alpha_j, t, \omega)| \quad 3.8$$

The pointwise error $e(\alpha_j, t, \omega)$ and the estimate in segment j are given by equations 3.4 and 3.5 respectively. Since the powers of t form a Chebyshev set this problem will have a solution for any interval (see [1]). Sophisticated algorithms for Chebyshev approximation by polynomials over discrete (finite) point sets are available [28]. For continuous problems the De La Vallee Poussin algorithm [1] can be used to obtain the optimal estimate.

The constraint set $A_j(\omega)$ and the two alternatives of interest for Γ are defined as for the L_p -case section 3.2.2. The problem, as for the L_p case, is to minimize $J_{\infty, N}(\Pi)$ over the set of all possible partitions of the interval $[0, T]$.

In practice the maximization over the sample-space Ω for the ensemble-based problem cannot be carried out due to limited information on the statistics of the stochastic process $x(t, \cdot)$. Assuming that a finite, denumerable set of sample functions is available, as discussed for the L_p case, a finite search can be carried out. The application of this approach

to the cardiographic problem is discussed in Chapter 5.

3.2.4 Constrained Approximations.

The piecewise polynomial approximations formulated can be required to satisfy various constraints at the knots. For the unconstrained case a discontinuous representation with jumps at knots will result. This may or may not be desirable from the point of view of representation. As mentioned earlier, a number of variants can be formulated to control the behavior at knots. Any set of constraints relating the actual data and the piecewise estimate in segment j is allowed, provided the estimate in segment j depends solely on data over segment j .

For the linear L_2 sample-based approximation (polynomials of degree $m = 1$) the following problem must be solved

$$J_{2,N}^* = \underset{T_1, T_2, \dots, T_{N-1}}{\text{Min}} \sum_{j=1}^N \int_{T_{j-1}}^{T_j} [x(t, \omega) - \alpha_{0j}^* - \alpha_{1j}^* t]^2 dt \quad 3.9$$

$$\frac{\partial}{\partial \alpha_{0j}} \int_{T_{j-1}}^{T_j} [x(t, \omega) - \alpha_{0j} - \alpha_{1j} t]^2 dt = 0 \quad 3.10$$

$$\frac{\partial}{\partial \alpha_{1j}} \int_{T_{j-1}}^{T_j} [x(t, \omega) - \alpha_{0j} - \alpha_{1j} t]^2 dt = 0 \quad 3.11$$

$$\alpha_{1j}^* = \frac{1}{(T_j - T_{j-1})^3} \left\{ 12 \int_{T_{j-1}}^{T_j} t x(t, \omega) dt - 6(T_j + T_{j-1}) \int_{T_{j-1}}^{T_j} x(t, \omega) dt \right\}$$

$$\alpha_{0j}^* = \frac{1}{(T_j - T_{j-1})} \int_{T_{j-1}}^{T_j} x(t, \omega) dt - \alpha_{1j}^* \frac{(T_j + T_{j-1})}{2} \quad 3.13$$

For linear segmented approximation we can also require that the line segments fit the data exactly at knots. Then the following constrained estimate is obtained

$$\hat{x}_j(t, \omega) = \frac{x(T_j, \omega) - x(T_{j-1}, \omega)}{(T_j - T_{j-1})} (t - T_{j-1}) + x(T_{j-1}, \omega) \quad T_{j-1} \leq t \leq T_j \quad 3.14$$

If such is the case, then there is no parameter to optimize over and the knot locations, together with the data at the knots, uniquely determine the approximation; the representation is obtained by merely joining the data at the knots with straight lines. This leads to a continuous representation. This case has been studied experimentally for the cardiographic problem, as discussed in Chapter 5.

For a quadratic segmented approximation (polynomials of degree $m = 2$) it can be required that the quadratics fit the data exactly at knots. Then the following must hold for segment j :

$$\begin{aligned} [\alpha_{0j} + \alpha_{1j}t + \alpha_{2j}t^2] \Big|_{t=T_{j-1}} &= x(T_{j-1}, \omega) \triangleq x_{j-1} \\ [\alpha_{0j} + \alpha_{1j}t + \alpha_{2j}t^2] \Big|_{t=T_j} &= x(T_j, \omega) \triangleq x_j \end{aligned} \quad 3.15$$

The constraints of equation 3.15 imply that one of the three coefficients

$\{\alpha_{0j}, \alpha_{1j}, \alpha_{2j}\}$ is free. Solving for α_{0j} and α_{1j} in terms of α_{2j} , for example:

$$\alpha_{0j} = \left(\frac{x_{j-1}T_j - x_jT_{j-1}}{T_j - T_{j-1}} \right) + (T_j T_{j-1}) \alpha_{2j} \quad 3.16$$

$$\alpha_{1j} = \left(\frac{x_j - x_{j-1}}{T_j - T_{j-1}} \right) - (T_j + T_{j-1}) \alpha_{2j}$$

the remaining independent parameter α_{2j} can be optimized by minimizing the appropriate cost over segment j . For the L_2 case the following problem results

$$\text{Min}_{\alpha_{2j}} \left[\int_{T_{j-1}}^{T_j} \left\{ x(t, \omega) - \left(\frac{x_{j-1}T_j - x_jT_{j-1}}{T_j - T_{j-1}} \right) - T_j T_{j-1} \alpha_{2j} - \left(\frac{x_j - x_{j-1}}{T_j - T_{j-1}} \right) t + (T_j + T_{j-1}) \alpha_{2j} t - \alpha_{2j} t^2 \right\}^2 dt \right] \quad 3.17$$

Differentiating with respect to α_{2j} and setting equal to zero

$$\int_{T_{j-1}}^{T_j} \left\{ x(t, \omega) - \left(\frac{x_{j-1}T_j - x_jT_{j-1}}{T_j - T_{j-1}} \right) - T_j T_{j-1} \alpha_{2j} - \left(\frac{x_j - x_{j-1}}{T_j - T_{j-1}} \right) t + (T_j + T_{j-1}) \alpha_{2j} t - \alpha_{2j} t^2 \right\} \{ t(T_j + T_{j-1}) - T_j T_{j-1} - t^2 \} dt = 0$$

3.18

This equation can easily be solved for α_{2j} in terms of data, $x(t, \omega)$, and knots T_{j-1} and T_j .

The following minimization problem must be solved for the case of Chebyshev approximation.

$$\text{Min}_{\alpha_{2j}} \text{Max}_{T_{j-1} \leq t \leq T_j} \left| x(t, \omega) - \left(\frac{x_{j-1}T_j - x_jT_{j-1}}{T_j - T_{j-1}} \right) - \left(\frac{x_j - x_{j-1}}{T_j - T_{j-1}} \right) t - \alpha_{2j} (T_j T_{j-1} + t^2 - (T_j + T_{j-1})t) \right|$$

3.19

This is, in general, a difficult problem. In the discrete case, however, this problem can be solved using available algorithms discussed in [28].

For higher order piecewise polynomials, an exact fit at the knots can still be required. Then the optimization must be carried out over the remaining parameters. It can also be required that the approximation fit the derivatives of the data at the knots. In the cubic case specifying that the approximation fit the data and its first derivative at both ends of every segment leaves no parameters for optimization. In general, due to the difficulties with differentiating data (since all real observations are noisy), it appears that requiring exact fit at the knots and determining the remaining parameters via best fits is more appropriate than fitting derivatives if continuous representations are desired.

By sacrificing smoothness at knots, it is clear that better interior fits can be obtained. The unconstrained minimization for the coefficients will always yield a cost lower than, or at most equal to, the cost incurred for a constrained case. The trade-off of continuity and

smoothness at knots versus cost must be judged for the particular representation problem at hand. It has been shown here that the representation formulated is general enough to allow various degrees of smoothness at knots.

3.3 Determination of Optimal Knots.

3.3.1 Introduction.

The problem of determining optimal knot locations is essential and computationally demanding in general. No satisfactory characterization or computational scheme has been developed by researchers in the relatively new field of variable-knot splines. The first consideration of an optimal segmentation problem is treated in Stone's paper [39]. The problem considered there is the determination of the $2N+2$ constants $a_i, b_i, i=1, \dots, N+1$ and the N points of subdivision T_1, T_2, \dots, T_N so as to minimize the function

$$J(a_1, \dots, a_{N+1}; b_1, \dots, b_{N+1}; T_1, \dots, T_N) = \sum_{j=1}^{N+1} \int_{T_{j-1}}^{T_j} [f(t) - a_j - b_j t]^2 dt \quad 3.20$$

where $T_0 = 0$ and $T_{N+1} = T$ and $T_0 \leq T_1 \leq T_2 \leq \dots \leq T$. The function $f(t)$ is a given function. Stone derives the necessary conditions for minimizing J and shows that the problem has an easy computational solution only when $f(t)$ is a quadratic function. Bellman in [38] suggests a dynamic programming approach to this problem and gives the basic recurrence relation.

In this section the recurrence relation is derived in general and developed to treat the various approximation problems formulated in the previous sections. In particular the Chebyshev norm case is developed and

both the sample-function and ensemble-based knot-determination problems are considered. The solutions obtained are guaranteed to be the globally optimal ones in all cases due to the principle of optimality which underlies the dynamic programming algorithm [21].

Various specific formulations have been tried for the cardiographic problem and have proved the computational tractability and feasibility of the approaches discussed here. These will be discussed in Chapter 5.

3.3.2 The L_p -Case.

The optimal knot determination problem for the L_p -case ($1 \leq p < \infty$) is the problem of solving for

$$J_{p,N}^*(\pi^*) = \min_{\pi} J_{p,N}(\pi) \quad 3.21$$

It will now be shown how $J_{p,N}^*$ of equation 3.21 can be computed recursively by imbedding the cost functional in a class of functionals dependent on the last knot.

Assume that only one interior knot (two segments $j=1,2$) is allowed in the interval $T_0 \leq t \leq \tau$ at $t = T_1$. Then define

$$J_{p,2}^*(\tau) = \min_{T_0 \leq T_1 \leq \tau} \left\{ \mathcal{E} J_p^*(T_0, T_1, \omega) + \mathcal{E} J_p^*(T_1, \tau, \omega) \right\} \quad \tau \in [0, T] \quad 3.22$$

Note that $J_{p,2}^*(T)$ is the optimal cost associated with subdividing the total interval $[0, T]$ into two segments. Now if two knots, at $t = T_1$ and $t = T_2$, (thus three segments), are allowed in the interval

$T_0 \leq t \leq \tau$, then

$$J_{p,3}^*(\tau) = \text{Min}_{T_1, T_2} \left\{ \mathcal{E} J_p^*(T_0, T_1, \omega) + \mathcal{E} J_p^*(T_1, T_2, \omega) + \mathcal{E} J_p^*(T_2, \tau, \omega) \right\}$$

$$T_1 < T_2; T_1, T_2 \in [0, \tau]; \tau \in [0, T] \quad 3.23$$

Since the minimization over T_1 only involves the first two terms of equation 3.23, that equation can be rewritten as

$$J_{p,3}^*(\tau) = \text{Min}_{T_2} \left\{ \text{Min}_{T_1} \left(\mathcal{E} J_p^*(T_0, T_1, \omega) + \mathcal{E} J_p^*(T_1, T_2, \omega) \right) + \mathcal{E} J_p^*(T_2, \tau, \omega) \right\}$$

3.24

But by equation 3.22, the first term in the brackets of equation 3.24 is simply $J_{p,2}^*(T_2)$. Thus equation 3.24 becomes

$$J_{p,3}^*(\tau) = \text{Min}_{T_2} \left\{ J_{p,2}^*(T_2) + \mathcal{E} J_p^*(T_2, \tau, \omega) \right\}$$

3.25

It can now be seen that the general recursive functional equation is

$$J_{p, M+1}^*(\tau) = \text{Min}_{T_0 \leq T_M \leq \tau} \left\{ J_{p, M}^*(T_M) + \mathcal{E} \mathcal{J}_p^*(T_M, \tau, \omega) \right\}$$

$$M = 1, 2, \dots, N-1$$

$$\tau \in [0, T]$$
3.26

For $M=1$, the initial cost is

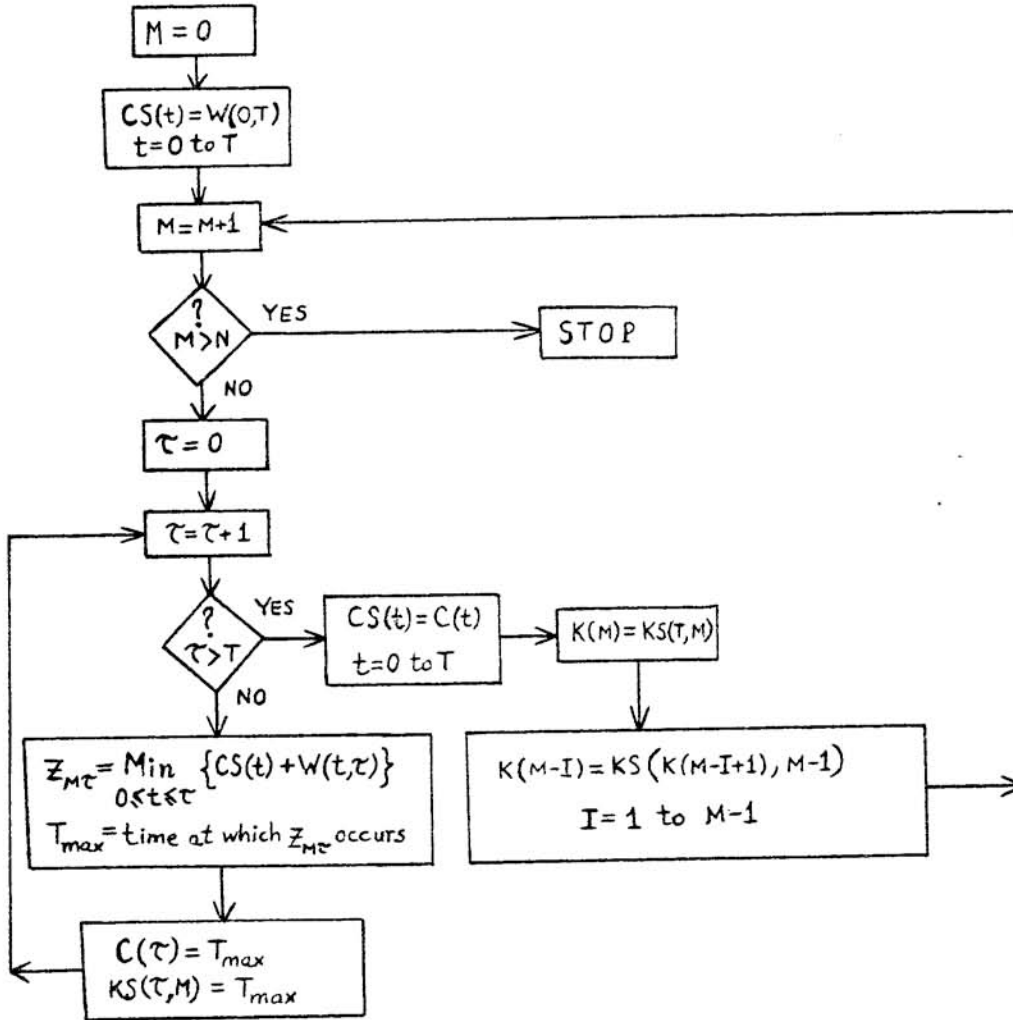
$$J_{p, 1}^*(\tau) = \mathcal{E} \mathcal{J}_p^*(0, \tau, \omega) \quad \tau \in [0, T]$$
3.27

$J_{p, 1}^*(\tau)$ is simply the optimal L_p -cost incurred by a global fit of an m -th degree polynomial over the total interval $[0, T]$ subject to any relevant constraints. In the case of $M=1$ no interior knots are used and the interval $[0, T]$ constitutes one segment.

Hence equations 3.26 and 3.27 give a computational scheme for determining the N optimal knots. Note that at each stage of the dynamic programming $J_{p, M}^*(\tau)$ must be computed and stored over $0 \leq \tau \leq T$, for use in the next stage. Finally $J_{p, N}^*(\tau)$ is obtained which, when evaluated at $\tau=T$ gives the optimal cost of equation 3.21. That is:

$$J_{p, N}^*(T) = J_{p, N}^*(\Pi^*) = \text{Min}_{\Pi} J_{p, N}(\Pi)$$
3.28

Also note that, at each stage, all knots are readjusted. In other words, all previous knots vary when one more knot is added. The actual dynamic programming algorithm for obtaining the optimal knot locations



- $[0, T]$ Total time interval to be segmented
- $W(t, \tau) = \mathcal{E} \mathcal{J}_p(t, \tau, \omega)$ Cost-to-go matrix
- N Total number of interior knots desired
- $K(I)$ Array of optimal knot locations
- $Z_{M\tau}, T_{max}, CS, C, KS$ Intermediate variables and storage arrays

Flow Chart 3.1: Dynamic Programming for Optimal Knot Locations in the L_p -Case.

is summarized in Chart 3.1.

In practical applications, the expected value in the integrands can be replaced by sample means, as discussed in section 3.2.2.

The computational aspects of the ensemble and sample-based L_p problems are very similar except that setting up the estimate of the expected cost, $\frac{1}{P} \sum_{\omega=1}^P J_p^*(t_1, t_2, \omega)$, in the ensemble-based case can be quite demanding for large data bases. The advantage, however, from the point of view of approximation, is that the knots are determined only once, off-line, and do not form part of the set of parameters needed to characterize sample-waveforms.

The ensemble and sample-based L_p knot optimization algorithms have been developed and applied to the cardiographic problem as discussed in Chapter 5.

3.3.3 The Chebyshev Case.

The optimal knot determination problem for the Chebyshev case (L_∞) is the problem of solving for

$$J_{\infty, N}^*(\pi^*) = \text{Min}_{\pi} J_{\infty, N}(\pi) \quad 3.29$$

It will now be shown how $J_{\infty, N}^*$ of equation 3.29 can be computed recursively by imbedding the cost functional in a class of functionals dependent on the last knot.

Assume that only one interior knot (two segments, $j=1,2$) is allowed in the interval $T_0 \leq t \leq \tau$ at $t=T_1$. Then define

$$J_{\infty, 2}^*(\tau) = \text{Min}_{0 \leq T_1 \leq \tau} \text{Max}_{\omega \in \Gamma} \text{Max} [J_{\infty}^*(T_0, T_1, \omega); J_{\infty}^*(T_1, \tau, \omega)]$$

3.30

Note that $J_{\infty,2}^*(T)$ is the optimal Chebyshev cost of using two segments over the total interval $[0, T]$. Now, if two knots, at $t=T_1$, and $t=T_2$, (thus three segments) are allowed in the interval $T_0 \leq t \leq \tau$, then

$$J_{\infty,3}^*(\tau) = \min_{T_1, T_2} \max_{\omega \in \Gamma} \max \left[J_{\infty}^*(T_0, T_1, \omega); J_{\infty}^*(T_1, T_2, \omega); J_{\infty}^*(T_2, \tau, \omega) \right]$$

$$T_1 < T_2; T_1, T_2 \in [0, \tau]; \tau \in [0, T]$$

3.31

But the maximum function commutes with other maximum functions and also enjoys the following property:

$$\max(a, b, c) = \max \{ \max(a, b); c \}$$

3.32

Thus $J_{\infty,3}^*(\tau)$ can be rewritten as

$$J_{\infty,3}^*(\tau) = \min_{T_1, T_2} \max \left[\max \left(\max_{\omega \in \Gamma} J_{\infty}^*(T_0, T_1, \omega); \max_{\omega \in \Gamma} J_{\infty}^*(T_1, T_2, \omega) \right); \max_{\omega \in \Gamma} J_{\infty}^*(T_2, \tau, \omega) \right]$$

3.33

$$T_1 < T_2; T_1, T_2 \in [0, \tau]; \tau \in [0, T]$$

Let

$$a(T_1) = \text{Max}_{\omega \in \Gamma} J_{\infty}^*(T_0, T_1, \omega)$$

$$b(T_1, T_2) = \text{Max}_{\omega \in \Gamma} J_{\infty}^*(T_1, T_2, \omega)$$

3.34

$$c(T_2) = \text{Max}_{\omega \in \Gamma} J_{\infty}^*(T_2, \tau, \omega)$$

Then equation 3.33 reduces to

$$J_{\infty,3}^*(\tau) = \text{Min}_{T_2} \text{Min}_{T_1} \text{Max} [\text{Max}(a(T_1); b(T_1, T_2)); c(T_2)]$$

3.35

Now also define

$$f(T_1, T_2) = \text{Max} \{a(T_1); b(T_1, T_2)\}$$

3.36

Then

$$J_{\infty,3}^*(\tau) = \text{Min}_{T_2} \text{Min}_{T_1} \text{Max} \{f(T_1, T_2); c(T_2)\}$$

3.37

Suppose T_2 is fixed and consider the minimization over T_1 . Suppress the T_2 dependence in the notation since the problem now considered is

$$\text{Min}_{T_1} \text{Max} \{ f(T_1); c \} \quad 3.38$$

Define

$$f(T_1^*) = \text{Min}_{T_1} f(T_1) \quad 3.39$$

Then by definition

$$f(T_1^*) \leq f(T_1) \quad \forall T_1 \in [0, T] \quad 3.40$$

Therefore it is clear that

$$\text{Max} \{ f(T_1); c \} \geq \text{Max} \{ f(T_1^*); c \} \quad \forall T_1 \in [0, T] \quad 3.41$$

In particular

$$\text{Min}_{T_1} \text{Max} \{ f(T_1); c \} \geq \text{Max} \{ f(T_1^*); c \} \quad 3.42$$

But by definition of the minimum

$$\text{Min}_{T_1} \text{Max} \{ f(T_1); c \} \leq \text{Max} \{ f(T_1); c \} \quad \forall T_1 \in [0, T] \quad 3.43$$

In particular

$$\text{Min}_{T_1} \text{Max} \{ f(T_1); c \} \leq \text{Max} \{ f(T_1^*); c \} \quad 3.44$$

By equations 3.42 and 3.44 it is concluded that

$$\min_{T_1} \max \{f(T_1); c\} = \max \{f(T_1^*); c\} = \max \left\{ \min_{T_1} f(T_1); c \right\} \quad 3.45$$

Therefore using equation 3.45 in equation 3.37

$$J_{\infty,3}^*(\tau) = \min_{T_2} \max \left\{ \min_{T_1} f(T_1, T_2); c(T_2) \right\} \quad 3.46$$

Substituting for $f(T_1, T_2)$ and $c(T_2)$ from equations 3.34 and 3.36 the following is obtained

$$J_{\infty,3}^*(\tau) = \min_{T_2} \max \left\{ \min_{T_1} \max \{a(T_1); b(T_1, T_2)\}; c(T_2) \right\} \quad 3.47$$

But the first argument of the first maximum function can be recognized in equation 3.47 as $J_{\infty,2}^*(T_2)$ of equation 3.30. Thus equation 3.47 becomes:

$$J_{\infty,3}^*(\tau) = \min_{0 \leq T_2 \leq \tau} \max \left\{ J_{\infty,2}^*(T_2); \max_{\omega \in \Gamma} J_{\infty}^*(T_2, \tau, \omega) \right\} \quad 3.48$$

By induction it can be seen that the recursive functional equation for the Chebyshev norm is:

$$J_{\infty, M+1}(\tau) = \min_{T_0 \leq T_M \leq \tau} \max \left\{ J_{\infty, M}^*(T_M); \max_{\omega \in \Gamma} J_{\infty}^*(T_M, \tau, \omega) \right\} \quad 3.49$$

$M = 1, 2, \dots, N-1$
 $\tau \in [0, T]$

The estimate used in equation 3.49 is the optimal fit of an m -th degree polynomial to $x(t, \omega)$ over each region subject to any constraints that may be imposed. The optimal fit may be chosen to be optimal in any desired norm. A consistent choice would be to use the Chebyshev norm. However, if computational expediency requires it, any other estimate may be used in conjunction with the Chebyshev norm for the knot optimization problem.

For $M=1$, the initial cost is

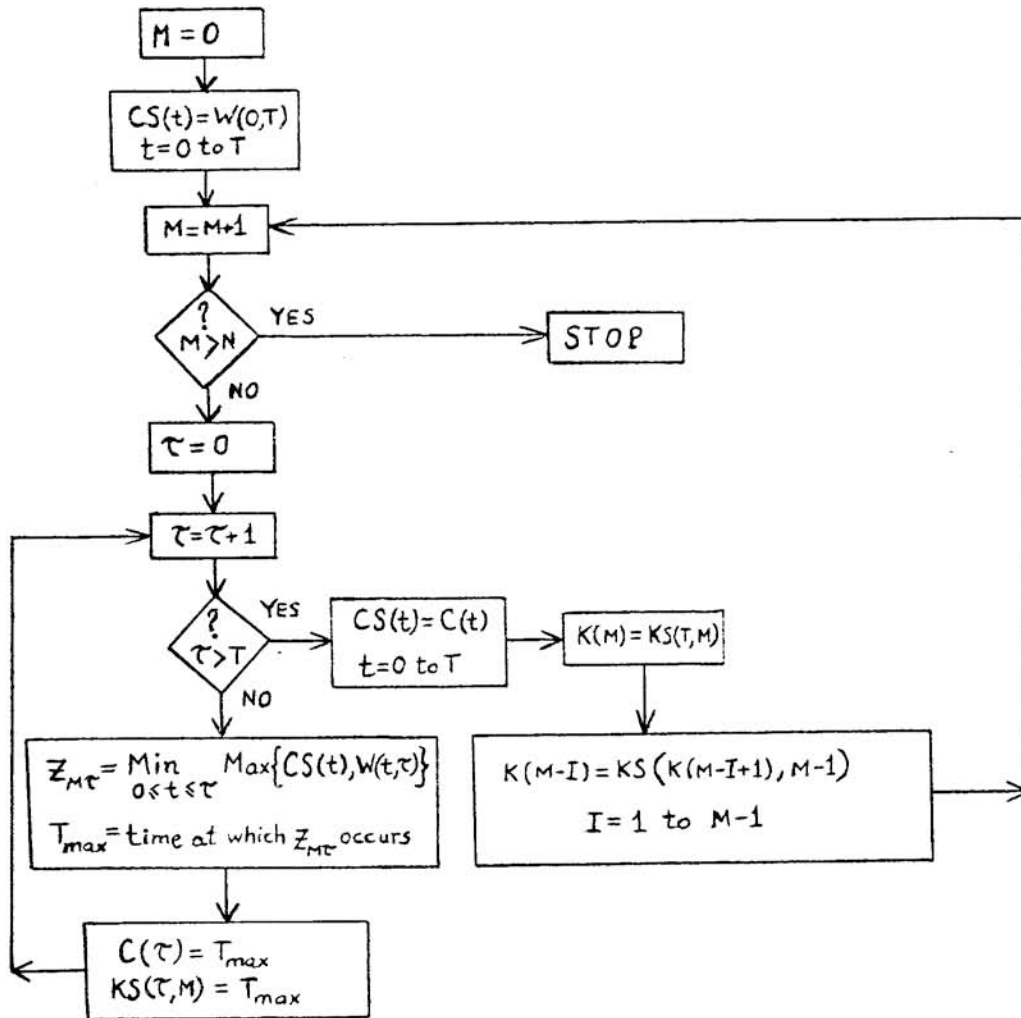
$$J_{\infty,1}^*(\tau) = \text{Max}_{\omega \in \Gamma} J_{\infty}(0, \tau, \omega) \quad \tau \in [0, T]$$

3.50

$J_{\infty,1}^*(\tau)$ is simply the Chebyshev cost (maximum absolute deviation) incurred by a global optimal fit of an m -th degree polynomial over the total interval $[0, T]$, subject to any relevant constraints on the estimate. In the case of $M=1$, no interior knots are used and the interval $[0, T]$ constitutes one segment.

Hence equations 3.49 and 3.50 provide a computational scheme for determining the N optimal knots provided the Ω space is a countable finite set, so that the maximization with respect to ω can be accomplished via a finite search.

Note that, if an expectation of the sample-function costs over the ensemble for this Chebyshev case had been taken, the problem would not have been tractable since expectation and maximization do not commute in general. The formulation given, however, does lead to a soluble problem as shown.



$[0, T]$ Total time interval to be segmented
 $W(t, \tau) = \text{Max}_{\omega \in \Gamma} \int_{\infty}^{\tau} (t, \tau, \omega)$ Cost-to-go matrix
 N Total number of interior knots desired
 $K(I)$ Array of optimal knot locations
 $Z_{M\tau}, T_{max}, CS, C, KS$. Intermediate variables and storage arrays

Flow Chart 3.2: Dynamic Programming for Optimal Knot Locations in the Chebyshev Case.

Note that, as in the L_p -norm case, each stage of the algorithm requires that $J_{\infty, M}^*(\tau)$ be computed and stored for $0 \leq \tau \leq T$, for use in the next stage. Finally, $J_{\infty, N}^*(T)$ provides the optimal cost of equation 3.29. That is

$$J_{\infty, N}^*(T) = J_{\infty, N}^*(\Pi^*) = \underset{\Pi}{\text{Min}} J_{\infty, N}(\Pi) \quad 3.51$$

Here again it must be noted that, at each stage, all knots are readjusted. Thus when one more knot is added, all previous knots must vary, as expected. Chart 3.2 summarizes the actual algorithm for obtaining the optimal knot locations.

The computational aspects of the ensemble and sample-based Chebyshev problems are very similar except for the setting up of $\text{Max}_{\omega \in \Gamma} J_{\infty}(t_1, t_2, \omega)$ which can be computationally quite demanding for the ensemble-based case with large data bases. The advantage, again, from the point of view of approximation, is that the knots are determined off-line and are not characterizing parameters (features) for sample-waveforms.

The ensemble and sample-based Chebyshev knot optimization algorithms have been developed and applied to the cardiographic problem as discussed in Chapter 5.

3.4 Error Analysis.

3.4.1 Introduction.

Upper bounds on the errors incurred by the various approximations formulated in this chapter are generally difficult to obtain due to the nonlinearity of the knot determination problem. Nevertheless various

useful bounds from spline-theory may be extended and adapted to the formulations developed here. In particular Burchard's [34] and Phillips' [5] results on the degree of convergence of variable-knot splines can be applied to the deterministic sample-function problem for both the L_p and Chebyshev cases.

For the ensemble-based representations, the error analysis of fixed-knot (linear) spline approximation of De Boor [40] is applicable. Error bounds for fixed-knot splines are discussed in Prenter [30] and Schumaker [28] as well.

The direct theorems of analysis relating smoothness properties of classes of functions to the order of the error in approximating them by classes of polynomials are well known and date back to Jackson's work [28]. Even for classes of global polynomials the methods for obtaining these error estimates are not particularly simple and upper bounds obtained can be misleading without more information on their sharpness. Such information is usually gained only through extensive computational experience with the approximations.

3.4.2 The Ensemble-Based Problems.

Let

$$E_{m,N}^e(x(t,\omega), 0, T) = \left\{ \sum_{j=1}^N \int_{T_{j-1}^*}^{T_j^*} [x(t,\omega) - \hat{x}_j(t,\omega)]^2 dt \right\}^{1/2}$$

3.52

denote the L_2 error incurred by the optimal fit \hat{x}_j^* to x using the fixed ensemble-optimal knots $\{T_j^*\}$, where \hat{x}_j^* is an m -th degree polynomial for each segment of $[0, T]$. The error $E_{m,N}^e$ is that incurred for representing a particular sample-waveform $x(t, \omega)$ using the ensemble-based formulation.

The most immediate error analysis for spline approximates (including deficient splines) to a given function f on an interval $[0, T]$ follows from the so-called first and second integral relations for odd degree splines. The basic result developed by Ahlberg, Nilson, and Walsh [29] for the Chebyshev norm is

$$E_{\infty, m, N}^e(x(t, \omega), 0, T) = \text{Max}_{1 \leq j \leq N} \text{Max}_{T_{j-1}^* \leq t \leq T_j^*} |x(t, \omega) - \hat{x}_j^*(t, \omega)|$$

3.53

where \hat{x}_j^* is the optimal estimate in the sense defined in this chapter. The error estimate result is

$$E_{\infty, m, N}^e \leq K \|\Delta\|^{2m-1}$$

3.54

with

$$\|\Delta\| = \text{Max}_{1 \leq j \leq N} [T_j^* - T_{j-1}^*]$$

3.55

and K a constant dependent on the smoothness of $x(t, \omega)$.

Hall [41] proves similar error bounds for $x(t, \omega) \in \mathcal{E}^4[0, T]$.

For such a case the result is:

$$E_{m,N}^e \leq \frac{5}{384} \left\{ \int_0^T \left[\frac{d^4 x(t,\omega)}{dt^4} \right]^2 dt \right\}^{1/2} \quad 3.56$$

Prenter [30] discusses various other error bounds of this sort for fixed-knot splines.

From the practical point of view, these bounds are of little use since they require estimation of high order derivatives of $x(t,\omega)$ which may not exist, or may not be obtainable due to noisy measurements.

De Boor, however, using a very elegant projection method has obtained a result on the order of Chebyshev approximation by splines as a function of knot spacing (i.e. for the fixed-knot problem) that can be adapted fruitfully to the formulations developed here:

$$E_{\infty,m,N}^e = \Theta(\omega[x:\|\Delta\|]) \quad 3.57$$

where $\|\Delta\|$ is given by equation 3.55 and $\omega(x:\cdot)$ is the modulus of continuity of the sample function x represented [30]. The modulus of continuity of a function $x(t)$ given over an interval I is defined as follows

$$\omega(x:h) \triangleq \sup \left\{ |x(t+\bar{h}) - x(t)| \mid t, t+\bar{h} \in I, |\bar{h}| \leq h, h > 0 \right\}$$

3.58

for fixed h , ω is a measure of the oscillatory nature of x . For example, if $x(t) = \sin \frac{1}{t}$ on $(0, \pi)$ then $\omega(f: h) \rightarrow 1$ for all h , no matter how small. On the other hand one can prove that $x(t)$ is uniformly continuous on an interval I if and only if $\omega(x: h) \rightarrow 0$ as $h \rightarrow 0$

Marsden [42] sharpens De Boor's result for $m \geq 2$ by the following bound

$$E_{\infty, m, N}^e \leq \left[\sqrt{\frac{m}{12}} + 1 \right] \omega(x: \|\Delta\|) \quad m \geq 2 \quad 3.59$$

The modulus of continuity can be estimated easily for each sample-function in practice. Hence bounds of the form of 3.59 are applicable and useful for the ensemble-based formulations.

3.4.3 The Sample-Based Problems.

Let

$$E_{m, N}(x(t, \omega), 0, T) = \text{Inf} \left\{ \sum_{j=1}^N \int_{T_{j-1}}^{T_j} [x(t, \omega) - \hat{x}_j(t, \omega)]^2 dt \right\}^{1/2} \quad 3.60$$

denote the L_2 error incurred by the optimal fit \hat{x}_j to x over all possible partitions $\{T_j | j=0, 1, \dots, N\}$ of the interval $[0, T]$, where the estimate \hat{x}_j is taken from the class of m -th degree polynomials. Assume, furthermore, that no constraints at knots are imposed. Then

Phillips' extension [5] of Meinardus's formula [2] gives the following error bound:

$$E_{m,N} \leq \sqrt{\frac{2N}{2m+3}} 2^{m+1} \frac{1}{\binom{2m+2}{m+1}} \left[\frac{T}{2N} \right]^{m+\frac{3}{2}} \frac{1}{(m+1)!} \text{Max}_{0 \leq t \leq T} \left| \frac{d^{m+1} x(t, \omega)}{dt^{m+1}} \right|$$

3.61

This result has limited applicability in practice since even for $m=1$ (linear segmented approximation) the bound involves second derivatives of the sample-function $x(t, \omega)$ which are difficult to estimate for real (noisy) data. In general such derivatives may not even exist, depending on the smoothness of the process $x(t, \cdot)$.

Asymptotic results on the behavior of the error as the number of knots tends to infinity have been obtained by Ream [43] and Mc Clure [36] as well. Phillips' bound of equation 3.61 leads to the following asymptotic result for the problems studied here:

$$\lim_{N \rightarrow \infty} \left\{ N^{m+1} E_{m,N}(x(t, \omega), 0, T) \right\} = \sqrt{\frac{2}{2m+3}} 2^{m+1} \frac{1}{\binom{2m+2}{m+1}} \frac{1}{(m+1)!} \left\{ \frac{1}{2} \int_0^T \left| \frac{d^{m+1} x(t, \omega)}{dt^{m+1}} \right|^{\frac{1}{m+\frac{3}{2}}} dt \right\}^{m+\frac{3}{2}}$$

3.62

For the Chebyshev case the analogs of equations 3.61 and 3.62, also treated in [36], are:

$$E_{\infty, m, N} \leq \frac{1}{2^m} \left[\frac{T}{2N} \right]^{m+1} \frac{1}{(m+1)!} \text{Max}_{0 \leq t \leq T} \left| \frac{dx^{m+1}(t, \omega)}{dt^{m+1}} \right|$$

3.63

and

$$\lim_{N \rightarrow \infty} \left\{ N^{m+1} E_{\infty, m, N} \right\} = \frac{1}{2^m} \left\{ \frac{1}{2} \int_0^T \left| \frac{dx^{m+1}(t, \omega)}{dt^{m+1}} \right|^{1/m+1} dt \right\}^{m+1} \frac{1}{(m+1)!}$$

3.64

where

$$E_{\infty, m, N} = \text{Inf} \text{Max}_{1 \leq j \leq N} \text{Max}_{T_{j-1} \leq t \leq T_j} |x(t, \omega) - \hat{x}_j(t, \omega)|$$

3.65

Burchard in [34], generalizing on an interesting result of Rice [27], obtains bounds on variable-knot polynomial spline approximations. These bounds apply to the present variable-knot formulations for both the L_p and Chebyshev norms.

The bounds give for large N :

$$E_{m,N} \leq K_m \frac{1}{N^{m+1}} \left\{ \int_0^T \left| \frac{dx^{m+1}(t,\omega)}{dt^{m+1}} \right|^\sigma dt \right\}^{1/\sigma} \quad \sigma = \frac{1}{m+3/2}$$

3.66

$$E_{\infty,m,N} \leq K_m \frac{1}{N^{m+1}} \left\{ \int_0^T \left| \frac{dx^{m+1}(t,\omega)}{dt^{m+1}} \right|^\sigma dt \right\}^{1/\sigma} \quad \sigma = \frac{1}{m+1}$$

3.67

with K_m a constant. Note that Burchard's results, although obtained using a very different approach, are equivalent, for large N , to the asymptotic results of equations 3.72, and 3.74 derived by Phillips.

Rice's interesting result which Burchard generalizes is reported in [27]. It is a special case of equation 3.77 for $m=0$. Rice, however, shows his result to hold for both $m=0$ and $m=1$ (approximation by constants and straight line segments). The result is:

$$E_{\infty,m,N} \leq \frac{V}{N} \quad m=0,1 \quad 3.68$$

where V is the (bounded) variation of $x(t,\omega)$ over the interval $[0,T]$. The only conditions on $x(t,\omega)$ are that it be continuous and of bounded variation over $[0,T]$. As such this result for line segment approximation is probably the most useful from the practical viewpoint.

Although equation 3.68 is very simple, it is more powerful than results obtainable by classical approximation theory involving fixed knots or global polynomials. Bernstein's and Zygmund's converse theorems discussed in [34] prove that such results could not hold for global polynomial approximation. That variable-knot splines converge much faster than fixed knot ones can be seen from comparing Burchard's result to the order of convergence of fixed-knot splines (for further discussion see [34]).

CHAPTER 4

OPTIMAL SEGMENTED FEATURE EXTRACTION

4.1 Introduction.

Data reduction, or feature extraction in general, is largely dependent on the choice of structure for the feature extractor (linear, nonlinear, etc.) as well as the cost criterion to be optimized. The strictly mathematical question of the computability and tractability of the data reduction process often directs the choice of structure and cost to be used. The feature extraction problem is concerned with the assignment of such analytically and computationally tractable representations to patterns, that concisely eliminate redundancy, while optimally preserving the salient global and local characteristics of individual sample waveforms.

The global L_2 measure of error leading to the K-L expansion is in many ways a compromise in which accuracy of representation in specific local regions of waveforms and for individual sample waveforms is traded-off for simplicity of the feature extractor. For a given number of allowed features, and restricting the feature extractor to be linear, the global L_2 -error has been shown to be minimized with a K-L system. This property, discussed in Chapter 2, however, does not indicate how best to increase the number of features such as to achieve higher representation accuracy in a given region. Taking higher order K-L terms may be inefficient as too many may be required to approximate

the given region to the desired accuracy. It is easy to see the problem in the limiting case where, say, a certain point of the waveform needs to be known precisely, while the error in other portions of the waves is unimportant. In this case all terms of the K-L expansion would be required although a much more efficient feature extractor could be devised by taking as the single feature the value of the waveform at the time in question. The K-L expansion does not provide a means to independently control the approximation accuracy in local regions. The first few terms of the K-L expansion very efficiently approximate global characteristics of waveforms. But once the desired level of accuracy is reached for any portion of the waveforms, the efficiency of approximation in other regions, where subtle deviations are important, may be highly increased by use of methods other than taking more global K-L terms.

Another major limitation of the K-L method is that the representation accuracy for a particular sample waveform cannot be controlled independently. The number of allowed features is fixed a priori based on expected error rates over the ensemble. The truncated K-L representation may perform very poorly for certain sample waveforms, although the number of terms has been fixed to yield a low expected error for the ensemble. Hence two of the major limitations of the K-L method derive from the fact that representations are based solely on global and ensemble considerations. These considerations are closely linked to the linearity of the K-L method as will be seen in the context of a more general non-linear approach.

In Chapter 3, an entirely different approach to the representation problem was investigated. In order to achieve local control of the error

and to ensure that each sample waveform is represented accurately, approximation-theoretic formulations have been studied. A variable-knot (nonlinear) segmented function approximation theory has been introduced and developed. The formulation considered is a generalization of spline function approximation. It was shown how the error could be controlled locally with the introduction of variable-knots. Allowing the knots to adapt to the specific waveform being represented, made the problem highly nonlinear. Feature-extraction was thus reduced to deterministic curve-fitting on a sample by sample basis. The characteristics of each waveform could now be captured accurately via variable-knots.

The essential drawback of this approach is that no use of ensemble information is made in the design of the feature extractor. Each sample waveform is treated deterministically and the statistical structure of the underlying process is disregarded. In a sense the methods of Chapter 3 stand in sharp contrast to the K-L method of Chapter 2, and their essential limitations derive from the fact that such representations are based solely on local and sample-function considerations.

In this chapter, a nonlinear representation which incorporates the desirable aspects of both the K-L expansion and the generalized spline approximation methods is developed. This novel representation reduces to either the K-L expansion or to a spline function type approximation under specific restrictions. The feature extractors developed, therefore, subsume the previous linear and nonlinear approaches discussed, as special cases. The proposed schemes retain analytic and computational tractability while successfully unifying global-local and ensemble-sample function

considerations and satisfying optimality with respect to well-defined error criteria.

4.2 Structure of Representations.

Let $x(t, \omega)$ denote the ω -th sample-function from the real-valued, L_2 , non-stationary stochastic process $x(t, \cdot)$ defined over the interval $[0, T]$, with mean zero and covariance function $R(t, \tau)$. A finite-dimensional representation of $x(t, \omega)$ for all $\omega \in \Omega$ denoted by $\hat{x}(t, \omega)$ is sought. The process $x(t, \cdot)$ is defined over the probability space introduced in Chapter 2.

In the approximations of this chapter, the sample function $x(t, \omega)$ is allowed to exhibit "segmented behavior" by virtue of the following representation structure.

Let

$$\Pi = \{T_j\}; \quad j = 0, 1, 2, \dots, N \quad 4.1$$

form a partition of the interval $[0, T]$ such that

$$0 = T_0 < T_1 < T_2 < \dots < T_N = T \quad 4.2$$

The set Π will be referred to as the set of knots for the sample function $x(t, \omega)$

Let

$$\hat{x}(t, \omega) = \hat{x}_j(t, \omega) = \sum_{i=1}^{m_j} \alpha_{ij}(\omega) \phi_{ij}(t) \quad \begin{array}{l} T_{j-1} \leq t \leq T_j \\ j = 1, 2, \dots, N \end{array}$$

4.3

where

$$\begin{aligned} \alpha_{ij}(\omega) &\in \mathbb{R}^1 \\ \phi_{ij}(t) &\in L_2[0, T] \\ m_j, N &\in \mathbb{Z}^+ \end{aligned} \quad 4.4$$

The following conditions are imposed on the set $\{\phi_j(t)\}$:

$$\begin{aligned} \int_{T_{j-1}}^{T_j} \phi_{ij}(t) \omega(t) \phi_{kj}(t) dt &= \delta_{ik} \quad \forall i, j, k \\ \omega(t) &\geq 0 \quad \forall t \in [0, T] \end{aligned} \quad 4.5$$

and

$$\phi_{ij}(t) = 0 \quad t \notin [T_{j-1}, T_j] \quad \forall i, j \quad 4.6$$

Hence $\hat{x}(t, \omega)$ denotes the finite-dimensional representation which, for t in the j -th segment, is an m_j -term linear expansion of $x(t, \omega)$ using the orthonormal basis functions $\{\phi_j(t)\}$ appropriate for the partition Π . The set $\{\alpha_j(\omega)\}$ denotes the coefficients of the linear expansion for the partition Π and sample-function ω . The parameters of the estimate $\hat{x}(t, \omega)$ are, therefore: the coefficients of the expansion, $\{\alpha_j(\omega)\}$, the basis functions

of the expansion, $\{\phi_j(t)\}$, the set of knot locations, Π , the local expansion orders, $\{m_j\}$, and the total number of segments, N .

There are two possibilities with respect to each of the above parameters which are to determine optimal parameters (i) over the ensemble waveforms: the ensemble-based problem; (ii) for each sample-wave form: the sample based problem.

The above alternatives have been discussed as they apply to the optimal knot locations Π , in section 3.2.1. From the point of view of feature extraction, or data compression, selecting basis functions for each sample-waveform must be precluded in order that a low-dimensional feature space may be obtained. The basis functions $\{\phi_j(t)\}$ should therefore not be made sample-dependent. All of the remaining parameters may be chosen on an ensemble or sample-basis independently. The coefficients $\{\alpha_j(\omega)\}$ are always sample-dependent regardless of whether the ensemble or sample-based problem is considered. They constitute the linear (also the only) features of the fully-ensemble-based feature extractor, and the linear components of the nonlinear feature extractor that results when any of the parameters are selected on a sample basis. The features, then, consist of the coefficients and any of the nonlinear parameters that are selected on a sample basis.

The representation problem is considered for the L_2 and Chebyshev norms. The L_2 norm is treated since it leads to an analytically and practically soluble problem. The Chebyshev norm is treated because of its usefulness in practice. Obtaining ensemble (or sample)-optimal basis functions using the Chebyshev approach, however, is not considered due

to the lack of a tractable analytic or computational characterization of an optimal solution for this case. In both the ensemble and sample-based Chebyshev problems, the basis functions of the L_2 ensemble case are selected as the canonical basis for expansion. The basis functions (and therefore the coefficients) having been selected a priori for the Chebyshev case, the remaining parameters (knot locations, local expansion orders, and the total number of segments) may be treated, as for the case, on either an ensemble or sample-basis.

In the approach taken, coefficients, basis functions and knot locations are parameters used to minimize a global cost. The local expansion orders and the total number of segments are parameters selected with a view to obtaining a minimal number of features consistent with satisfying a set of specified L_2 or Chebyshev local error constraints imposed on an ensemble or sample-basis.

A weighting function in the cost functionals is included for the L_2 -problems. It is shown how weighting functions can be chosen to improve the smoothness of the representations across the knots, since the representations considered are not necessarily continuous at the knots. It is shown how the error at the knots can be made arbitrarily small by suitable penalty techniques. Then the magnitude of the discontinuity in $\hat{x}(t, \omega)$ across knots can be controlled, thereby improving smoothness.

Finally the feature extractors developed here are compared to the global K-L and piecewise polynomial approaches of the previous chapters. It is pointed out how both of these previous methods are special cases of this more general approach to feature extraction.

4.3 The L_2 -Case.

4.3.1 Global Cost Function.

In this formulation consider the following global cost functional:

$$J_{2,N}(\{\underline{\alpha}_j\}, \{\underline{\phi}_j\}, \{m_j\}, \Pi) = \mathcal{E} \sum_{j=1}^N \mathcal{J}_2(\underline{\alpha}_j, \{\underline{\phi}_j\}, m_j, T_{j-1}, T_j, \omega) \quad 4.7$$

where the segment L_2 cost is

$$\mathcal{J}_2(\underline{\alpha}_j, \{\underline{\phi}_j\}, m_j, T_{j-1}, T_j, \omega) = \int_{t=T_{j-1}}^{T_j} [e(\underline{\alpha}_j, \{\underline{\phi}_j\}, m_j, t, \omega)]^2 w(t) dt \quad 4.8$$

and the pointwise approximation error is

$$e(\underline{\alpha}_j, \{\underline{\phi}_j\}, m_j, t, \omega) = x(t, \omega) - \hat{x}_j(t, \omega) \quad \begin{array}{l} T_{j-1} \leq t \leq T_j \\ j = 1, 2, \dots, N \end{array} \quad 4.9$$

with the estimate in segment j given by

$$\hat{x}_j(t, \omega) = \sum_{i=0}^{m_j} \alpha_{ij}(\omega) \phi_{ij}(t) = \underline{\alpha}_j(\omega) \cdot \underline{\phi}_j(t) \quad \begin{array}{l} T_{j-1} \leq t \leq T_j \\ j = 1, 2, \dots, N \end{array} \quad 4.10$$

The function $w(t)$ is a given weighting function such that

$$w(t) \geq 0 \quad \forall t \in [0, T] \quad 4.11$$

The expectation operation in equation 4.7 is defined as in equation 3.6 leading to the two alternatives considered throughout: the linear ensemble-based problem, and the nonlinear sample-based problem. The same considerations discussed in section 3.2.2 apply to this formulation.

The optimization problem considered here is

$$J_{2,N}^* (\{\alpha_j^*\}, \{\phi_j^*\}, \{m_j\}, \Pi^*) = \text{Min}_{\{\alpha_j\}, \{\phi_j\}, \Pi} J_{2,N} (\{\alpha_j\}, \{\phi_j\}, \{m_j\}, \Pi)$$

4.12

The local orders of expansion $\{m_j\}$ and the total number of segments N are parameters to be optimized in later sections with the objective of satisfying local error constraints and minimizing a "feature extraction cost" (related to the total number of features used).

4.3.2 Optimal Coefficients.

In view of the orthonormality of the basis functions as given in equation 4.5, any sample function $x(t, \omega)$ can be expanded over any segment j using the complete orthonormal set $\{\phi_{ij}(t)\}$. That is:

$$x(t, \omega) = \sum_{i=1}^{\infty} \alpha_{ij}(\omega) \phi_{ij}(t) \quad \forall t \in [T_{j-1}, T_j]$$

4.13

The coefficients $\alpha_{ij}(\omega)$ can be determined by the orthonormality condition for the $\{\phi_{ij}(t)\}$. The approach here parallels closely

that of section 2.3 for the K-L expansion

$$\int_{T_{j-1}}^{T_j} x(t, \omega) w(t) \phi_{k_j}(t) dt = \sum_{i=1}^{\infty} \alpha_{ij}(\omega) \int_{T_{j-1}}^{T_j} \phi_{ij}(t) w(t) \phi_{k_j}(t) dt \quad 4.14$$

$$\int_{T_{j-1}}^{T_j} x(t, \omega) w(t) \phi_{k_j}(t) dt = \sum_{i=1}^{\infty} \alpha_{ij}(\omega) \delta_{ik} = \alpha_{k_j}(\omega) \quad 4.15$$

One may at first suspect that for an m-term truncated expansion of

$x(t, \omega)$ one may better approximate by the $\{\phi_{1j}(t), \phi_{2j}(t), \dots, \phi_{mj}(t)\}$ using coefficients $\alpha'_{ij}(\omega)$ which are different from those $\alpha_{ij}(\omega)$ given by equation 4.15. But it is easy to see that this is not the case. It will be shown that

$$\int_{T_{j-1}}^{T_j} [x(t, \omega) - \sum_{i=1}^m \alpha_{ij}(\omega) \phi_{ij}(t)]^2 w(t) dt \leq \int_{T_{j-1}}^{T_j} [x(t, \omega) - \sum_{i=1}^m \alpha'_{ij}(\omega) \phi_{ij}(t)]^2 w(t) dt \quad 4.16$$

whenever $\alpha'_{ij}(\omega) \neq \alpha_{ij}(\omega)$. The left hand side of equation

4.16 is simply: $\int \sum_{i=m+1}^{\infty} [\alpha_{ij}(\omega)]^2$

Therefore, expanding $x(t, \omega)$ on the right hand side of 4.16 and

using the orthonormality of $\{\phi_{ij}(t)\}$

$$\mathcal{E} \sum_{i=m+1}^{\infty} [\alpha_{ij}(\omega)]^2 \leq \mathcal{E} \int_{T_{j-1}}^{T_j} \left[\sum_{i=1}^{\infty} \alpha_{ij}(\omega) \phi_{ij}(t) - \sum_{i=1}^m \alpha'_{ij}(\omega) \phi_{ij}(t) \right]^2 w(t) dt \quad 4.17$$

$$\mathcal{E} \sum_{i=m+1}^{\infty} [\alpha_{ij}(\omega)]^2 \leq \mathcal{E} \sum_{i=1}^m [\alpha_{ij}(\omega) - \alpha'_{ij}(\omega)]^2 + \mathcal{E} \sum_{i=m+1}^{\infty} [\alpha_{ij}(\omega)]^2 \quad 4.18$$

Equation 4.18 obviously checks and equality holds only when $\alpha'_{ij}(\omega) = \alpha_{ij}(\omega)$. Thus the $\alpha_{ij}(\omega)$ given by equation 4.15 are optimal.

The integrand of the cost of equation 4.7 can now be expanded and the orthonormality of the basis functions and equation 4.15 for $\{\alpha_{ij}^*(\omega)\}$ used to obtain:

$$J_{2,N} = \mathcal{E} \left\{ \sum_{j=1}^N \int_{T_{j-1}}^{T_j} x^2(t, \omega) w(t) dt - \sum_{j=1}^N \sum_{i=1}^{m_j} [\alpha_{ij}(\omega)]^2 \right\} \quad 4.19$$

Now substitute for $\alpha_{ij}^*(\omega)$ from equation 4.15 to arrive at:

$$J_{2,N} = \sum_{j=1}^N \int_{T_{j-1}}^{T_j} \mathcal{E} \left(x^2(t, \omega) \right) w(t) dt - \sum_{j=1}^N \sum_{i=1}^{m_j} \mathcal{E} \left(\left(\int_{T_{j-1}}^{T_j} x(t, \omega) w(t) \phi_{ij}(t) dt \right)^2 \right)$$

4.20

Define

$$\mathcal{E} \left\{ x(t, \omega) x(t', \omega) \right\} \triangleq R(t, t')$$

4.21

For $\Gamma = \Omega$ this is the covariance function of the process.

and for $\Gamma = \omega_p$ it is simply the product of the value of the sample-function ω_p at two different times.

Then

$$J_{2,N} = \sum_{j=1}^N \int_{T_{j-1}}^{T_j} R(t, t) w(t) dt - \sum_{j=1}^N \sum_{i=1}^{m_j} \int_{T_{j-1}}^{T_j} \int_{T_{j-1}}^{T_j} R(t, t') w(t) w(t') \phi_{ij}(t) \phi_{ij}(t') dt' dt$$

4.22

Now it remains to minimize over the set $\{\phi_{ij}(t)\}$ subject to the constraint

$$\int_{T_{j-1}}^{T_j} \phi_{ij}(t) w(t) \phi_{kj}(t) dt = \delta_{ik} \quad 4.23$$

4.3.3 Optimal Basis Functions.

Consider the problem:

$$J_{2,N}^* = \underset{\{\phi_j\}}{\text{Min}} J_{2,N}(\{\alpha_j^*\}, \{\phi_j\}, \{m_j\}, \Pi) \quad 4.24$$

Dynamic programming will be used to solve this problem. The solution parallels closely that of section 2.4 for the K-L expansion.

Define

$$\begin{aligned} J_{m_1, m_2, \dots, m_N}(\alpha^*, \phi^*) &= \underset{\{\phi_{ij} \dots \phi_{m_j, j}\}}{\text{Min}} J_{m_1, m_2, \dots, m_N}(\alpha^*, \phi) \\ &\quad \forall j \\ &= \underset{\phi_{m_k, k}}{\text{Min}} J_{m_1, m_2, \dots, (m_k-1), \dots, m_N}(\alpha^*, \phi^*) \end{aligned} \quad 4.25$$

Equation 4.25 is a recursion relation for the minimal cost (with appropriately simplified notation) where the recursion is on the index m_k indicating the number of basis functions used in segment k .

The minimization must be carried out using the constraint equation 4.5 which is adjoined to the cost using Lagrange multipliers $\{\gamma_{ij}\}$.

Consider using one basis function in segment k .

$$\begin{aligned}
 J_{m_1, \dots, m_k=1, \dots, m_N}(\alpha^*, \phi) = & \sum_{j=1}^N \left[\int_{T_{j-1}}^{T_j} R(t, t) w(t) dt - \sum_{i=1}^{m_j} \int_{t, t'=T_{j-1}}^{T_j} \phi_{ij}(t) w(t) R(t, t') w(t') \phi_{ij}(t') dt dt' \right] \\
 & + \sum_{j=1}^N \sum_{i=1}^{m_j} \gamma_{ij} \left(\int_{T_{j-1}}^{T_j} \phi_{ij}(t) w(t) \phi_{ij}(t) dt - 1 \right) \quad 4.26
 \end{aligned}$$

Then set

$$\frac{\partial J_{m_1, \dots, m_k=1, \dots, m_N}(\alpha^*, \phi)}{\partial \phi_{ik}(t)} = 0$$

4.27

which yields

$$-2 \int_{t'=T_{k-1}}^{T_k} w(t) R(t, t') w(t') \phi_{1k}(t') dt' + 2 \gamma_{1k} w(t) \phi_{1k}(t) = C$$

4.28

or

$$w(t) \int_{t'=T_{k-1}}^{T_k} R(t, t') w(t') \phi_{1k}(t') dt' = \gamma_{1k} w(t) \phi_{1k}(t)$$

4.29

Since $w(t) \neq 0 \forall t \in [T_{k-1}, T_k]$ it must be that

$$\int_{t'=T_{k-1}}^{T_k} R(t, t') w(t') \phi_{1k}(t') dt' = \gamma_{1k} \phi_{1k}(t)$$

4.30

Substituting from equation 4.30 into J as given by equation 4.26

$$J_{m_1, \dots, m_k=1, \dots, m_N}(\alpha^*, \phi) = \sum_{j=1}^N \left[\int_{T_{j-1}}^{T_j} w(t) R(t, t) dt - \sum_{i=1}^{m_j} \int_{t=T_{j-1}}^{T_j} \phi_{ij}(t) w(t) \left\{ \int_{t'=T_{j-1}}^{T_j} R(t, t') w(t') \phi_{ij}(t') dt' \right\} dt \right]$$

$$+ \sum_{\substack{j=1 \\ j \neq k}}^N \sum_{i=1}^{m_j} \gamma_{ij} \left(\int_{T_{j-1}}^{T_j} \phi_{ij}(t) w(t) \phi_{ij}(t) dt - 1 \right)$$

4.31

The inner integral in the second term becomes $\gamma_{1k}^* \phi_{1k}(t)$ in segment k (for j=k). Then the second term becomes γ_{1k}^* for j=k due to the orthonormality of the $\{\phi_{ij}\}$'s.

$$\begin{aligned}
 J_{m_1, \dots, m_k=1, \dots, m_N}(\alpha^*, \phi) &= \sum_{j=1}^N \int_{T_{j-1}}^{T_j} w(t) R(t, t) dt - \sum_{\substack{j=1 \\ j \neq k}}^N \sum_{i=1}^{m_j} \int_{T_{j-1}}^{T_j} \phi_{ij}(t) w(t) \int_{T_{j-1}}^{T_j} R(t, t') w(t') \phi_{ij}(t') dt' dt \\
 &\quad - \gamma_{1k}^* + \sum_{\substack{j=1 \\ j \neq k}}^N \sum_{i=1}^{m_j} \gamma_{ij} \left(\int_{T_{j-1}}^{T_j} \phi_{ij}(t) w(t) \phi_{ij}(t) dt - 1 \right)
 \end{aligned}$$

4.32

The constraint for j=k is satisfied, hence that term drops out of the summation over the constraints. Clearly γ_{1k}^* must be the maximum eigenvalue of the integral equation of 4.30 since this will minimize $J_{m_1, \dots, m_k=1, \dots, m_N}$.

Staying in segment k, the next stage is to look for $\phi_{2k}^*(t)$

Clearly,

$$J_{m_1, \dots, m_k=2, \dots, m_N}(\alpha^*, \phi) = J_{m_1, \dots, m_k=1, \dots, m_N}(\alpha^*, \phi) - \int_{T_{k-1}}^{T_k} \int_{T_{k-1}}^{T_k} \phi_{2k}(t) w(t) R(t, t') w(t') \phi_{2k}(t') dt dt'$$

4.33

Now using the recursive relation of equation 4.25 it is only required to minimize over $\phi_{2k}(t)$:

$$J_{m_1 \dots m_k=2 \dots m_N}(\alpha^*, \phi) = \text{Min}_{\phi_{2k}(t)} \left\{ J_{m_1 \dots m_k=1 \dots m_N}(\alpha^*, \phi^*) - \int_{t, t'=T_{k-1}}^{T_k} \phi_{2k}(t) w(t) R(t, t') w(t') \phi_{2k}(t') dt' dt \right. \\ \left. + \gamma_{2k} \left(\int_{T_{k-1}}^{T_k} \phi_{2k}(t) w(t) \phi_{2k}(t) dt - 1 \right) \right\} \quad 4.34$$

Setting

$$\frac{\partial J_{m_1 \dots m_k=2 \dots m_N}(\alpha^*, \phi)}{\partial \phi_{2k}(t)} = 0 \quad 4.35$$

it is again obtained that

$$\int_{t'=T_{k-1}}^{T_k} R(t, t') w(t') \phi_{2k}(t') dt' = \gamma_{2k} \phi_{2k}(t) \quad 4.36$$

Substituting from equation 4.36 into equation 4.34

$$J_{m_1 \dots m_k=2 \dots m_N}(\alpha^*, \phi^*) = J_{m_1 \dots m_k=1 \dots m_N}(\alpha^*, \phi^*) - \gamma_{2k}^* \quad 4.37$$

Clearly γ_{2k}^* must be the second largest eigenvalue of the integral equation of 4.36 in order to minimize the right-hand-side of equation 4.37.

Proceeding in this manner it is concluded that, if the eigenvalues of the integral equation of 4.36 are ordered monotonically as

$$\gamma_{1k}^* > \gamma_{2k}^* > \gamma_{3k}^* \dots \quad k = 1, 2, \dots, N \quad 4.38$$

then the optimal basis function $\phi_{ik}^*(t)$ is the eigenfunction corresponding to γ_{ik}^* .

Finally Mercer's theorem [19] can be invoked to rewrite the optimal cost. By Mercer's theorem

$$R(t, t') = \sum_{i=1}^{\infty} \gamma_{ik} \phi_{ik}(t) \phi_{ik}(t') \quad \forall t, t' \in [T_{k-1}, T_k] \quad 4.39$$

Thus

$$R(t, t) = \sum_{i=1}^{\infty} \gamma_{ik} \phi_{ik}^2(t) \quad \forall t \in [T_{k-1}, T_k] \quad 4.40$$

Therefore

$$\begin{aligned} \sum_{j=1}^N \int_{T_{j-1}}^{T_j} w(t) R(t, t) dt &= \sum_{j=1}^N \sum_{i=1}^{\infty} \gamma_{ij} \int_{T_{j-1}}^{T_j} \phi_{ij}(t) w(t) \phi_{ij}(t) dt \\ &= \sum_{j=1}^N \sum_{i=1}^{\infty} \gamma_{ij} \end{aligned} \quad 4.41$$

Hence the optimal cost using m_1, m_2, \dots, m_N features respectively in segments $1, 2, \dots, N$ is:

$$J_{m_1, m_2, \dots, m_N}(\alpha^*, \phi^*) = \sum_{j=1}^N \sum_{i=m_j+1}^{\infty} \gamma_{ij} \quad 4.42$$

or in terms of the expected energy of the process $x(t, \cdot)$, this can be restated as:

$$J_{m_1, m_2, \dots, m_N}(\alpha^*, \phi^*) = \sum_{j=1}^N \left[\int_{T_{j-1}}^{T_j} w(t) R(t, t) dt - \sum_{i=1}^{m_j} \gamma_{ij}^* \right] \quad 4.43$$

4.3.4 Optimal Knots.

The next stage of the optimization is to determine the partition Π^* with respect to which the general ensemble representation is truly optimal. Given a set of knots, a set of local-expansion orders, and a fixed number of segments for the representation, the representation that minimizes the expected global cost over the ensemble has been obtained in the last sections. It is now desired to optimize this ensemble representation with respect to the set of knots, Π , still assuming N and $\{m_j\}$ to be given. The problem considered is therefore

$$\underset{\Pi}{\text{Min}} J_{2,N}(\{\alpha_j^*\}, \{\phi_j^*\}, \{m_j\}, \Pi) \quad 4.44$$

Dynamic programming is again used to determine the optimal segmentation. Now the cost functional of equation 4.44 is imbedded in a class of functionals dependent on the last knot. Define

$$J_{2,N}^*(T) = \text{Min}_{T_1, T_2, \dots, T_{N-1}} J_{2,N}(T_0, T_1, \dots, T_{N-1}, T) \quad 4.45$$

(Note that $T_0 = 0$ and $T_N = T$ are fixed).

The derivation of section 3.3.2 is followed to obtain the recursive equation for the cost. The recursion is on the number of knots used as before

$$J_{2,M+1}^*(\tau) = \text{Min}_{T_0 \leq T_M \leq \tau} \{ J_{2,M}^*(T_M) + h_2(T_M, \tau) \} \quad 4.46$$

and $0 \leq \tau \leq T$ for $M = 1, 2, \dots, N-1$ with

$$J_{2,1}^*(\tau) = h_2(0, \tau) \quad \tau \in [0, T] \quad 4.47$$

and

$$h_2(t_1, t_2) = \mathcal{E} \int_2(\alpha, \{\underline{\phi}\}, m, t_1, t_2, \omega)$$

$$\begin{aligned} 0 &\leq t_1 < t_2 \\ t_2 &\in [0, T] \end{aligned}$$

4.48

$J_{2,1}^*(\tau)$ of equation 4.47 is just the expected global K-L cost over the interval $[0, \tau]$ for a K-L-expansion with m_1 terms. The incremental cost $h_2(T_M, \tau)$ is just the cost incurred in the segment from T_M to τ . This cost has been computed in section 4.3.3 and is simply

$$h(T_M, \tau) = \sum_{i > m_{M+1}} \gamma_{iM+1}^* = \int_{T_M}^{\tau} R(t, t) w(t) dt - \sum_{i=1}^{m_{M+1}} \gamma_{iM+1}^* \quad 4.49$$

where $\{\gamma_{iM+1}^*\}$ are the ordered eigenvalues of the local covariance kernel over the segment $[T_M, \tau]$. Hence the recursive equation of 4.46 now becomes

$$J_{2, M+1}^*(\tau) = \text{Min}_{0 \leq T_M \leq \tau} \left\{ J_{2, M}^*(T_M) + \int_{T_M}^{\tau} R(t, t) w(t) dt - \sum_{i=1}^{m_{M+1}} \gamma_{iM+1}^* \right\} \\ M=1, 2, \dots, N-1 \quad 4.50$$

or

$$J_{2, M+1}^*(\tau) = \text{Min}_{0 \leq T_M \leq \tau} \left\{ J_{2, M}^*(T_M) + \sum_{i > m_{M+1}} \gamma_{iM+1}^* \right\} \\ M=1, 2, \dots, N-1 \quad 4.51$$

for

In order to carry out the dynamic programming of equation 4.51, the following needs to be computed

$$E(t_1, t_2) = \int_{t_1}^{t_2} R(t, t) w(t) dt \quad \forall t_1 < t_2 \quad t_1, t_2 \in [0, T] \quad 4.52$$

where $E(t_1, t_2)$ is the weighted expected energy of the process $x(t, \cdot)$

in the interval $[t_1, t_2]$ or the weighted energy of the single sample-function ω_p depending on whether Γ is Ω or ω_p .

The dominant m_{max} eigenvalues and eigenfunctions of the following integral equations must also be computed:

$$\int_{\tau=t_1}^{t_2} R(t, \tau) w(\tau) \phi(\tau) d\tau = \gamma \phi(\tau) \quad \forall t_1 < t_2$$

$$t_1, t_2 \in [0, T] \quad 4.53$$

where

$$m_{max} = \text{Max} \{m_1, m_2, \dots, m_N\} \quad 4.54$$

Once $E(t_1, t_2)$ and all the above basis functions and eigenvalues are available, the recursive equation 4.51 can be solved for the optimal cost $J_{2,N}^*(T)$ for using N segments (or $N-1$ knots) over the interval $[0, T]$ and the optimal knot locations can be determined as well as in section 3.3.2. In the next section it is demonstrated how optimal local orders $\{m_j^*\}$ can be determined by constraining the error to satisfy local constraints. Then it is not needed to compute as many as m_{max} eigenfunctions for each region.

4.3.5 Local Error Constraints and Optimal Local Expansion Orders.

In the optimization problem only an ensemble global-error has so far been considered. Suppose that an ensemble local-error tolerance function $\mathcal{E}(t_1, t_2)$ can be defined as follows. The total expected energy of the weighted error allowed in region $[t_1, t_2]$ is at most $\mathcal{E}(t_1, t_2)$.

That is:

$$h_2(t_1, t_2) \leq \varepsilon(t_1, t_2) \quad \forall t_1 < t_2 \quad t_1, t_2 \in [0, T]$$

4.55

The local-error tolerance function $\varepsilon(t_1, t_2)$ is assumed to be prescribed for the problem at hand. Note that $\varepsilon(t_1, t_2)$ must obey the following positivity and monotonicity requirements since it is a cumulative error function over the interval $[t_1, t_2]$:

$$\varepsilon(t_1, t_2) \geq 0 \quad \forall t_1 < t_2 \quad t_1, t_2 \in [0, T]$$

4.56

with

$$\varepsilon(t_1, t_2) = 0 \quad \text{iff } t_1 = t_2$$

Also given $t_1 < t_2$, $t_3 < t_4$, and $[t_1, t_2] \subset [t_3, t_4]$,

it must be that

$$\varepsilon(t_1, t_2) \leq \varepsilon(t_3, t_4) \quad \forall t_1, t_2, t_3, t_4 \in [0, T]$$

4.57

Finally the following upper-bound must hold:

$$\varepsilon(t_1, t_2) \leq E(t_1, t_2) \quad \forall t_1 < t_2 \quad t_1, t_2 \in [0, T]$$

4.58

Equation 4.58 states that the expected error energy in any interval is upper bounded by the expected energy of the process over that interval. Therefore to make the local constraints inactive over any interval $[t_1, t_2]$, one only need prescribe $\varepsilon(t_3, t_4)$ to satisfy equation 4.58 with equality for all $[t_3, t_4] \subset [t_1, t_2]$.

Assuming that the $\varepsilon(t_1, t_2)$ appropriate for the problem is given, the local constraints of equation 4.55 can be directly incorporated into the dynamic programming for the knots of equation 4.46. From equation 4.49, and constraints of equation 4.55, the following is obtained

$$h_2(t_1, t_2) = \sum_{i > m} \gamma_i^* \leq \varepsilon(t_1, t_2) \quad 4.59$$

Therefore m , denoting the order of expansion needed over the interval $[t_1, t_2]$, must be chosen to satisfy equation 4.59. Since the objective is to achieve a representation with a minimal number of features, the smallest order m^* to satisfy the local constraint for the region $[t_1, t_2]$ must be selected.

The dynamic programming of equation 4.46 or 4.51 is now constrained to satisfy equation 4.55. The appropriate local orders of expansion can be incorporated directly into the computation of $h_2(t_1, t_2)$. The number of dominant eigenfunctions of the integral equations 4.53 needed will be determined uniquely via the constraints of equation 4.59. The local constraints bound the expected error energy in any particular interval for the ensemble-based formulation, $\Gamma = \Omega$. In the sample-based problem, $\Gamma = \omega_p$, the actual error energy for sample-function

is bounded on each interval.

4.4 The Chebyshev Case.

4.4.1 Global Cost Function.

In this formulation, consider the following global cost functional:

$$J_{\infty, N}(\{\alpha_j\}, \{\phi_j\}, \{m_j\}, \Pi) = \text{Max}_{\omega \in \Gamma} \text{Max}_{j=1, \dots, N} \mathcal{J}_{\infty}(\alpha_j, \{\phi_j\}, m_j, T_{j-1}, T_j, \omega) \quad 4.60$$

where the segment Chebyshev cost is

$$\mathcal{J}_{\infty}(\alpha_j, \{\phi_j\}, m_j, T_{j-1}, T_j, \omega) = \text{Max}_{T_{j-1} \leq t \leq T_j} |e(\alpha_j, \{\phi_j\}, m_j, t, \omega)| \quad 4.61$$

The pointwise error $e(\alpha_j, \{\phi_j\}, m_j, t, \omega)$ and the estimate in segment j are given by equations 4.9 and 4.10 respectively. The ensemble-based and sample-based alternatives result, again, depending on whether $\Gamma = \Omega$ or $\Gamma = \omega_p$. For the case $\Gamma = \Omega$ the same considerations discussed in 3.2.3 apply.

The optimization problem considered here is

$$J_{\infty, N}^*(\{\alpha_j^e\}, \{\phi_j^e\}, \{m_j\}, \Pi^*) = \text{Min}_{\Pi} J_{\infty, N}(\{\alpha_j^e\}, \{\phi_j^e\}, \{m_j\}, \Pi) \quad 4.62$$

Optimizing for the basis functions $\{\phi_j\}$ (and thereby coefficients $\{\alpha_j\}$) is not meaningful in the case of the sample-based problem ($\Gamma = \omega_p$) if the objective is feature extraction. The reason is that basis functions then become features leading to an infinite-dimensional feature space as discussed earlier. In case of the ensemble-based

Chebyshev problem, optimizing for the basis functions is analytically intractable and is a difficult problem in practice. Therefore optimization with respect to the basis functions is not considered for either the ensemble or sample-based Chebyshev problems. Instead, the L_2 -ensemble-optimal basis functions (here denoted by $\{\Phi_j^e\}$) derived in section 4.3.3 for $\Gamma = \Omega$, are chosen as a canonical basis that incorporates ensemble information. Having selected this basis, the optimal coefficients $\{\alpha_j^e\}$ follow as before (section 4.3.2).

The local orders of expansion $\{m_j\}$ and the total number of segments N are parameters to be optimized in later sections with the objective of satisfying local error constraints and minimizing a "feature extraction cost" (related to the total number of features used).

4.4.2 Optimal Knots.

Dynamic programming is again used by formulating a recursion on the knots. Following the derivation of section 3.3.3 a closely similar recursive equation is obtained

$$J_{\infty, M+1}^*(\tau) = \text{Min}_{T_0 \leq T_M \leq \tau} \left\{ \text{Max}_{M=1,2,\dots,N-1} \left[J_{\infty, M}^*(T_M) ; h_{\infty}(T_M, \tau) \right] \right\} \quad 4.63$$

with

$$J_{\infty, 1}^*(\tau) = h_{\infty}(0, \tau) \quad \tau \in [0, T] \quad 4.64$$

The cost $J_{\infty, 1}^*(T)$ of equation 4.64 is the actual maximum weighted pointwise error over the interval $[0, T]$ incurred in representing

sample-function ω , using a global K-L expansion with m_1 terms.

In order to carry out the dynamic programming of equation 4.63 the quantity $\mathcal{J}_\infty(\alpha_j, \{\phi_j\}, m_j, T_{j-1}, T_j; \omega)$ must be computed on line, that is,

$$h_\infty(t_1, t_2) = \text{Max}_{\omega \in \Gamma} \mathcal{J}_\infty(\alpha, \{\phi\}, m, t_1, t_2, \omega) \quad 4.65$$

To compute $h_\infty(t_1, t_2)$ the set $\{m_j\}$ and N are required.

These parameters can be chosen based on some ensemble consideration.

It is, however, also feasible to impose sample function local constraints to determine a set of sample-dependent local expansion orders (features).

This consideration is treated in the next section.

4.4.3 Local Error Constraints and Optimal Local Expansion Orders.

With the Chebyshev formulation, it can be required that the representation satisfy pointwise local constraints. Given an appropriate measure of tolerance $\epsilon_\infty(t_1, t_2)$, the following constraints are imposed.

$$h_\infty(t_1, t_2) \leq \epsilon_\infty(t_1, t_2) \quad 4.66$$

The error tolerance function $\epsilon_\infty(t_1, t_2)$ must obey the same positivity and monotonicity requirements as given by equations 4.56 and 4.57. The upper bound of equation 4.58 must now be replaced by

$$\epsilon_\infty(t_1, t_2) \leq \text{Max}_{\omega \in \Gamma} \text{Max}_{t_1 \leq t \leq t_2} |x(t, \omega)| \quad 4.67$$

Letting $\epsilon_{\infty}(t_1, t_2)$ satisfy equation 4.67 with equality for all $[t_3, t_4] \subset [t_1, t_2]$ will render the local constraints inactive over the interval $[t_1, t_2]$.

Assuming that the $\epsilon_{\infty}(t_1, t_2)$ appropriate for the problem at hand is given, the local constraints of equation 4.67 can be directly incorporated into the dynamic programming for the knots of equation 4.63. Again, the smallest local expansion order m_j^* to satisfy the local constraint for the region indexed by j must be selected. The dynamic programming of equation 4.63 is now constrained to satisfy the local constraints of 4.67. The appropriate local orders of expansion are thus directly incorporated into the computation of $h_{\infty}(t_1, t_2)$.

The Chebyshev norm approach is a highly desirable one in practice since the representation error is then controlled for each time-point and possibly for each sample-function if the sample-based case is used. Choosing an appropriate tolerance function $\epsilon_{\infty}(t_1, t_2)$ is also relatively easy since this corresponds to the maximum absolute error allowed over the region $[t_1, t_2]$.

4.5 Optimal Number of Segments for Feature Extraction.

4.5.1 Introduction.

Throughout the optimization of the feature extractor N , the number of segments used was considered to be fixed a priori. So far, the optimal segmented representation, given the number of segments, N , that minimizes expected global error while satisfying local expected error constraints was determined.

Since the goal of the representation is feature extraction, a measure of the cost of using the features required to achieve the local constraints must now be optimized while minimizing expected global error. The features needed to characterize a sample waveform $x(t, \omega)$ will depend on whether the ensemble or sample-based problem is considered. The measure of the "cost of feature extraction" can be taken to be the total number of features in the case of the linear ensemble-based problem. In the case of the nonlinear sample-based problems various weight factors should be considered to account for the "relative cost" of using linear vs. nonlinear or real vs. integer features.

4.5.2 Linear Feature Extraction.

In the ensemble-based problem for the L_2 -norm, where $\Gamma = \Omega$ and the expectations are therefore taken over the whole sample space, the optimal basis functions $\{\phi_j^*\}$, the optimal knots Π^* , and the minimal local expansion orders $\{m_j^*\}$, are determined once and fixed for the entire ensemble. These parameters are common to all sample-functions and are therefore not features. The only sample-function-dependent parameters are then the coefficients $\{\alpha_j^*(\omega)\}$. These coefficients are linear in the data $x(t, \omega)$ as shown earlier. Thus the ensemble-based problem leads to a linear feature extractor.

In the ensemble-based problem, the total number of features required for a given number of segments N , is then

$$F(N) = \sum_{j=1}^N m_j^* \quad 4.68$$

For $N = 1$ the global K-L expansion over the 1 segment (the total interval) $[0, T]$ is obtained. The quantity $F(1)$ is the total number of global K-L terms needed to satisfy the local constraints specified by the local error tolerance function $\epsilon_2(t_1, t_2)$.

The behavior of $F(N)$ as a function of N will depend on the problem at hand and on the choice of the error tolerance function. The optimal number of segments, N^* , to use, from the point of view of feature extraction, can be determined by searching for:

$$F(N^*) = \underset{N}{\text{Min}} F(N) = \underset{N}{\text{Min}} \sum_{j=1}^N m_j^* \quad 4.69$$

Note that $F(N)$ can be computed very easily at each stage of the dynamic programming for the knots. The behavior of the (constrained) feature-extractor as N increases can thus be tracked. Suppose that there is an upper limit, N_{\max} , to the number of features allowed. The absolutely minimum number of local features needed is one per segment, regardless of the number of segments. Therefore, if $\epsilon(t_1, t_2) < E(t_1, t_2)$ for all $t_1 < t_2, t_1, t_2 \in [0, T]$, then

$$F(N) \geq N_{\max} \quad \text{for } N \geq N_{\max} \quad 4.70$$

Thus the search for the minimum of $F(N)$ of equation 4.69 can then be replaced by a finite search:

$$F(N^*) = \text{Min} \{F(1), F(2), \dots, F(N_{\max})\} \quad 4.71$$

to t_2 . In Figure 4.1 the following reasonable assumptions were made:

$$(i) \quad \varepsilon_2(t_1, t_2) < E(t_1, t_2) \quad \text{for } t_1 < t_2, \text{ and } t_1, t_2 \in [0, T] \quad 4.72$$

(ii) The longest segment tends to zero as N tends to infinity; i.e.

$$\lim_{N \rightarrow \infty} \left\{ \max_j [T_j - T_{j-1}] \right\} = 0 \quad 4.73$$

(iii) The error incurred with the single dominant K-L term tends to zero, as the segment length becomes vanishingly small, faster than the tolerance function, i.e.:

$$\lim_{\Delta t \rightarrow 0} \left[\int_t^{t+\Delta t} R(\tau, \tau) d\tau - \gamma_{\max}^*(t, t+\Delta t) \right] \leq \lim_{\Delta t \rightarrow 0} \varepsilon_2(t, t+\Delta t) \leq \lim_{\Delta t \rightarrow 0} \int_t^{t+\Delta t} R(\tau, \tau) d\tau \quad 4.74$$

If conditions (i) and (ii) hold, then

$$\int_{T_{j-1}}^{T_j} R(t, t) dt - \gamma_{\max}^*(T_{j-1}, T_j) \leq \varepsilon_2(T_{j-1}, T_j) \quad \forall j, \forall N \geq N_5 \quad 4.75$$

for some sufficiently large, fixed, N_5 . Then

$$F(N) = N \quad \forall N \geq N_5 \quad 4.76$$

as depicted in Figure 4.1.

Note that N^* is fixed once for the entire ensemble and as such does not become a feature in the feature extraction problem.

The general behavior of $F(N)$ is depicted in Figure 4.1.

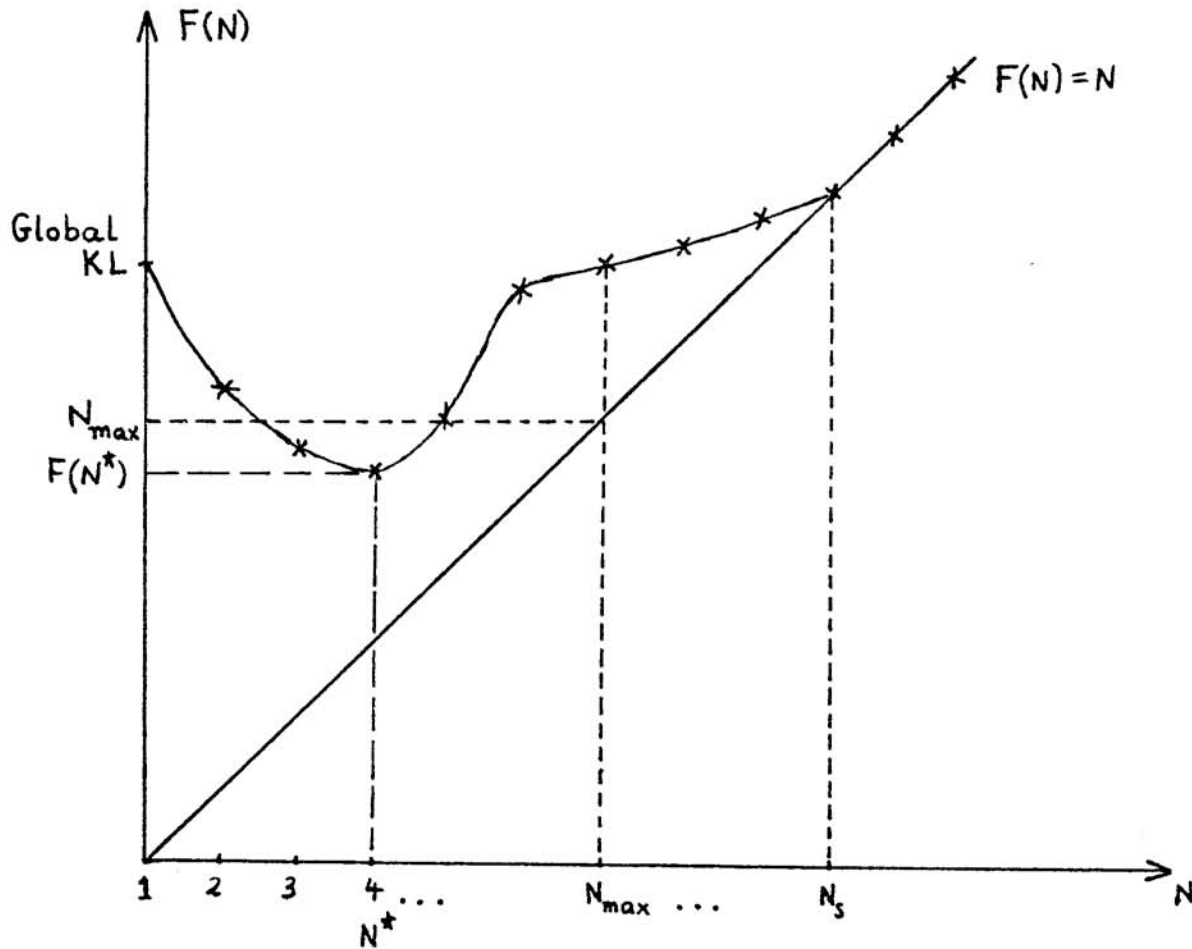


Figure 4.1: Total Number of Features as a Function of the Number of Segments for Linear Feature Extraction.

The $F(N)$ curve can never lie below N . The behavior of $F(N)$ as N becomes large will depend on the behavior of $\epsilon_2(t_1, t_2)$ as t_1 tends

4.5.3 Nonlinear Feature Extraction.

In the sample-based problems (for L_2 and Chebyshev norms), where $\Gamma = \omega_p$ and the expectations become trivial, the optimal knots Π^* , the minimal local expansion orders $\{m_j^*\}$ as well as the coefficients $\{\alpha_j^*(\omega)\}$ become sample-dependent. As discussed earlier, the $\{\phi_j\}$ can be chosen in an ensemble-sense to lead to a meaningful and finite-dimensional feature extraction problem. In that case, the basis functions used are common to all sample functions and therefore not features. Although the coefficients $\{\alpha_j^*(\omega)\}$ are still linear in the data $[X(t, \omega)]$, the knots Π^* , and the local expansion orders $\{m_j^*\}$ are highly nonlinear functions of the data.

The optimal total number of segments N^* is also a parameter that varies with each sample-function in the sample-based problems. It too is a feature and is highly nonlinear in the data. Therefore the resulting feature extractor is a nonlinear one.

Let $K(N)$ denote the total "cost of features" for the sample-based nonlinear representations with N segments. Then

$$K(N) = r_0 \underbrace{\sum_{j=1}^N m_j^*}_{\text{linear coefficients}} + \underbrace{r_1(N-1)}_{\text{nonlinear knot locations}} + \underbrace{r_2 N}_{\text{nonlinear local expansion orders}} + \underbrace{r_3(1)}_{\text{nonlinear number of segments}} \quad 4.77$$

$$K(N) = r_0 \sum_{j=1}^N m_j^* + (r_1 + r_2) N + (r_3 - r_1) \quad 4.78$$

The weights r_0, r_1, r_2, r_3 (all non-negative reals) have been included to account for the fact that coefficients and knot locations are real numbers whereas local expansion orders and the number of segments are (non-negative) integers. The "relative cost" of using real vs. integer or linear vs. nonlinear features in the feature extraction process can thus be accounted for by use of these weight factors.

The behavior of $K(N)$ as a function of N will depend on the problem at hand and on the choice of the error tolerance function. The optimal number of segments, N^* , to use, from the point of view of feature extraction, can be determined by searching for

$$K(N^*) = \underset{N}{\text{Min}} K(N) = \underset{N}{\text{Min}} \left\{ r_0 \sum_{j=1}^N m_j^* + (r_1 + r_2)N \right\} + (r_3 - r_1) \quad 4.79$$

Note that $K(N)$ can be computed very easily at each stage of the dynamic programming for the knots. The behavior of the (constrained) feature-extractor as N increases can thus be tracked. The absolutely minimum number of coefficients needed is one per segment, regardless of the number of segments, if $\epsilon_2(t_1, t_2) < E(t_1, t_2)$ for all $t_1 < t_2$ and $t_1, t_2 \in [0, T]$. Therefore,

$$K(N) \geq (r_0 + r_1 + r_2)N + (r_3 - r_1) \quad 4.80$$

Suppose that there is an upper bound, K_{max} , to the total cost of features allowed. By virtue of equation 4.80.

$$K(N) \geq K_{max} \quad \text{for} \quad N \geq \frac{K_{max} - (r_3 - r_1)}{(r_0 + r_1 + r_2)} \quad 4.81$$

Thus the search for the minimum of $K(N)$ of equation 4.79 can be replaced by a finite search

$$K(N^*) = \text{Min} \{K(1), K(2), \dots, K(I_{\max})\} \quad 4.82$$

where I_{\max} is the smallest integer larger than $\left(\frac{K_{\max} - (r_3 - r_1)}{r_0 + r_1 + r_2}\right)$.
 Provided the dynamic programming for the knots is carried up to I_{\max} , the optimal number of segments to use for representing $x(t, \omega)$ can be automatically determined.

The general behavior of $K(N)$ is depicted in Figure 4.2.

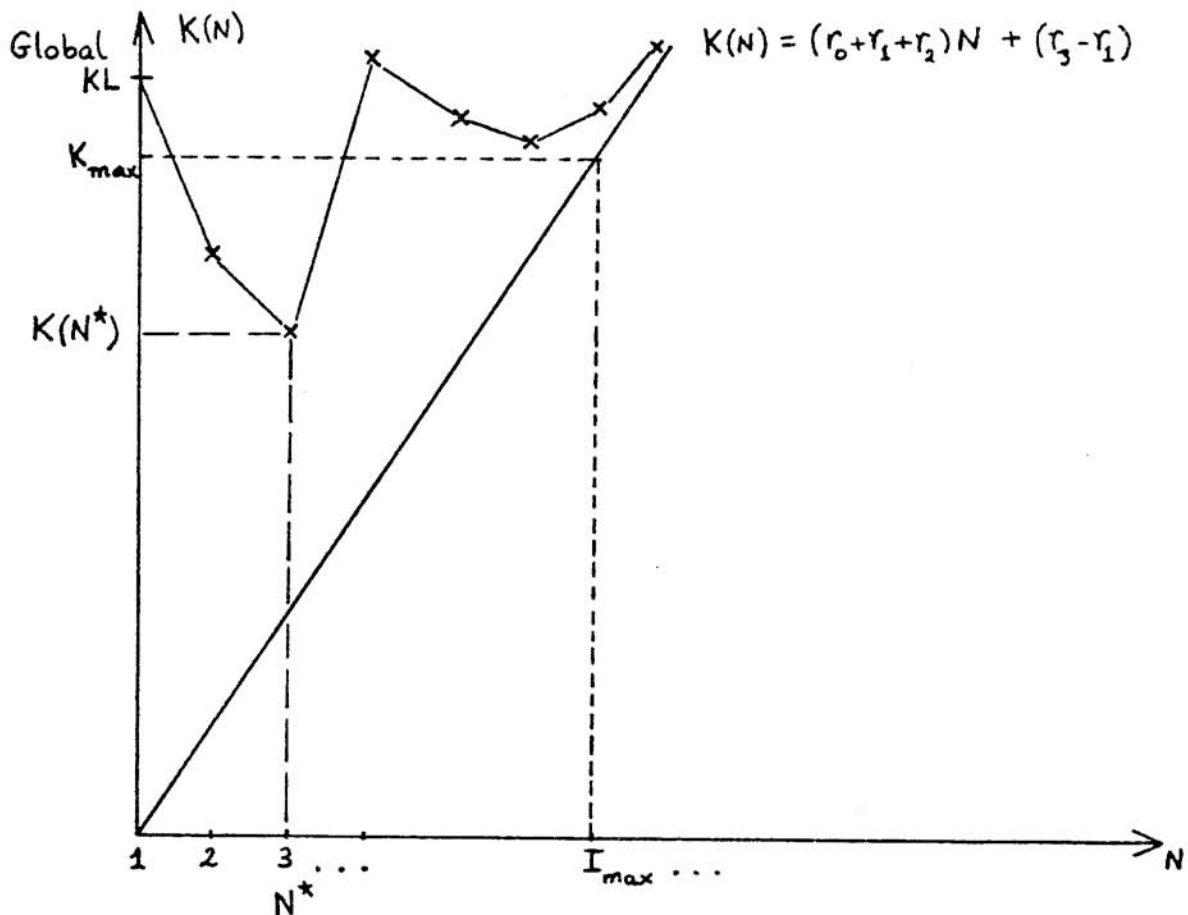


Figure 4.2: Total Number of Features as a Function of the Number of Segments for Nonlinear Feature Extraction.

The $K(N)$ curve can never lie below $(r_0 + r_1 + r_2)N + (r_3 - r_1)$. It is conjectured that for most problems of interest and useful tolerance functions, $K(N)$ tends to $(r_0 + r_1 + r_2)N + (r_3 - r_1)$ for very large N . In any case, in practice, it is the behavior of $K(N)$ for small N that is important. This behavior is entirely problem dependent. However the finite search for $K(N^*)$ can easily be performed together with the dynamic programming for the knots.

The case $N=1$, again, corresponds to a global K-L expansion over the 1-segment (the total interval) $[0, T]$. The quantity

$$\left(\frac{K(1) - (r_2 + r_3)}{r_0} \right) \text{ is the total number of global K-L terms needed}$$

to satisfy the local constraints specified by the error tolerance function. Hence the global K-L is also a special case of these optimal, nonlinear, sample-based representations.

4.6 Error Weighting for Improving Smoothness.

The segmented representations introduced in this chapter are not necessarily continuous across knots. In other words

$$\lim_{\epsilon \rightarrow 0} \hat{x}(T_j - \epsilon, \omega) \neq \lim_{\delta \rightarrow 0} \hat{x}(T_j + \delta, \omega) \quad 4.83$$

A way to control non-smoothness at knots is by penalizing the actual representation error at knots. The estimates are then forced to approach the same limiting value (the actual data point) on either side of knots, as the penalty weights are increased.

Let the weighting function $w(t)$ be given by

$$w(t) = [1 + \lambda(t)] [\delta(t - T_{j-1}) + \delta(t - T_j)] \quad T_{j-1} \leq t \leq T_j \quad 4.84$$

where $\lambda(t) \geq 0$, a continuous function on $[0, T]$, is the penalty for non-smooth behavior at time point t . The following convention for δ -functions will be followed

$$\int_{T_{j-1}}^{T_j} f(t) [\delta(t - T_j) + \delta(t - T_{j-1})] dt = \frac{1}{2} [f(T_{j-1}) + f(T_j)] \quad 4.85$$

The global cost of equation 4.7 now becomes:

$$\begin{aligned} J_{2,N} = \mathcal{E} \left\{ \sum_{j=1}^N \int_{T_{j-1}}^{T_j} [x(t, \omega) - \hat{x}(t, \omega)]^2 dt + \sum_{j=1}^{N-1} \lambda(T_j) \mathcal{E} [x(T_j, \omega) - \hat{x}(T_j, \omega)]^2 \right. \\ \left. + \frac{1}{2} \lambda(0) \mathcal{E} [x(0, \omega) - \hat{x}(0, \omega)]^2 + \lambda(T) \mathcal{E} [x(T, \omega) - \hat{x}(T, \omega)]^2 \right\} \end{aligned} \quad 4.86$$

This is the unweighted expected global cost plus the weighted variance of the error at the knots. The expected error is zero everywhere by construction of the process and the estimate [zero mean process $x(t, \cdot)$ and unbiased estimate $\hat{x}(t, \cdot)$]. Hence it is the variance at the knots that is penalized.

The weighting function of equation 4.83 can be used to independently control the smoothness at knots by an appropriate choice of $\lambda(t)$. As $\lambda(t) \rightarrow \infty$ the optimal eigenfunctions will tend to delta functions centered at the knots in order to pick out the data points $x(T_j, \omega)$ exactly and keep $J_{2,N}$ finite. For finite $\lambda(t)$, the eigenfunctions and coefficients

will be such as to increase accuracy of representations at knots.

Given $\lambda(t)$ the weighting function, $w(t)$, can be incorporated into all phases of the optimization. In practice, the problem will be discretized so that the discrete δ -function will replace the continuous δ -function and no computational difficulties will arise.

The weighting function $w(t)$ of the L_2 representation problem is thus determined by $\lambda(t)$ and the optimal set of knots π^* . This weighting function, in turn, determines the optimal set of ensemble basis functions $\{\phi_j^*\}$ (everything is actually co-determined via the dynamic programming).

Controlling smoothness for the Chebyshev case will be achieved directly via the local constraints. Since the global cost here is a pointwise cost, estimation error at the knots is treated the same way as estimation error over the segment intervals. Upper bounds to both can be specified using the local constraints. The L_∞ approach is again very desirable in practice, this time from the point of view of controlling continuity across the knots. An independent weighting function in the cost is unnecessary here since the same effect can be obtained via the tolerance function.

4.7 Comparisons to Global K-L and Piecewise Polynomial Approximations.

It is worthwhile to compare the K-L expansion of Chapter 2, piecewise polynomial approximation of Chapter 3, and the optimally segmented local K-L methods of this chapter on the basis of their conceptual and fundamental differences. This is done in Table 4.1 for 10 relevant issues. The principal advantage of the KL technique is smoothness and minimization of global L_2 cost for a fixed number of features. The methods of this chapter are superior to the K-L in every other respect and to piecewise polynomials in every respect. Piecewise polynomials, on the other hand, are superior to the K-L in local adaptability and error control, and the

fact that timing (dynamic) information is available in features. The K-L is superior to piecewise polynomials in its use of ensemble information and in its noise rejection capability and smoothness. The optimal methods of this chapter attempt to exploit the advantages of both the K-L and piecewise-polynomial methods, while minimizing the disadvantages, by combining them in a systematic way.

The general methods developed in this chapter reduce to the global K-L or to piecewise polynomials as special limiting cases under specific conditions. Piecewise polynomials are special cases when

- 1) Basis functions are fixed a priori
- 2) The orders of expansion are fixed a priori via the order of the approximating polynomials.
- 3) Local constraints are not imposed.
- 4) Knots are fixed a priori in the case of fixed-knot piecewise polynomials.

The K-L expansion is a special case when

- 1) Only 1-segment is allowed (only two knots, at 0 and T).
- 2) Local constraints are not imposed.
- 3) The cost is restricted to be a weighted L_2 norm.
- 4) The order of the expansion is fixed a priori.

It is also of interest to rank the piecewise polynomial (P.P) and optimally segmented local K-L (OSKL) methods according to the global expected error for a fixed number of features. The following rankings will clearly hold "ceteris paribus", for any measure of the global error

(disregarding the number of features).

- 1) Fixed-knot OSKL no worse than fixed-knot P.P.
- 2) Variable-knot OSKL no worse than fixed-knot OSKL.
- 3) Variable-knot P.P. no worse than fixed-knot P.P.
- 4) Variable-knot OSKL no worse than fixed-knot P.P.

(1) holds since the P.P. case is a special case of the OSKL case.

(2) and (3) hold since the fixed-knot case is a special case of the variable-knot case. (4) holds because of (1) and (2). The only remaining comparisons are:

- 5) Variable-knot P.P. vs. fixed-knot OSKL.
- 6) Variable-knot OSKL vs. variable-knot P.P.

It is in general difficult to rank comparisons (5) and (6).

For (5) the error bounds for variable-knot P.P. of Section 3.4 can be tried and compared to the precomputable expected error rate for the fixed-knot OSKL. This approach may or may not provide a ranking depending on the tightness of the bounds of section 3.4. For (6) the ranking should be obtained via experience with the data to be approximated.

The global K-L of chapter 2 is better than all fixed-knot approaches (since they are linear) for a fixed number of features if the L_2 -norm is used. For other norms and for variable-knot methods the KL may be inferior even for global error minimization for a fixed number of features, depending on the process to be approximated.

Issue	K-L	P.P. Fixed-Knots	P.P. Variable Knots	OSKL Fixed-Knots	OSKL Variable Knots
Type of Feature Extractor	Linear	Linear	Non-Linear	Linear	Non-linear
Features	Coefficients	Coefficients	Coefficients, Knots	Coefficients	Coefficients, Knots, Expansion Orders, Number of Segments
Cost Function	Global Weighted L_2	Arbitrary	Arbitrary	Local Weighted L_2	Arbitrary
Optimal Aspects	Basis Functions over Ensemble	Knots over Ensemble	Knots for Each Sample	Knots and Basis Functions over Ensemble	Knots for Each Sample, Basis Functions over Ensemble (Expansion Orders and Number of Segments)
Use of Ensemble Statistics (A Priori Information)	Yes	Yes	No	Yes	Yes
Adaptability to Individual Sample-Functions	No	Variable	Yes	Yes	Yes
Possibility for Local Control of Error	No	Variable	Yes	Yes	Yes
Noise Rejection	Yes	No	No	Yes	Yes
Smoothness	Yes	Variable	Variable	Variable but generally good	Variable but generally good
On-Line Computation	Fast	Fast	Medium	Fast	Medium-to-Fast with Suboptimal Schemes

Table 4.1

Comparison of K-L, P.P., and OSKL Techniques

CHAPTER 5

APPLICATION TO APPROXIMATION OF CARDIOGRAMS

5.1 Introduction

The global K-L techniques of Chapter 2, the piecewise polynomial techniques (P.P.) of Chapter 3, and the optimally segmented local K-L techniques (OSKL) of Chapter 4 have all been applied to the approximation of cardiographic waveforms.

Cardiography generally deals with the potential differences resulting from the activity of the heart and measured on the surface of the body. The mechanical events of the heart cycle are initiated and accompanied by electrical events. This relationship is exploited by physicians to assess the physiological condition of the heart. There is a considerable body of empirical knowledge that relates the heart's physical condition with potential differences measured by strategically placed sensor leads on the human torso. One of the standard recordings used for clinical diagnosis consists of three time signals known as the vector-cardiogram (VCG) [14]. An idealized plot of the potential difference between two electrodes for the duration of a complete heart cycle is given in Figure 5.1. For a fuller discussion of the generation of the electrical fields and cardiography in general the reader is referred to standard texts [44,45].

The routine analysis of cardiograms is costly in terms of a trained physician's time. Starting in the late 1950's there have been numerous efforts to automate the classification of cardiograms into either normal

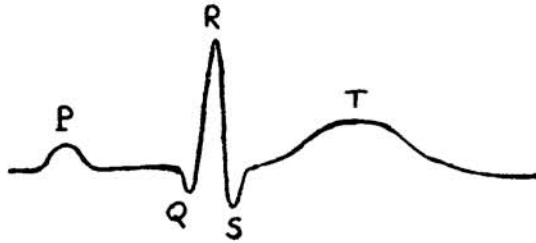


Figure 5.1: Idealized Plot of a Heart Cycle

or various abnormal groups. With most of these techniques, the effort has been to abstract from the waveforms those criteria which physicians have empirically correlated with important aspects of the heart's functioning. These computerized techniques are essentially designed to mimic the cardiographer. However, the imprecise nature of present clinical diagnosis techniques has been illustrated by a study in which 125 patients were analyzed twice independently by nine experienced interpreters. The results were consistent on the average in only 73% of the cases [46]. This is both an argument for automatic classification, and a warning that diagnostic rules based on imitating the cardiographer are not very reliable or consistent.

Although interest in cycle to cycle variation in cardiograms is increasing, most attention to date has been focused on morphological analysis of a single beat, usually a "typical" or average beat taken from a recording. The approximation and analysis here is directed to the morphology of the cardiograms rather than their rhythm characteristics.

Any automated scheme for cardiographic classification must involve basically three steps:

1. Noise, artifact and "bad data" removal;
2. Reduction of the clean typical data;
3. Design of an algorithm for classification.

The study here is concerned with the second step above with respect to the VCG problem. This step represents feature extraction that the VCG must undergo prior to pattern recognition. The pattern recognition problem itself is not investigated here. For studies on the classification of cardiograms using some of the techniques developed here see [6,7,8].

As discussed in section 1.2, in the conservative approach to feature extraction considered here, the objective is to minimize approximation error, over a specified ensemble of records (the data-base), of the reconstructed estimates of each member of the ensemble. Clearly, if all members of an appropriately chosen ensemble can be accurately reconstructed (using visual inspection as a criterion) from lower-dimensional estimates, then diagnostic information will have been retained.

In previous works [6,7] the K-L expansion and the P.P. methods have been used on VCG data with promising results. The objective of these efforts has been to perform a series of extensive trade-off studies

on a data base of 936 patients carefully selected and supplied by the U.S. Air Force School of Aerospace Medicine (USAFSAM). As a result of these studies a prototype VCG Interpretation System which is operational on an IBM/360 computer at USAFSAM has been developed [6].

The original analog VCG data for each patient is sampled at 250 Hz and processed to remove baseline noise and to produce a typical heartbeat wave by averaging up to about 30 heartbeat cycles synchronized at the peaks of the R-waves for averaging. This preprocessing of VCG's is documented more extensively in [13,6]. The resulting discrete data consists of a total of 600 samples for each patient: 200 samples per lead for the 3-lead VCG recorded using a Frank-lead system [45].

5.2 Karhunen-Loève Techniques

Extensive analyses using K-L techniques on the 936 patient data base are reported in [6]. Various factors such as the effects of sampling rate, of using combined vs. separate lead expansions, and of using a weighting factor in the P wave region to reduce the reconstruction errors in that region are studied.

Experimental results indicate that K-L reconstructions require up to 60 terms in the expansion (20 vectors per lead separate, or 60 vectors combined expansion) to approach a generally tolerable level of accuracy from the point of view of a cardiographer. However, even with 60 global K-L features, the 5 or more worst case reconstructions over the 936 patient data-base may not be acceptable. Furthermore using a weighting over the P wave region causes the T wave reconstructions to deteriorate.

Lead 3



Lead 2



Lead 1

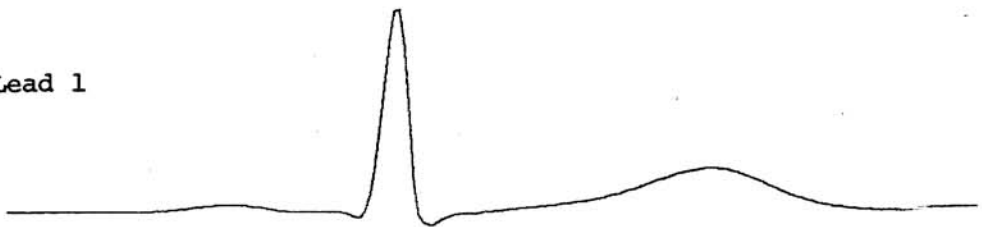


Figure 5.2: Ensemble Mean VCG waveforms for Data-Base of 936 patients.

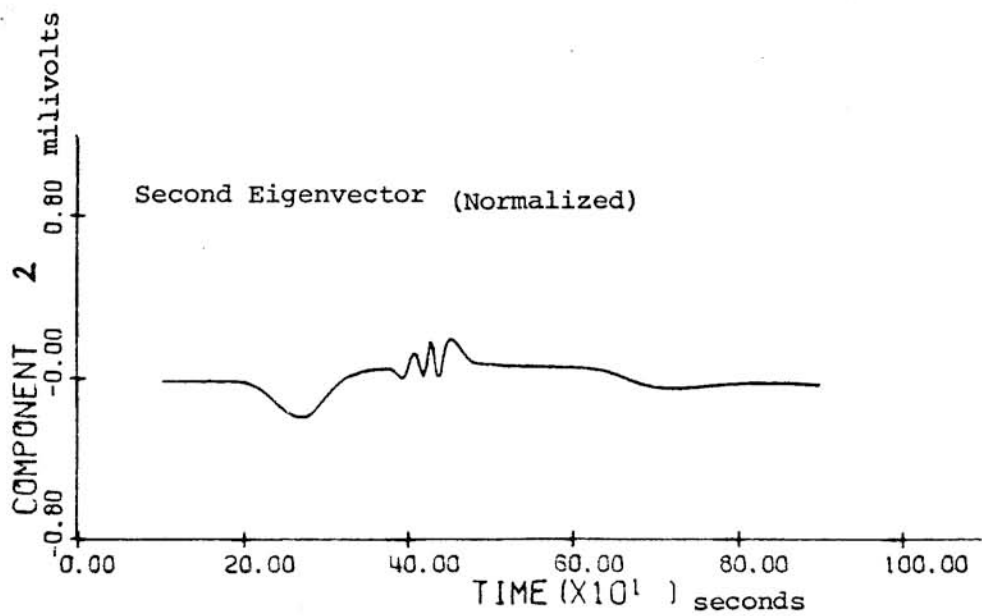
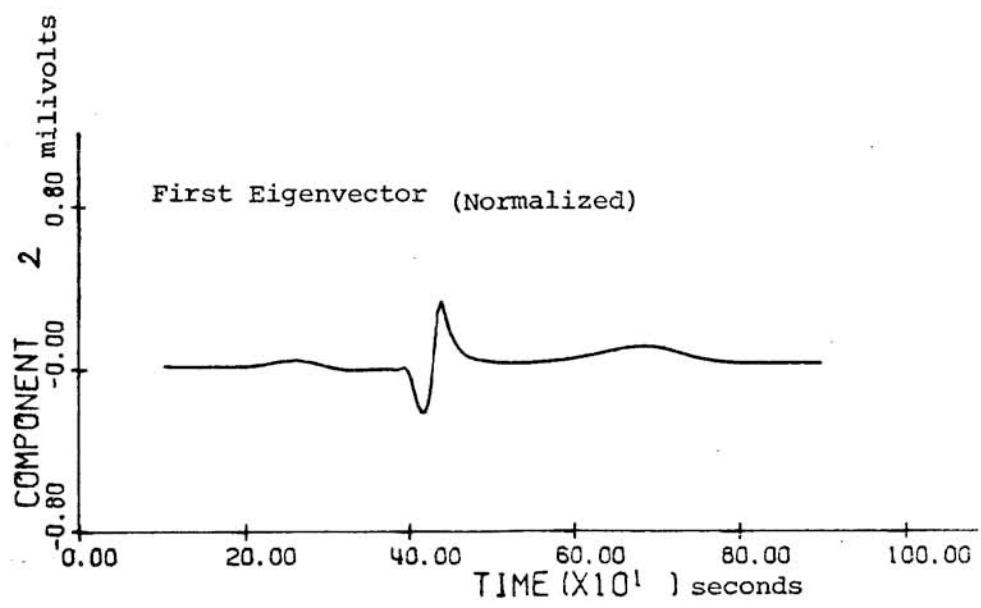


Figure 5.3: First Two Eigenvectors of the 60-th Order Separate-Lead K-L Expansion for Lead 2.

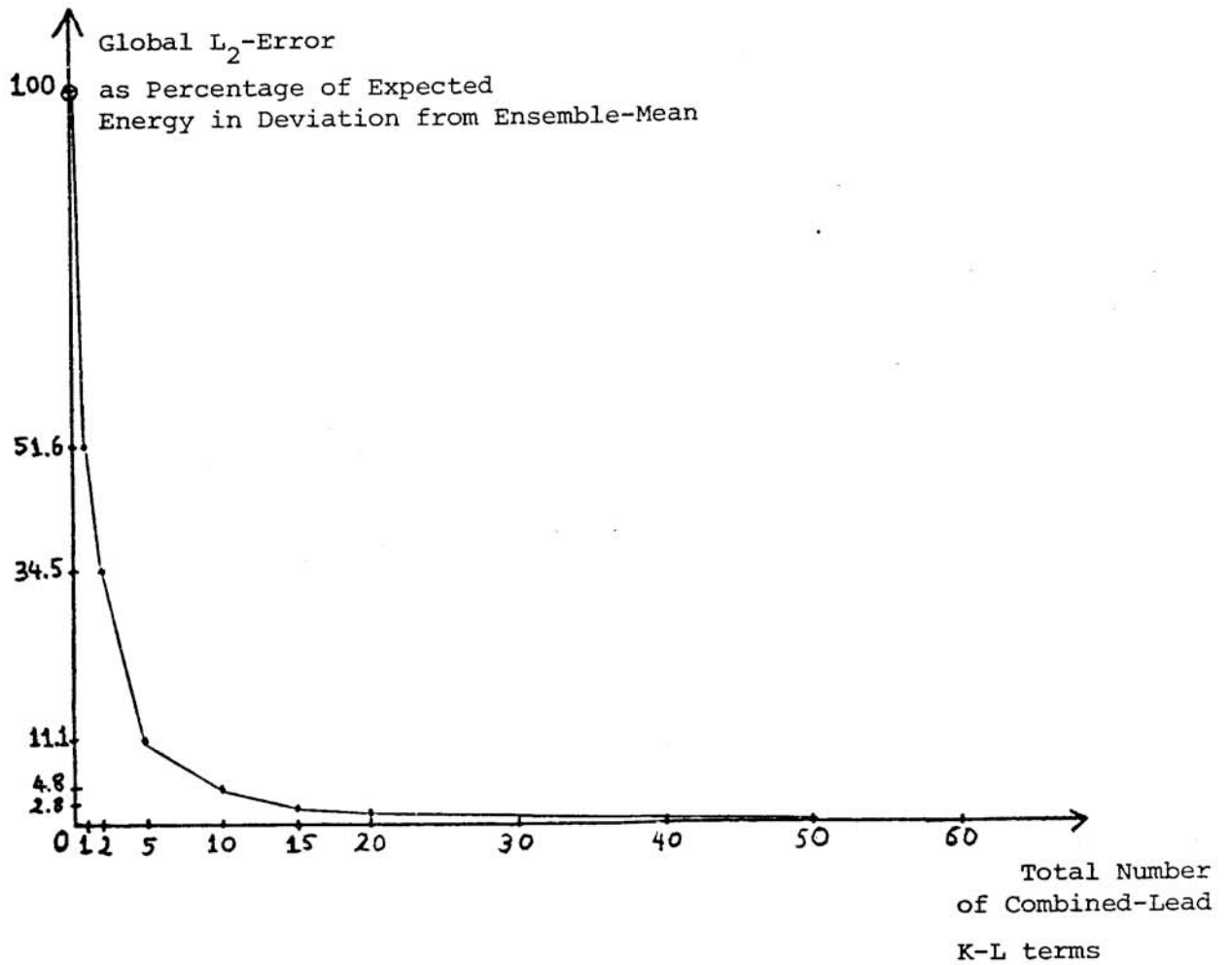


Figure 5.4: Convergence of 60-th Order Combined-Lead
Global K-L as a Function of the Order of Expansion.

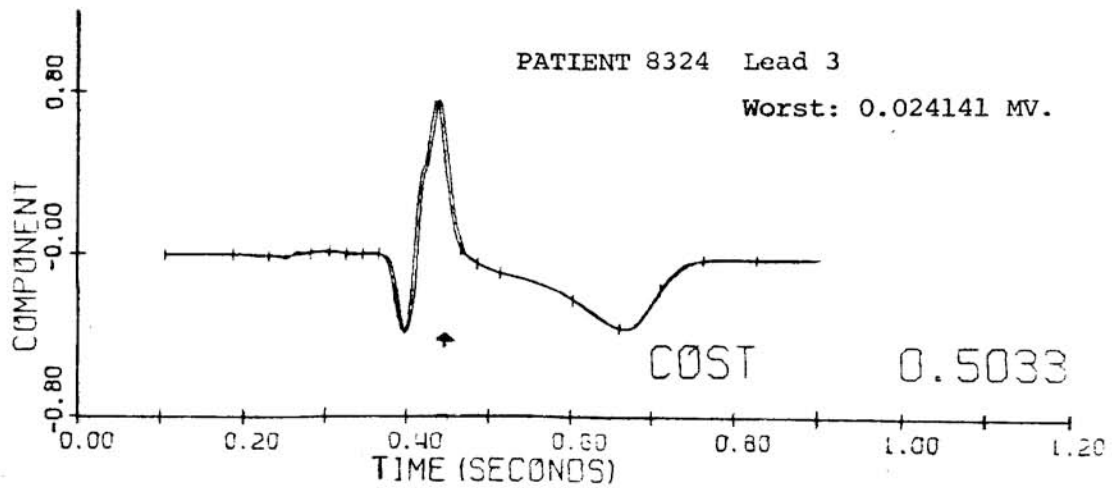
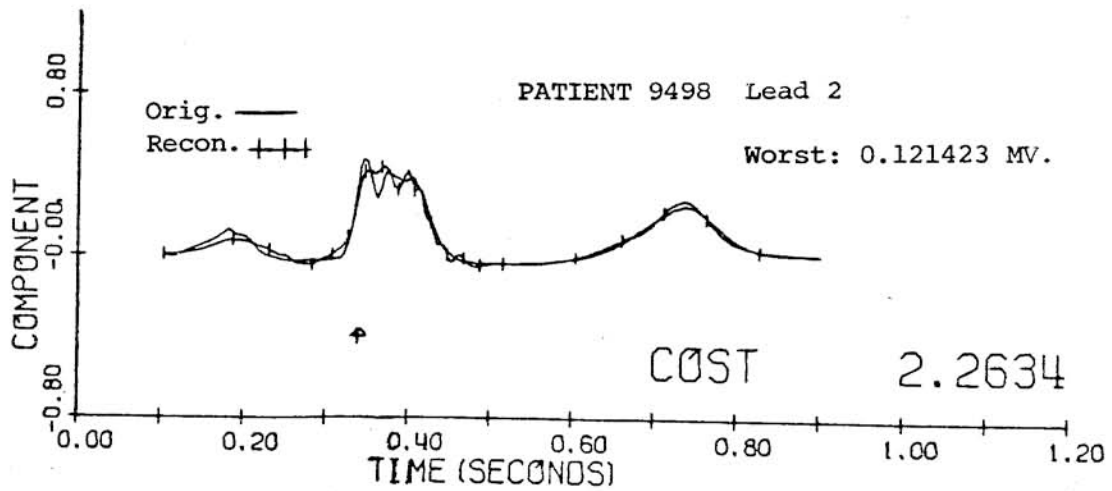


Figure 5.5: 60-th Order Combined-Lead K-L Reconstructions for Patients 9498 (in "Worst" Class) and 8324 (in First 10).

On the other hand, most of the patients in the ensemble are reconstructed to within visual accuracy by using 20 vectors per lead (60 total features). The data compression is from 600 samples to 60 features, or 10 to 1 with the 60-th order K-L.

In Figure 5.2 the ensemble mean VCG waveforms over the data base of 936 patients are shown. Figure 5.3 depicts the first two normalized eigenvectors of the 60th order *separate* lead K-L expansion for lead 2. The percentage of residual expected error energy not captured by the expansion is plotted as a function of the order of the expansion in Figure 5.4. (Note that this is the percentage of expected energy of the deviation from the mean). The reconstructions of VCG lead 2 and lead 3 data are shown for patients 9498 and 8324 respectively in Figure 5.5. Patient 9498 is among the five patients of the whole data-base for which the 60-th order K-L expansion yields the largest absolute pointwise error (L_{∞} cost). Patient 8324 is a typical case. All reconstruction plots depict the original and the reconstructed waveforms superposed on each other for comparison. The location of the largest pointwise absolute error is indicated by a pointer and the actual error at that point is printed next to the label "worst". The L_2 cost incurred is also shown next to the label "cost". The vertical axes are all scaled in milivolts (mv).

5.3 Piecewise Polynomial Techniques

Extensive analyses using P.P. techniques on 60 of the 936 patients are reported in [6]. Several variants of P.P. were tried:

1) Linear (L): This method uses a linear segmented approximation with the estimate constrained to match the data exactly at the knots as discussed in section 3.3.

2) Quadratic (Q): This method uses a quadratic approximation with the estimate constrained to match the data exactly at the knots and at the central sample points between knots: i.e., over each segment the estimate is obtained as the least squares constrained fit of a quadratic to the data.

3) Linear Envelope (LE): This method uses knots computed to minimize approximation error over the vector magnitude (envelope) of the 3-lead VCG data. The same knot locations are then used on each of the separate leads.

In all the methods presented here the optimal knot locations were found for each individual VCG record separately (the sample-based problem, $\Gamma = \omega_p$), with the number of knots fixed a priori. Fixing knots on an ensemble basis yielded results which were generally inferior and unacceptable. Therefore the ensemble-based problem has not been pursued further.

Table 5.1 shows the number of features corresponding to several different numbers of knots. The number of features is the total number of parameter values per lead which must be stored to reconstruct the waveform approximations. The linear features (coefficients) and the nonlinear features (knot locations) are given equal weight in computing the total number of features here. As discussed for the OSKL approach later, the nonlinear features do not require as much storage space as the linear ones because they are unsigned integer parameters while linear features are signed real parameters. In the P.P. data presented in Table 5.1, this is not accounted for. The dynamic programming for the knot locations is performed

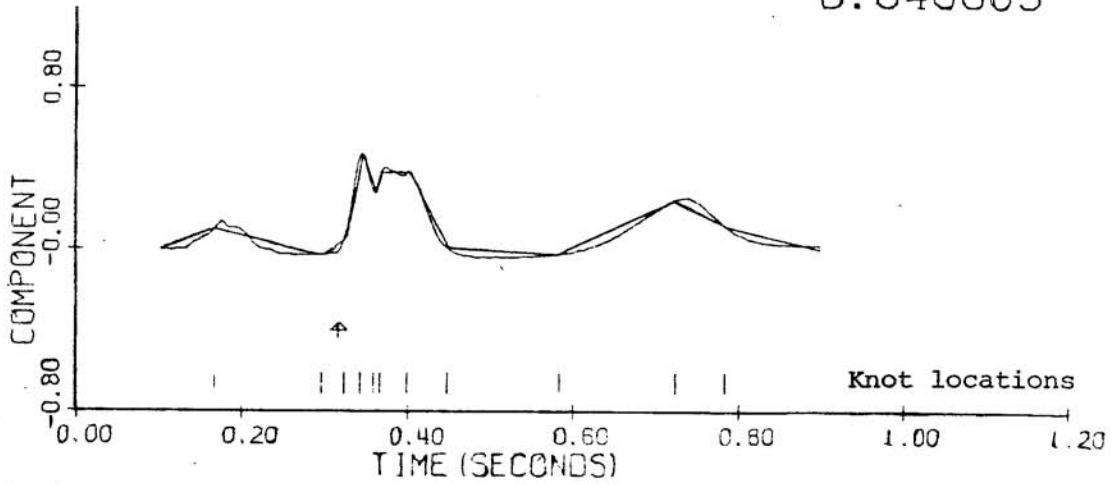
Number of Interior Knots	P.P. Approximation Method Used		
	L	Q	LE
7	16	24	11.33
11	24	36	16.67
14	30		20.67
15	32		22
22	46		31.33

Table 5.1: Number of Features vs. Number of Knots for P.P. Approximation

LINEAR SPLINE LE

PATIENT 9498 LEAD 2 11 KNOTS

0.048689



LINEAR SPLINE L

PATIENT 8329 LEAD 3 15 KNOTS

0.025365

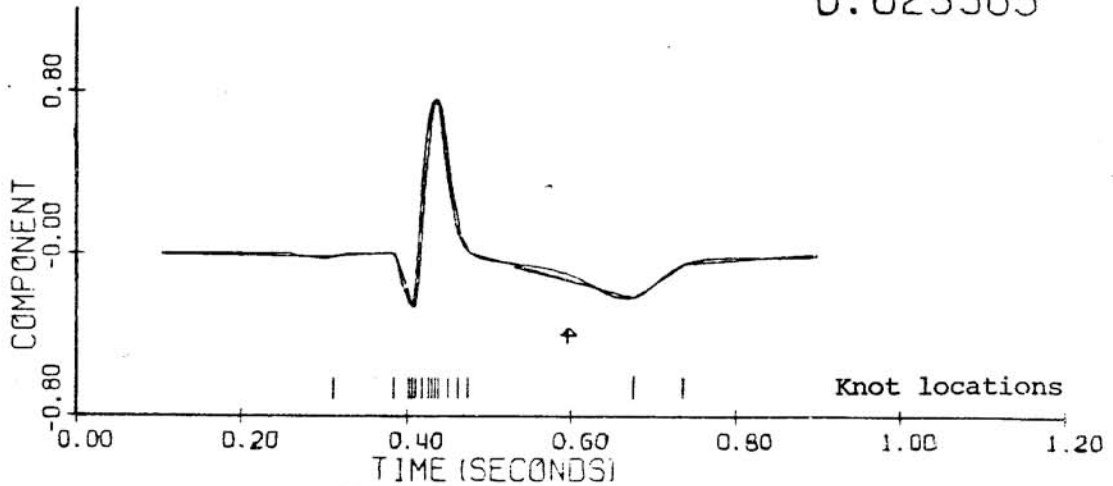


Figure 5.6: Piecewise Polynomial VCG Reconstructions for Patients 9498 (in "Worst" Class) and 8329 (in First 10).

on the full set of 200 possible knot locations for each lead and no suboptimal approaches are used to reduce computations.

Reconstructions for patients 9498 and 8329 using P.P. techniques are shown in Figure 5.6. The optimal knot locations are marked above the time axis and the P.P. variant used is also indicated.

5.4 Optimally Segmented Karhunen-Loève Technique

The OSKL methods developed in Chapter 4 were applied to the cardiogram problem. L_2 -norm ensemble-based, and Chebyshev norm sample-based formulations were tried. In all cases, due to the limited on-line memory available on the computer used for the OSKL technique (a CDC 6400), the original data's sampling rate was halved yielding data of 100 samples per lead, or 300 samples in total per patient, instead of the 600 used for the K-L and P.P. techniques. The computational experience, with this approach, however, indicates that using the original sampling rate is entirely feasible on a computer with larger memory, say an IBM 360, as used for the K-L and P.P. techniques. For purposes of the dynamic programming for the knot locations, a suboptimal approach was used. The total interval, $[0, T]$ in continuous time, or $[1, 100]$ in the discrete case, was partitioned into 10 equal regions with 9 interior knots. The only knots considered for the optimization over knot locations were the 9 equally spaced interior knots. This approach, although clearly suboptimal, still yielded successful results that can be compared with the previous K-L and P-P techniques. Ideally the grid of allowed knots should have a spacing which is within the resolution of the QRS complex. The computational experience gained with the suboptimal scheme presented here indicates that it is entirely feasible

to take a grid twice as dense as the current one (20 regions, 19 interior knots). This has not been pursued here since the results with the coarse grid are sufficient to demonstrate the desirable aspects of the OSKL techniques.

With the suboptimal scheme using a maximum of 9 interior knots for segmentation, there are 55 possible regions to consider for the dynamic programming. Local K-L basis vectors over each of the 55 regions are first determined. The local expansion orders are limited to a maximum of 10. (Note that over the shortest regions between consecutive grid points, there are only 10 time samples). Each lead of the VCG is considered separately, again due to memory limitations in the CDC 6400. A combined lead vector approach, as with the global K-L, is entirely feasible on a large computer.

Several studies were made corresponding to the various formulations of Chapter 4. Methods (1) and (2) described below correspond to the ensemble based problem, $\Gamma = \Omega$, with the L_2 norm. Methods (3) and (4) correspond to the sample-based problem, $\Gamma = \omega_p$, with the L_∞ norm.

1) Fixed Knots, Fixed Uniform Local Orders of Expansion (FKULO):

The knot locations are fixed for all patients and are optimal with respect to the entire-data base. The local expansion orders are fixed in all cases to be 5 ($m_j = 5$). The total number of segments is fixed to be 4 ($N = 4$). The number of segments $N = 4$ is chosen in view of the behavior of the L_2 -ensemble cost as a function of the number of segments shown in Figure 5.7. It can be seen that the ensemble cost reduces slowly for $N > 4$. The four resulting fixed segments correspond roughly, in order of importance,

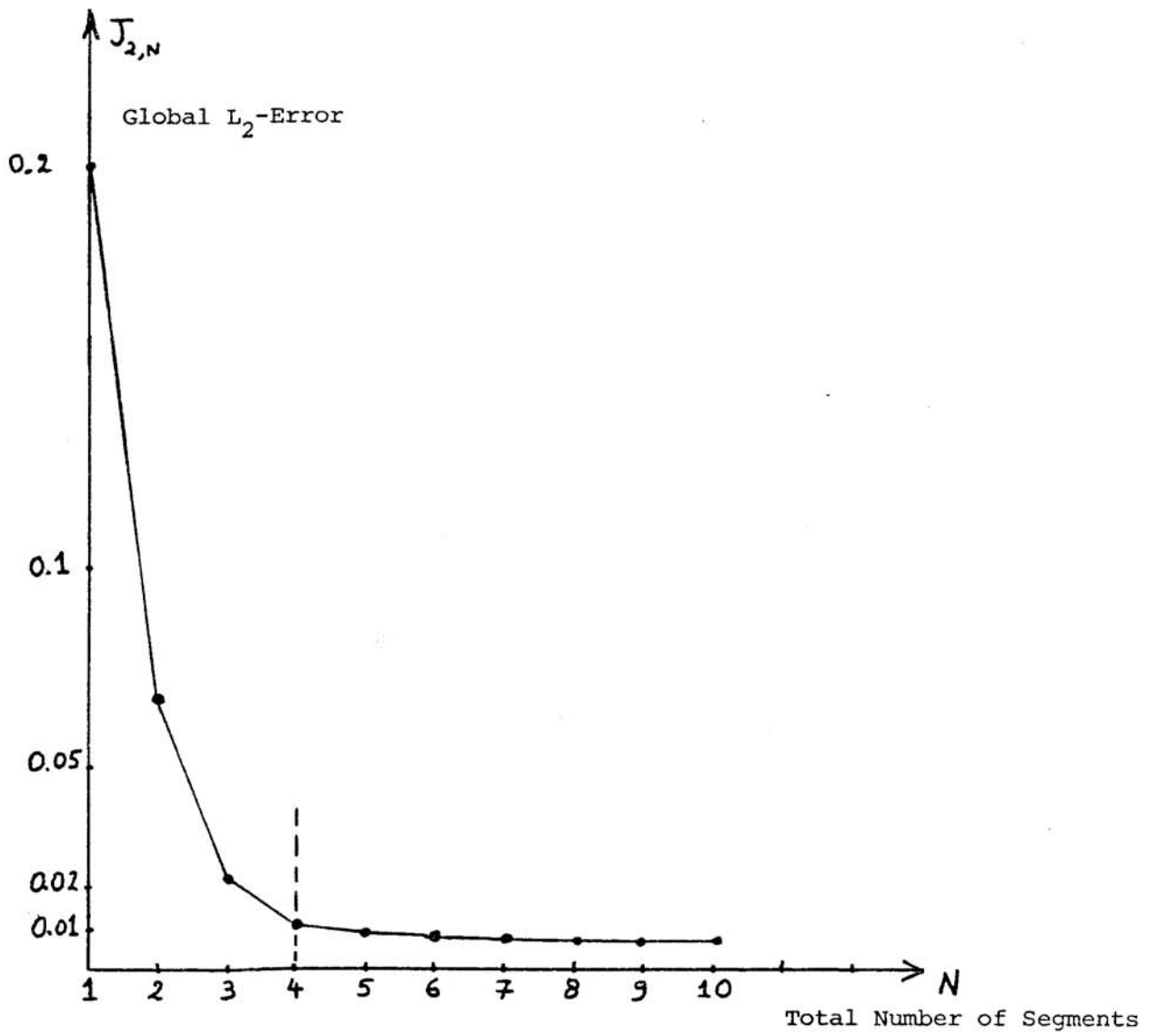
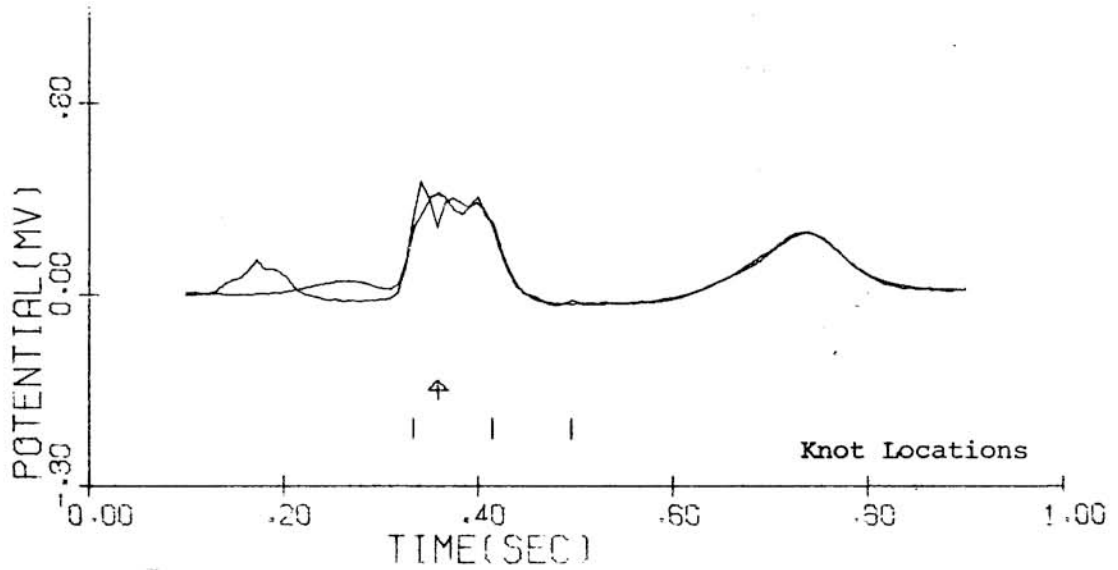


Figure 5.7: Convergence of FKULO Method with 5 Vectors/Segment as a Function of the Number of Segments.

ENSEMBLE-BASED OSKL FKULO
PATIENT 9498 LEAD 2
ERROR .14257 20.0 FEATURES



ENSEMBLE-BASED OSKL FKULO
PATIENT 8324 LEAD 2
ERROR .06553 20.0 FEATURES

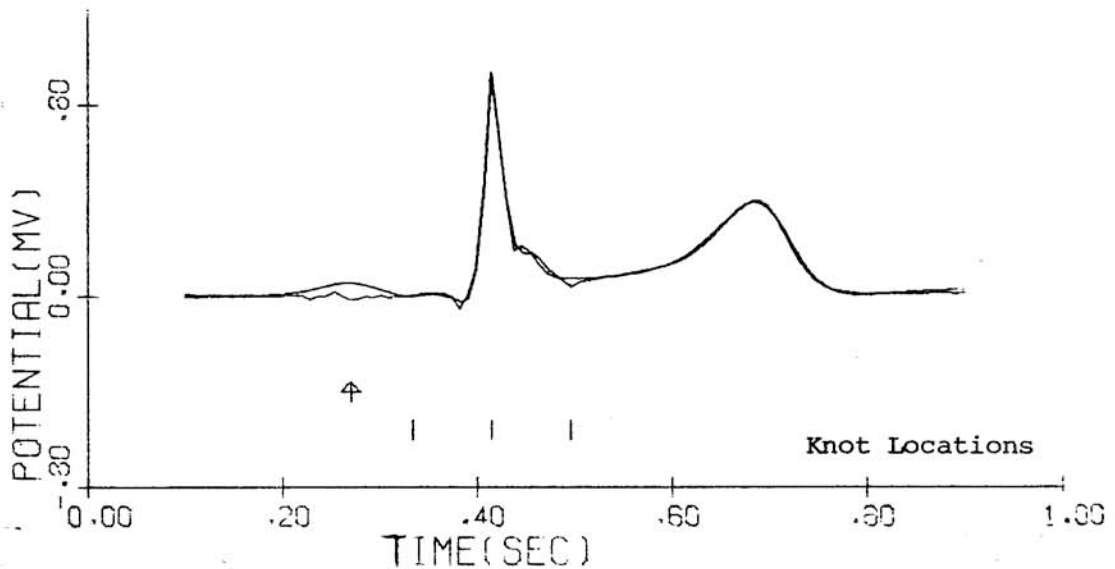


Figure 5.8: Reconstructions for FKULO Variant of OSKL for Patients 9498 (in "Worst" Class) and 8324 (among first 10).

to the QRS, ST, T, and P waves. Note that the actual segmented modes of the data could be better captured if a finer grid was allowed for the dynamic programming. The orders of expansion were fixed to yield 20 features per lead once the number of segments was selected. Typical reconstructions are shown in Figure 5.8.

2) Fixed Knots, Fixed Non-Uniform Local Orders of Expansion (FKNLO):

The knots are again fixed for the entire data base. The local orders of expansion are fixed but determined to satisfy local L_2 constraints on an ensemble basis. The local constraints are chosen such that 2.8% of the total expected energy of the deviation of the sample waveforms from the mean is uniformly distributed over the total interval. Here the local error tolerance function is

$$\mathcal{E}(t_1, t_2) = \left[\frac{t_2 - t_1}{T} \right] (2.8\%) \int_0^T R(t, t) dt \quad 5.1$$

where

$$R(t, t) = \mathcal{E} [x(t) - \bar{x}(t)]^2 \quad 5.2$$

In the discrete case considered

$$\mathcal{E}(t_1, t_2) = \left[\frac{t_2 - t_1}{100} \right] (2.8\%) \text{tr } R \quad 5.3$$

where R is the 100×100 covariance matrix for the random vector \underline{x} . A plot of the expected L_2 global error versus the number of segments is

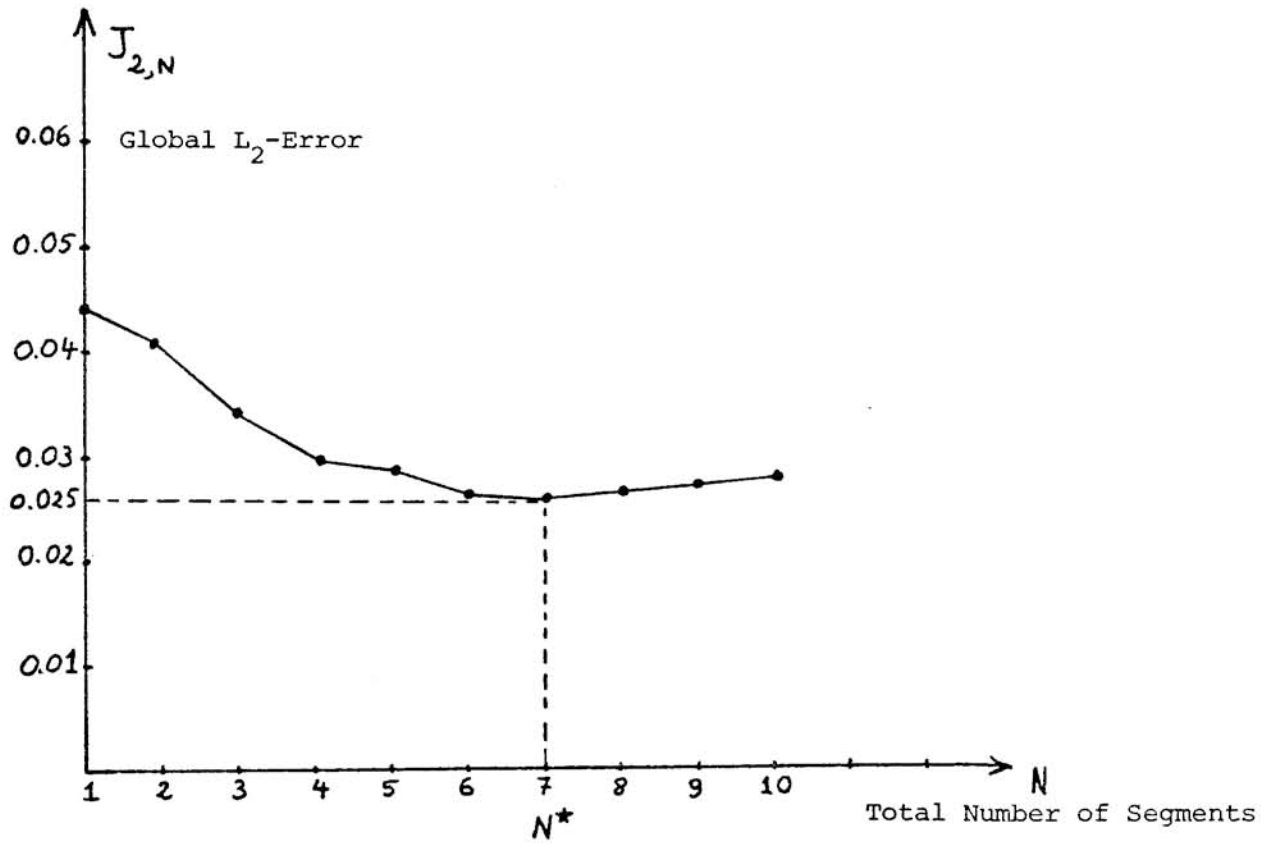


Figure 5.9: Global L_2 -Error as a Function of the Total Number of Segments for FKNLO Method.

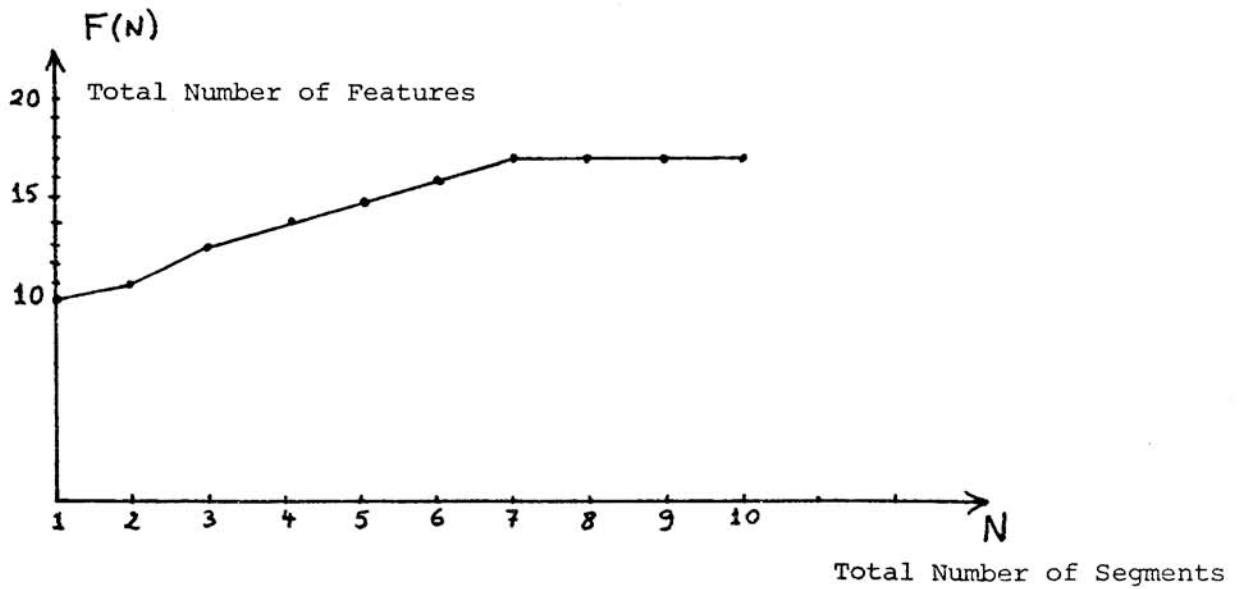
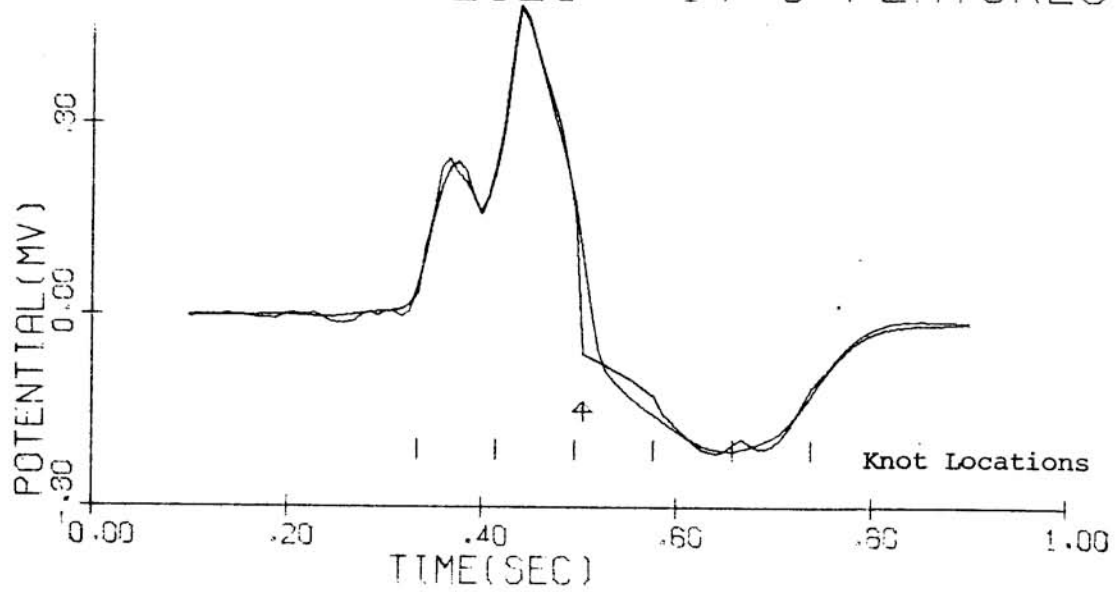


Figure 5.10: Total Number of Features Required as a Function of the Total Number of Segments Used for FKNLO Method.

ENSEMBLE-BASED OSKL FKNLO
PATIENT 9070 LEAD 3
ERROR .42826 17.0 FEATURES



ENSEMBLE-BASED OSKL FKNLO
PATIENT 8322 LEAD 3
ERROR .02080 17.0 FEATURES

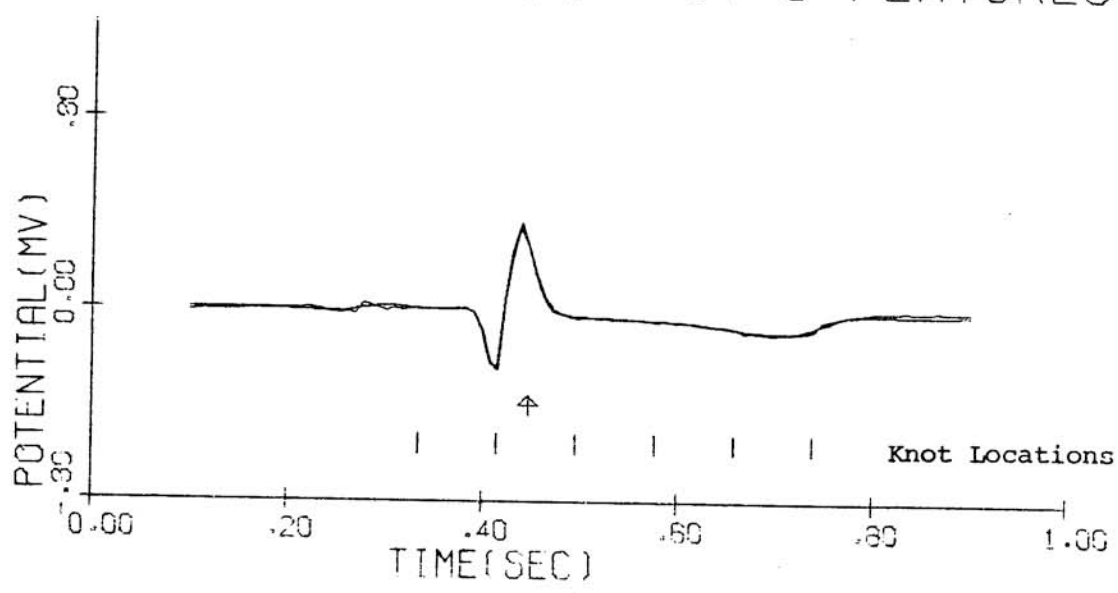


Figure 5.11: Reconstructions for FKNLO Variant of OSKL for Patients 9070 (in "Worst" Class) and 8322 (among first 10).

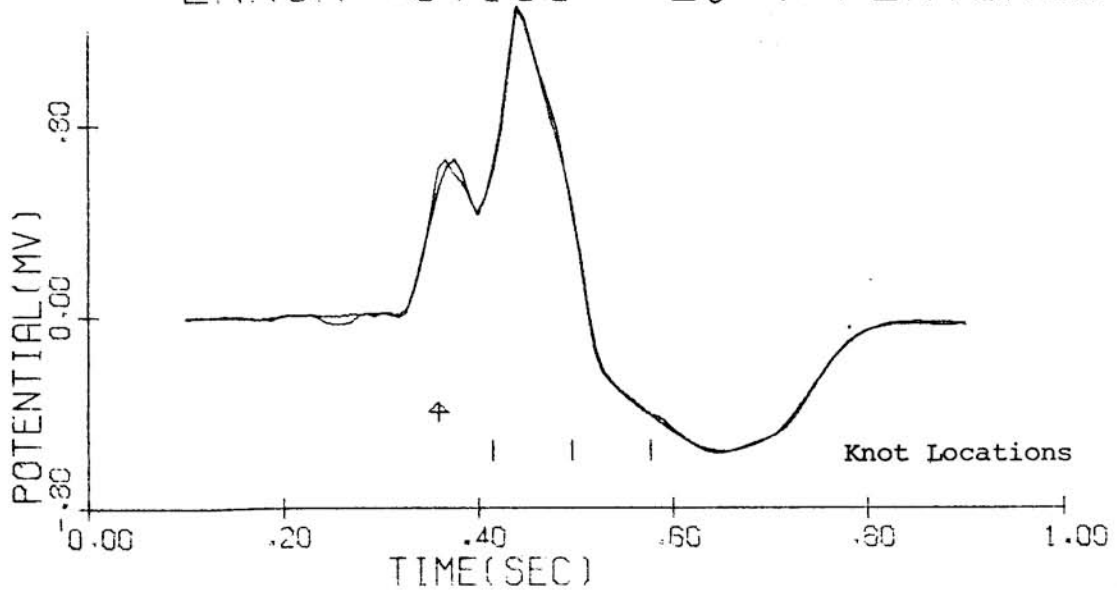
Optimal Knot Locations	Required Local Expansion Orders	Total Number of Features
$T_0 = 0$		
$T_1 = 40$	$m_1 = 1$	$\sum_{j=1}^7 m_j = 17$
$T_2 = 50$	$m_2 = 5$	
$T_3 = 60$	$m_3 = 5$	
$T_4 = 70$	$m_4 = 1$	
$T_5 = 80$	$m_5 = 2$	
$T_6 = 90$	$m_6 = 2$	
$T_7 = 100$	$m_7 = 1$	

Table 5.2: FKNLO Parameters for Expected Error not Exceeding 2.8% of Total Expected Energy in Process Deviation from the Norm.

shown in Figure 5.9. The total number of features required is plotted in Figure 5.10. It can be seen that the minimum expected L_2 -error is achieved for 7 segments. The local expansion orders required to meet the local constraints and the optimal knot locations are given in Table 5.2. The number of required features is 17 to capture 97.2% of the total expected energy in the deviation of the sample-functions from the mean. Furthermore the expected error is spread uniformly throughout the interval -- a result difficult to achieve with a weighted global K-L approach. Typical reconstructions are shown in Figure 5.11.

3) Variable Knots, Fixed Uniform Local Orders of Expansion (VKFULO): The optimal knots are determined using an L_∞ cost for each patient individually. The local expansion orders are fixed to be 5 per segment. It is again observed that using 4 segments is often needed and also enough for most patients analyzed. Therefore N is set to 4, hence yielding a total of 23 features composed of 20 linear local K-L coefficients and 3 nonlinear interior knot locations. The knot locations, being integers, require much less storage space than K-L coefficients as discussed in section 5.3. In fact, since knot locations are positive integers between 1 and 9 in this suboptimal scheme, and K-L coefficients are signed real numbers with at least four or five significant digits, the feature cost of knots is at least 4 times smaller than the feature cost of a K-L coefficient (1 significant digit with no sign, vs. 4 significant digits with a sign). Thus if a K-L coefficient is counted as a unit feature, then a knot location should be counted, with a conservative approach, as 1/4th of a feature. Then the total number of effective features is only about 20.75 rather than 23 with this method. Typical reconstructions are shown in Figure 5.12.

SAMPLE-BASED OSKL VKFULO
 PATIENT 9070 LEAD 3
 ERROR .07103 20.75 FEATURES



SAMPLE-BASED OSKL VKFULO
 PATIENT 9168 LEAD 2
 ERROR .02519 20.75 FEATURES

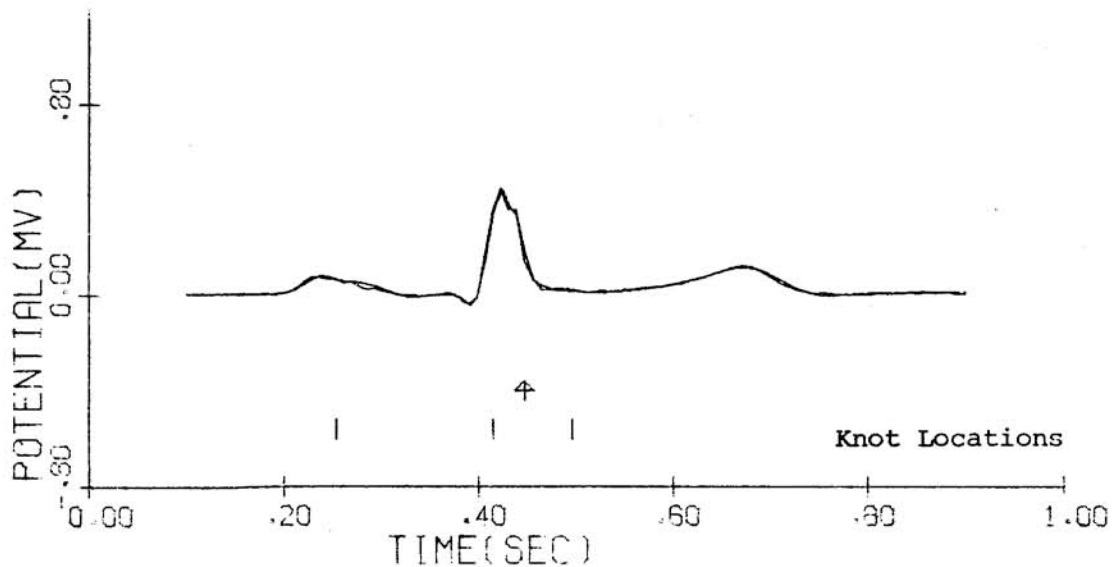
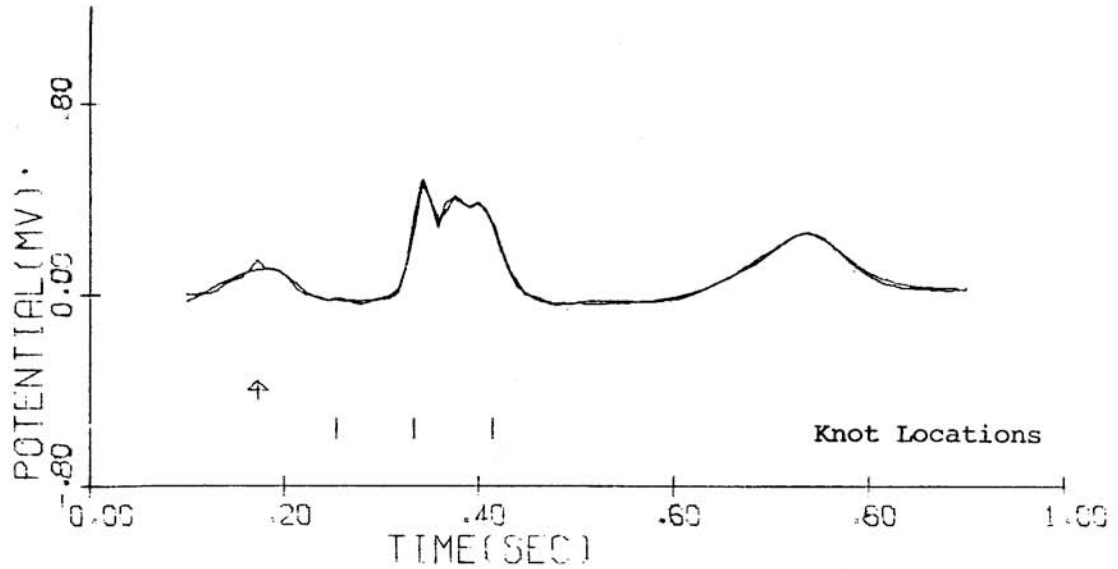


Figure 5.12: Reconstructions for VKFULO Variant of OSKL for Patients 9070 (in "Worst" Class) and 9168 (in "Best" Class).

SAMPLE-BASED OSKL VKLON
 PATIENT 9498 LEAD 2
 ERROR .03797 25.0 FEATURES



SAMPLE-BASED OSKL VKLON
 PATIENT 8325 LEAD 3
 ERROR .01909 19.75 FEATURES

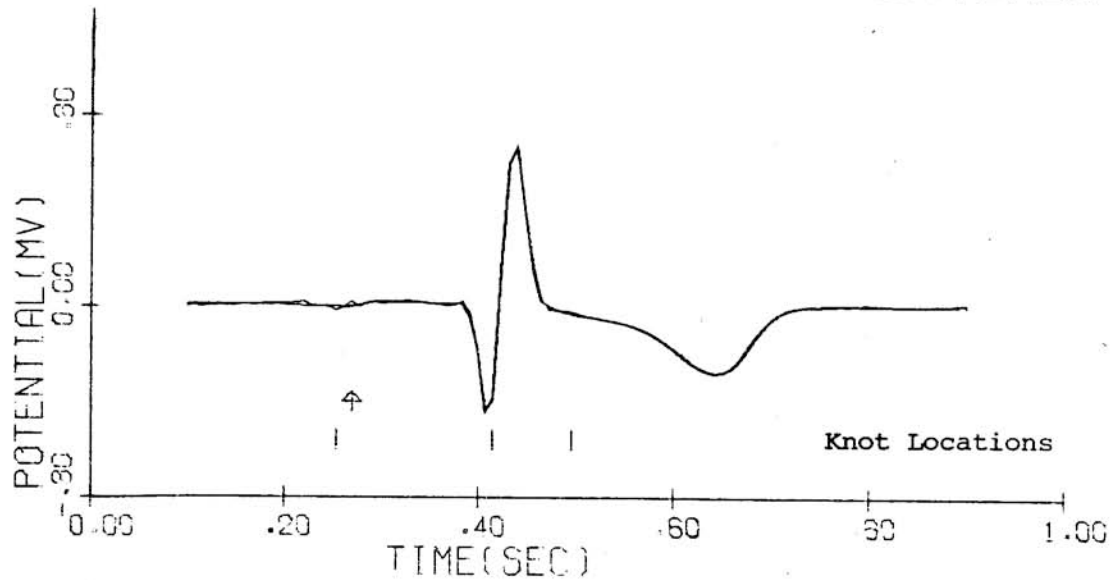


Figure 5.13: Reconstructions for VKLON Variant of OSKL for Patients 9498 (in "Worst" Class) and 8325 (among first 10).

4) Variable Knots, Variable Local Expansion Orders, Variable Number of Segments (VKLON): In this method every parameter, other than the basis functions, is determined optimally for each patient individually using an L_∞ cost.

Since local expansion orders and the total number of segments are positive integers that do not exceed 10, these nonlinear features also carry storage costs not exceeding 1/4th that for a K-L coefficient.

The local L_∞ constraints tried here have been chosen to be uniform over the whole interval. This way the pointwise global and local error is controlled uniformly. In table 5.3, results are shown for a uniform pointwise error constraint of .02 for the first ten patients of the data base. Extensive comparisons of this method with the previous fixed and variable knot OSKL methods have shown that this variant, where every parameter is allowed to adapt to the VCG waveform approximated, yields in all cases a lower L_∞ cost with a lower total number of effective features. Typical reconstructions are shown in Figure 5.13.

5.5 Comparison of Approximation Techniques

A comparison of the global K-L, P.P., and OSKL methods for 20 of the 936 patients is shown in Table 5.4. The first five patients indicated by W yield the worst pointwise absolute approximation errors over the data base with a 60th order combined-lead global K-L. The next five patients indicated by a B yield the lowest pointwise absolute errors. The remaining patients are the first ten patients of the data-base which is not ordered in any particular way. The lead used for the comparisons indicated by the lead number is chosen to be the lead for which the global 60th order K-L pointwise absolute error is largest.

Lead 3 Patient Number	L_{∞} -Cost	Number of Segments	Features		
			Linear	Nonlinear	Total
8322	.01946	3	13	6	14.5
8323	.01981	2	16	4	17
8324	.01953	2	10	4	11
8325	.01979	3	18	6	19.5
8327	.01858	4	23	8	25
8328	.01762	3	23	6	24.5
8329	.01677	2	16	4	17
8330	.01566	4	24	8	26
8331	.01517	4	26	8	28
8334	.01556	4	24	8	26

Table 5.3: VKLON Results for Uniform L_{∞} Error
Constraint of .02 for Lead 3 of First
10 Patients.

Of the various P.P. methods studied, the one yielding the lowest error is shown together with the number of corresponding features per lead. For the last 7 patients only the L and Q methods were tried as indicated. The OSKL method used for comparison is variant (4) where every parameter is allowed to adapt to the waveforms. The optimal number of segments N , the total number of linear features L (coefficients) and the total number of nonlinear features NL (knot locations, local expansion orders and N) are displayed separately. Finally a total number of effective features TOT is computed using $TOT = L + NL/4$. In the OSKL methods, the pointwise absolute error constraints are set to achieve the error performance of the global K-L. The resulting total number of features for OSKL is then compared to 20 which is the number of features per lead used in the K-L method. For the first five patients, the P.P. method performs better than the global K-L and therefore the OSKL approach is compared to the P.P. method separately in Table 5.5 for these patients by setting the pointwise absolute error constraints in the OSKL method to the level of error achieved by the relevant P.P. method. Finally, average worst pointwise absolute errors and average total number of features per lead are computed for all methods. Also an average of the cost per feature for each method is obtained by averaging the ratios of error to number of features used over the 20 patients studied. This number is indicative of the amount of features used in achieving a certain error level.

Table 5.4 indicates that, except for patients 8324 and 8327, the OSKL approach is clearly superior to the global K-L since it achieves lower error and uses fewer effective features. For these two patients, the costs are lower with OSKL but the total numbers of features used are 23 and 23.5 vs. 20 for the global K-L. Hence neither method has a distinct

advantage in those two cases. For all but the first five patients (the W class) the OSKL technique is distinctly superior to the P.P. technique as well. The average numbers indicate the general superiority of the OSKL technique: for an average cost of .045 the P.P. uses an average of 22.7 features, for an average cost of .044 the K-L used 20 features, whereas for an average cost of .040 the OSKL uses an average of 16.7 features.

The average cost per feature is also higher for the OSKL technique than the other techniques, indicating that relatively similar costs were achieved with fewer features on the average: in some sense, there is more "information" per feature with the OSKL approach. The most striking improvements of the OSKL method over the global K-L are for patients which are at the extremes of the performance range of the global K-L; e.g. patients 9426 and 9168 which fall respectively among the five worst and the five best category. This indicates that the OSKL method tends to outperform the K-L in cases for which K-L does poorly and cases for which it performs best.

In Table 5.5, the OSKL method is compared to the P.P. method for the first five patients. It appears that for roughly equivalent L_{∞} -costs the P.P. method uses fewer features than the OSKL method for these patients. It is interesting to note that these patients are the ones that yield the five worst pointwise errors over the data base of 936 patients for the K-L method. The OSKL technique improves greatly over the K-L for these patients and does almost as well as the P.P. technique for which, however, these five patients are not essentially different than the rest since no use of ensemble information is made in the P.P. technique. The OSKL retains

Number	PATIENT		K-L	P.P.		OSKL					
	Lead	Class		L _∞ -Cost	L _∞ -Cost	Type	Features	L _∞ -Cost	N	L	NL
9070	3	W	.074	.037	IE	20.67	.071	3	17	6	18.5
9368	1	W	.076	.049	IE	20.67	.070	3	17	6	18.5
9426	2	W	.095	.040	Q	24	.095	2	7	4	8
9498	2	W	.121	.041	IE	20.67	.117	3	13	6	14.5
9505	3	W	.116	.045	Q	24	.098	3	12	6	13.5
9168	2	B	.022	.021	Q	24	.021	2	12	4	13
9178	1	B	.018	.038	IE	20.67	.016	2	17	4	18
9254	1	B	.018	.032	IE	20.67	.016	3	18	6	19.5
9770	2	B	.014	.033	IE	20.67	.013	3	15	6	16.5
9829	3	B	.016	.032	IE	20.67	.013	3	17	6	18.5
8322	3		.028	.028	Q	24	.022	2	10	4	11
8323	2		.024	.054	L	24	.018	3	18	6	19.5
8324	2		.024	.055	IE	20.67	.018	4	21	8	23
8325	3		.033	.047	L*	24	.031	2	10	4	11
8327	2		.038	.043	L*	24	.034	3	22	6	23.5
8328	1		.035	.071	L*	24	.033	2	15	4	16
8329	2		.027	.034	Q*	24	.025	4	18	8	20
8330	3		.027	.078	L*	24	.025	3	17	6	18.5
8331	1		.041	.058	L*	24	.033	2	14	4	15
8334	3		.037	.057	L*	24	.033	2	16	4	17
Averages			.044	.045		22.67	.040	2.7	15.35	5.4	16.7
Average (Cost/Feature)			.0022	.0020							.0028

Table 5.4: Comparison of K-L, P.P., and OSKL Techniques for Cardiogram Approximation Problem.

Patient			P.P.				OSKL				
Number	Lead	Class	I_{∞} -Cost	Type	Features	I_{∞} -Cost	N	L	NL	TOT	
9070	3	W	.037	IE	$20\frac{2}{3}$.037	4	25	8	27	
9368	1	W	.049	IE	$20\frac{2}{3}$.047	3	23	6	24.5	
9426	2	W	.040	Q	24	.035	3	24	6	25.5	
9498	2	W	.041	IE	$20\frac{2}{3}$.038	4	23	8	25	
9505	3	W	.045	Q	24	.036	3	23	6	24.5	

Table 5.5: Comparison of OSKL and P.P. Techniques for Class W Patients.

some of its K-L character by performing more poorly for these patients than a non-statistical deterministic curve-fitting approach such as the P.P. method. Nevertheless the OSKL's performance is not far from that of the P.P. technique even for these worst case patients. It should be noted that the OSKL approximations are much smoother than P.P. approximations regardless of the pointwise errors. Also the optimal of three different P.P. techniques is compared to OSKL and the OSKL method may be improved when a finer grid is used in the dynamic programming. A further consideration is that in a combined-lead OSKL scheme the number of features required for 3 leads may not be three times the number required for each lead separately just as is the case with the LE vs. L P.P. cases.

The computational requirements of the various techniques developed here are shown in Table 5.6. It can be seen that the OSKL technique with the suboptimal scheme used here is a practicable and superior method for on-line application to the cardiogram approximation and analysis problem.

Technique	Off-Line Computations		On-Line Computations per Patient per Lead (Feature Extraction)		Computer Used
	Time (Seconds)	Memory (Words)	Time (Seconds)	Memory (Words)	
K-L	60	30K	<0.5	10K	IBM 360
P.P. Fixed Knots	20	20K	<0.5	<10K	IBM 360
P.P. Variable Knots	None	None	20	20K	IBM 360
OSKL Fixed Knots	220	30K	<0.5	15K	CDC 6400
OSKL Variable Knots	220	30K	<2	35K	CDC 6400

Table 5.6: Estimated Computational Requirements for Cardiogram Problem.

CHAPTER 6

CONCLUSION AND SUGGESTIONS FOR FURTHER RESEARCH

In this thesis, a new technique, the optimally segmented K-L method for the approximation and analysis of stochastic processes, was developed. This approximation method attempts to unify the desirable aspects of the Karhunen-Loève expansion and variable knot piecewise polynomial approximation. The novel approach is formulated such that expansion functions, knot locations, the total number of segments, and local expansion orders are selected on an optimal basis. Furthermore, the approximations are flexible enough to allow imposition of local error constraints and use of arbitrary norms. The formulation of the approximation problem can be considered on an ensemble or sample-function basis such that various possibilities exist with respect to use of statistical information on the stochastic process in the approximations. Finally, this new approximation technique can be derived using a finite-data base of realizations of the stochastic process being analyzed. Some statistical questions related to the convergence of finite-data base K-L methods were investigated and qualitative results as well as results amenable to numerical techniques for describing the asymptotic behavior of expected errors for truncated expansions were obtained.

The OSKL method was then applied to the feature extraction problem for vectorcardiograms and shown to yield generally better results than either the global K-L expansion or piecewise polynomial approximation from the point of view of data compression. The nonlinear features that resulted

may also capture important timing and phase information for the cardiographic problem that cannot be extracted using only linear methods. The information content of the OSKL features for the cardiogram problem is an important topic that needs thorough investigation.

Some suggestions for further research in this field are listed below:

1) A rigorous theoretical error analysis for the OSKL approach including practically useful error bounds should be developed. It is conjectured that the OSKL approach is superior to many currently available techniques for approximating process realizations for a large class of stochastic processes.

2) The nonlinear features are essentially different from the linear ones. An information-theoretic approach to the feature extraction problem in which nonlinear features are allowed should be investigated. A theoretical study of the information content of nonlinear features would be invaluable.

3) The classification part of the pattern recognition problem must be reconsidered if the OSKL method is used for feature extraction. The feature space, and clustering techniques in this new feature space, must be studied. Hierarchical schemes may have to be developed for dealing with the nonlinear features.

4) The OSKL approach may find application in some central problems of systems science such as system identification and reduced-order filtering. In problems where a minimal state space must be obtained from input-output data, the OSKL approach may yield a systematic approach and allow flexibility for constraint imposition.

5) From a practical and theoretical point of view it would be desirable to develop efficient suboptimal schemes to determine knot locations causally from the data. Alternatively it may be possible to devise a suboptimal dynamic programming algorithm with reduced computational requirements. Also developing parallel processing implementation for OSKL may be practically important.

6) Finally, the application of the OSKL approach to the study of other physical data such as seismic waves, economic time series, or brain waves may provide new insights into the nature of the physical processes underlying the observed associated phenomena.

REFERENCES

1. Rice, J.R., The Approximation of Functions: Linear Theory, Addison-Wesley, Reading, Mass. 1964.
2. Meinardus, G., Approximation of Functions: Theory and Numerical Methods, Springer-Verlag, 1967.
3. Rice, J.R., The Approximation of Functions: Nonlinear and Multivariate Theory, Addison-Wesley, Reading, Mass, 1959.
4. Esch, R.E., Eastman, W.L., "Computational Methods for Best Spline Function Approximation", J. of Approx. Theory Vol. 2, 1969, pp. 85-96.
5. Talbot, A., Editor, Approximation Theory, Proceedings of a Symposium held at Lancaster, July 1969, Academic Press 1970.
6. Gustafson, D.E., et al., "Automated VCG Interpretation Studies Using Signal Analysis Techniques", C.S. Draper Lab., Rept. R-1044, Cambridge, Mass., 1977.
7. Gustafson, D.E., Akant, A., and Mitter, S.K., "Cardiogram Analysis Feature Extraction and Clustering Studies", C.S. Draper Lab. Rept. R-936, Cambridge, Mass, 1975.
8. Gustafson, D.E., Johnson, T.L., and Akant, A., "Cardiogram Analysis and Classification Using Signal Analysis Techniques", C.S. Draper Lab. Rept. R-853, 1974.
9. Calvert, T.W., and Young, T.Y., Classification, Estimation, and Pattern Recognition, American Elsevier, N.Y., 1974.

10. Fukunaga, R., Introduction to Statistical Pattern Recognition, Academic Press, 1972.
11. Chien, Y.T., and Fu, K.S., "Selection and Ordering of Feature Observation in a Pattern Recognition System", *Inf. and Control*, Vol. 12, 1968, pp. 395-414.
12. Sebestyen, G.S., Decision-Making Processes in Pattern Recognition, MacMillan, N.Y., 1962.
13. Akant, A., Processing of Cardiograms for Pattern Recognition, S.M. thesis, M.I.T., 1974.
14. Burton, A.C., Physiology and Biophysics of the Circulation, Yearbook Medical Publishers, Chicago, 1965.
15. Watanabe, S., "Karhunen-Loève Expansion and Factor Analysis: Theoretical Remarks and Applications", *Proc. 4th Prague Conf. on Inf. Theory*; also Yale University T-Report 1965.
16. Dyson, F.J., "Correlations between Eigenvalues of a Random Matrix", *Comm. Mathematical Physics*, Vol. 19, 1970, pp. 235-250.
17. Van Trees, H.L., Detection, Estimation, and Modulation Theory: Part I., J. Wiley and Sons, N.Y., 1968.
18. Young, T.Y., "The Reliability of Linear Feature Extractors", *IEEE Trans. on Computers*, Vol. C-20, 1971, pp. 967-971.
19. Loève, M.M., Probability Theory, Van Nostrand, Princeton, 1963.
20. Ash, R.B., Information Theory, Interscience Publishers, N.Y., 1968.

21. Bellman, R.E., Dynamic Programming, Princeton University Press, 1957.
22. Wilks, S.S., Mathematical Statistics, Wiley, N.Y., 1963.
23. Faddeev, D.K., and Faddeeva, V.N., Computational Methods of Linear Algebra, Freeman, San Francisco, 1963.
24. Porter, C.E., Editor, Statistical Theories of Spectra: Fluctuations, A collection of original papers and reprints edited by C.E. Porter, Academic Press, 1965.
25. Mehta, M.L., Random Matrices and the Statistical Theory of Energy Levels, Academic Press, 1967.
26. Schoenberg, I., Cardinal Spline Interpolation, SIAM Regional Conference Series in Applied Mathematics, Philadelphia, 1973.
27. Schoenberg, I., Approximations with Special Emphasis on Spline Functions, Proceedings of a Symposium conducted by the Mathematics Research Center, U.S. Army, University of Wisconsin, Academic Press, 1969.
28. Greville, T.N.E., Editor, Theory and Applications of Spline Functions, N.Y. Academic Press, 1969.
29. Ahlberg, J.H., Nilson, E.N., and Walsh, J.L., The Theory of Splines and their Applications, N.Y., Academic Press, 1967.
30. Prenter, P.M., Splines and Variational Methods, Wiley, New York, 1975.
31. Braess, D., "Chebyshev Approximation by Spline Functions with Free Knots", *Numerische Math.*, Vol. 17, 1971, pp. 357-366.

32. De Boor, C., Rice, J.R., "Least Squares Cubic Spline Approximation: Variable Knots", Comp. Sc. Dept. Tech., Rept. 21, Purdue University, 1968.
33. Meir, A., and Sharma, A., Editors, Spline Functions and Approximation Theory, Proceedings of the Symposium held at University of Alberta, Birkhauser Verlag Basel, 1973.
34. Burchard, H.G., "Splines (with Optimal Knots) are Better", *Applicable Analysis*, Vol. 3, 1974, pp. 309-319.
35. Schumaker, L., "Uniform Approximation by Chebyshev Spline Functions: Free Knots", *SIAM J. Numerical Analysis*, Vol. 5., No. 4, Dec. 1968, pp. 647-656.
36. Mc Clure, D.E., "Nonlinear Segmented Function Approximation and Analysis of Line Patterns", *Quarterly of Applied Math.*, Vol. 23, No. 1, 1975, pp. 1-37.
37. Dodson, D.S., Doctoral Dissertation, Comp. Science Dept., Purdue University, 1972.
38. Bellman, R.E., "On the Approximation of Curves by Line Segments Using Dynamic Programming", *Comm. ACM*; Vol. 6, No. 4, June 1961, p. 284.
39. Stone, H., "Approximation of Curves by Line Segments", *Math. Comp.*, Vol. 15, 1961, pp. 40-47.
40. De Boor, C., "On Uniform Approximation by Splines", *J. of Approx. Theory*, Vol. 1, 1968, pp. 219-235.

41. Hall, C.A., "On Error Bounds for Spline Interpolation", J. of Approx. Theory, Vol. 1, 1968, pp. 209-218.
42. Marsden, M.J., "On Uniform Spline Approximation", J. of Approx. Theory, Vol. 6, 1972, pp. 249-253.
43. Ream, N., "Note on 'Approximation of Curves by Line Segments'", Math. of Comp., Vol. 15, 1961, pp. 418-419.
44. Goldman, M.J., Principles of Clinical Electrocardiography, Lange Medical Publications, Los Altos, California 1970.
45. Frank, E., "An Accurate, Clinically Practical System for Spatial Vectorcardiography", Circulation, Vol. 13- p. 737, 1956.
46. Yamada, K., et al., "Observer Variation in Electrocardiographic Interpretation", Ann. Rep. Res. Inst. Environ. Med., Nagoya University, Nagoya, Japan, Vol. 16, 1968, pp. 27-41.

BIOGRAPHY

Adnan Akant was born in Ankara, Turkey on July 23, 1951. He completed his primary and secondary education at Lycee Janson de Sailly in Paris, France, and Lycee de Galatasaray in Istanbul, Turkey. He then attended Wheelus American High School in Tripoli, Libya and was graduated from there in June 1968. In September 1968, he entered the Massachusetts Institute of Technology and received from there the S.B. and S.M. degrees in Electrical Engineering simultaneously in June 1974, and the Electrical Engineer degree in June 1975. While a graduate student at MIT, he was a teaching assistant in Electrodynamics, Statistical Mechanics and Thermodynamics, Signals, Circuits, and Systems, and Network Theory courses. From June 1973 to June 1976, he has worked as a research assistant and Draper Fellow at the Control and Flight Dynamics Division of Charles Stark Draper Laboratory, Inc. He has also held a Vinton-Hayes fellowship in Communication and a research assistantship at the M.I.T. Electronic Systems Laboratory. Mr. Akant is a member of Sigma Xi and Tau Beta Pi.

In the summer of 1976, he completed Officer's basic training at the Army School of Telecommunications in Ankara, Turkey. He was discharged from military duty with the rank of second lieutenant.

Mr. Akant is currently a candidate for the S.M. degree in Management, which he expects to receive in December 1977, from the Alfred P. Sloan School of Management, M.I.T. He is also working at Scientific Systems, Inc., Cambridge, Massachusetts. His interests are in the general field of systems science and its applications.